Stony Brook University

Harnessing Redox Regulation of PTP1B: a Novel Path to Therapeutic Design

A Dissertation Presented

by

Ioana A. Rus

to

The Graduate School

in Partial Fulfillment of the

Requirements

for the Degree of

Doctor of Philosophy

in

Genetics

Stony Brook University

May 2016

Stony Brook University

The Graduate School

Ioana A. Rus

We, the dissertation committee for the above candidate for the Doctor of Philosophy degree, hereby recommend acceptance of this dissertation.

Nicholas K. Tonks-Dissertation Advisor
Professor, Cold Spring Harbor Laboratory

Geoffrey Girnun-Chairperson of Defense
Associate Professor, Department of Pathology, Stony Brook University

Leemor Joshua-Tor
Professor
Cold Spring Harbor Laboratory

Richard Lin
Professor
Department of Physiology and Biophysics
Stony Brook University

Markus Seeliger
Assistant Professor
Department of Pharmacological Sciences
Stony Brook University

Anton Bennett
Professor
Department of Pharmacology and of
Comparative Medicine
Yale University

This dissertation is accepted by the Graduate School

Charles Taber
Dean of the Graduate School

Abstract of the Dissertation

Harnessing Redox Regulation of Protein Tyrosine Phosphatase 1B: a Novel Path to Therapeutic Design

by

Ioana A. Rus

Doctor of Philosophy

in

Genetics

Stony Brook University

2016

Protein tyrosine phosphatse 1B (PTP1B) is an important negative regulator of signaling by the insulin and leptin receptors. PTP1B-null mice are sensitized to insulin and resistant to diet-induced obesity, making PTP1B a prized target in the pharmaceutical industry for therapeutic intervention in type two diabetes and obesity. Efforts to develop inhibitors of PTP1B focused on the active site pocket; however, those efforts have been hindered by poor oral bioavailability of the compounds. Our lab has exploited the conformational changes associated with redox regulation of PTP1B to devise an alternative method of inhibiting the enzyme. Reactive oxygen species, generated in response to insulin receptor tyrosine kinase signaling, oxidize the thiol of the catalytic cysteine, temporarily inactivating PTP1B. Reversible oxidation of PTP1B (oxPTP1B) results in a profound conformational change at the catalytic site. We have identified by phage display a single chain variable fragment antibody (scFv45) that selectively binds oxPTP1B and stabilizes it. When expressed in cells, scFv45 leads to potentiation of insulin signaling. We have pursued molecular and structural studies to determine the basis for the interaction between scFv45 and oxPTP1B. By comparison with T-cell protein tyrosine phosphatase (TCPTP), with which it shares 74% sequence identity in the catalytic domain, we have found that a combination of both residue identity and conformational changes confer specificity to the binding interaction between scFv45 and oxPTP1B. These data suggest a strategy for development of small molecule inhibitors that mimic the effects of scFv45. This study is discussed in the context of identification of chelerythrine as a small molecule mimic of scFv45 and inhibitor of PTP1B function. Overall our data reveal a path to identification of therapeutic molecules that sensitize insulin signaling in type 2 diabetes and obesity by selectively inhibiting that pool of PTP1B that regulates insulin and leptin signaling.

to my parents

Table of Contents

LIST OF FIGURES

Figures for Chapter 1

Figures for Chapter 2

Figures for Chapter 3

Figures for Chapter 4

Figures for Chapter 5

Acknowledgments

First and foremost, I would like to thank my advisor, Dr. Nicholas K. Tonks for his support throughout the past 5 years. As a mentor he has worked with me tirelessly, offering advice and guidance when needed. He has allowed me the independence to grow, yet was always near when help, supervision or encouragement were much needed. He has been patient and kind at times when I am sure I tried his patience tremendously, and I am truly honored to have worked in his laboratory and with him. He has helped me develop into a scientist and has taught me more than I could have ever hoped to learn. I will also always appreciate the fact that I have now learned enzyme kinetics from a legend in the field.

I am grateful to each and every single one of my committee members for their guidance both during committee meetings and outside. I have received helpful reagents and had useful discussion with each and every one of you and I am thankful you have given me the opportunity to work with and learn from you. I would like to thank Dr. Leemor Joshua-Tor for adopting me into her research group and welcoming me to learn from them and conduct crystallography experiments in their lab. I would like to thank Dr. Markus Seeliger for helpful discussion about my structural work and supportive mentorship throughout my graduate career, both the PhD and the MD years. I would like to thank Dr. Geoffrey Girnun for being the chair of my committee and for his helpful discussions in regards to my experiments, for generously sharing reagents, and for challenging me. I am grateful to Dr. Richard Lin for his valuable input and focused guidance during this complicated process. Last, but certainly not least I am thankful that Dr. Anton Bennet has kindly agreed to join my thesis committee and for willing to share his expertise in the PTP field with me through this process.

I am grateful to the members of the Tonks lab both present and graduated: Gaofeng, Wei, LiLi, Mathangi, Mind, Fauzia, Siwei, Dongyan, Chris, Nava, Om, Ulla, Christie, Kevin and Lorraine. I feel compelled to thank two colleagues in particular, Aftab and Nava for their tireless efforts, support, helpful discussions and friendship throughout my time in the lab. I am thankful to Chris for his scientific collaboration, for countless helpful discussions and for his friendship since he joined the lab.

I am also thankful to each of the members of the Joshua Tor lab. Claus was my initial help when I undertook this project. Chris, Elad, Jack, Jon, Ken and Ante have been tremendously generous with their time and knowledge. They have provided technical help countless times and have been a 2nd home in addition to the Tonks lab.

Chapter 1

Introduction

1.1. Diabetes

Type two diabetes is a disease characterized by insulin resistance resulting in inability to maintain blood glucose homeostasis. Concurrent with increased prevalence in obesity, diabetes has become a major chronic disease primarily through progressive cardiovascular damage from hyperglycemia. Treatment of diabetes involves maintenance of blood glucose and ongoing medical care to prevent acute complications and long-term sequelae. In 2007 in the US the prevalence of type 2 diabetes was 23.6 million, or ~8% of the population. Once considered a disease of wealthy nations, worldwide statistics are becoming staggering with developing countries affected the most. In 1980 there were 108 million patients diagnosed with diabetes, by 2000 that number had almost doubled to 171 million and although it was suggested that this number would double by 2030, data show that by 2014 there were 422 million adults worldwide living with diabetes.

One of the worst features of the disease is the lead-time before diagnosis, which can be as long as 20 years. During this time patients are hyperglycemic but unaware of it as there are no readily available physical symptoms such as pain or discomfort, which drive people to the hospital in the case of other diseases. As a result, irreversible cardiovascular damage will occur in silence for decades before diagnosis of T2DM occurs and treatment starts. This delay in diagnosis causes morbidity and mortality, with diabetics in western society 3 times more likely to be hospitalized than non-diabetics. For example, in the US, diabetes is the leading cause of blindness, end-stage renal disease and non-traumatic lower extremity amputations. T2DM used to be referred to as “maturity onset” diabetes, but is now also becoming prevalent in children, with higher incidence that type 1 in some developing countries.

Diagnosis of diabetes is based on maintenance of plasma glucose homeostasis with the same tests used for both screening and diagnosis. The original tests used measurements of blood glucose randomly sampled or with fasting or after challenging the body with a large quantity of it. More recently glycation of hemoglobin ($HbA_{1c} \geq 6.5\%$) has been adopted as a measurement because it indicates blood glucose homeostasis over a period of 3 months and therefore has less variability that previously used tests. Based on their ability to control glucose homeostasis patients can be classified into categories such as pre-diabetes/high risk for diabetes and diabetes. Early testing is beneficial as there is a long asymptomatic phase to type 2 diabetes when intervention and lifestyle changes would reduce the development of disease.

The classification of diabetes includes four clinical cases. Type 1, mostly present in children, is characterized by insulin deficiency, due to β-cell destruction by anti-islet autoantibodies (90% of cases) or other insults such as pancreatitis. Type 2 results from progressive resistance to insulin, which culminates in insufficient insulin secretion. A third category is not overt diabetes, but rather gestational, diagnosed during pregnancy and is associated with development of type 2 diabetes later in life. A fourth group includes diabetes caused by drugs/chemicals or disease of the exocrine pancreas. All forms of diabetes, both inherited and acquired, are clinically characterized by hyperglycemia, some degree or absolute insulin deficiency and vascular damage.

1.1.1. Pathogenesis of Disease

Several mechanisms have been shown to contribute to the development of insulin resistance, with deregulation of metabolic control and obesity accounting for as much as 50% of cases (Reaven 2011). The constellation of conditions contributing to metabolic deregulation can be classified as a metabolic syndrome and includes central obesity, impaired glucose tolerance, diabetes mellitus, hypertension and dyslipidemia. The pathogenesis of metabolic syndrome is not fully elucidated, although thus far it is clear that it can be attributed to a combination of genetic predisposition, sedentary lifestyle and a diet of excess calories. When our food intake exceeds energy expenditure for an extended period, energy balance is lost and obesity develops. The healthy response is to increase anabolic reactions in times of nutrient consumption or excess and to increase catabolic reactions in nutrient shortage. If nutrient intake exceeds expenditure, anabolic reactions convert the excess carbohydrates, protein or lipid to fatty acids in the form of triglyceride stored as adipose tissue. If the storage capacity of adipose is exceeded, nutrients enter other tissues, typically thought of as non-storage, such as myocytes, hepatocytes, vascular cells and β-cells, and results in insulin resistance in these tissues. The association between lipids and insulin resistance is widely accepted.

An imbalance between calories taken in over calories used leads to increased storage of fat in adipose tissue, leading to development of obesity, and eventually an inability of adipocytes to store more triglycerides. As a result, levels of circulating fatty acids increase and fat is stored in other cell types such as liver and skeletal muscle, both of which lead to insulin resistance. It has been shown that intrahepatic lipid content is the cause of insulin resistance in liver, and not general abdominal adipose as previously suspected. Concurrently, immune cells infiltrate

adipose tissue in response to cytokines released by adipocytes further contributing to insulin resistance in muscle and liver. Insulin resistance in the brain also contributes to obesity and ultimately glucose intolerance by failing to suppress appetite.

At the molecular level although many mechanisms have been proposed, insulin resistance due to impaired insulin signaling has received most of the focus. Impaired insulin signaling due to increased serine phosphorylation and inactivation of the insulin receptor substrate-1, IRS-1, leads to insulin resistance. This serine phosphorylation prevents binding of IRβ and IRS-1, and its activation through tyrosine phosphorylation. Ultimately this leads to decreased binding of downstream phosphatidylinositol 3-kinase (PI3K), and decreased phosphorylation and activation of Akt. IRS-1 serine residues are phosphorylated by protein kinase C (PKC), which is activated by the lipid intermediate diacylglycerol or by the stress kinase c-Jun N-terminal kinase (JNK). JNK is activated by proinflammatory cytokines released due to increased adiposity.

The most important physiologic regulator of insulin secretion is glucose. Glucose enters the pancreatic β-cells by facilitated diffusion through the GLUT2 transporter. Glucose is phosphorylated to glucose-6-phosphate by the rate limiting enzyme glucokinase, which functions as a glucose sensor for the β-cell. Glycolysis produces ATP, which initiates insulin secretion by blocking the K_{ATP} channel on the membrane of β-cells, leading to depolarization, increase in intracellular Ca^{+2} and insulin secretion. Conversely, a fall in blood glucose levels results in decrease in glycolysis and in insulin secretion. The higher the blood glucose levels the more glucose enters the β-cells, the higher the rate of glycolysis and in response the rate of insulin secretion increases to compensate. The rate of glycolysis as determined by glucokinase activity is the primary response mechanism by which β-cells adapt to glucose changes. In obesity or other insulin-resistant states, β-cells increase sensitivity to glucose through increased expression of a hexokinase. Hexokinase has a lower K_m for glucose than glucokinase does, and thus functionally shifts the insulin-glucose dose-response curve left: more insulin is secreted in response to lower glucose concentrations. Whether insulin resistance progresses to diabetes mellitus depends directly on the ability of pancreatic β-cells to maintain high enough insulin levels to overcome insulin resistance and control hyperglycemia. Many pre-diabetics have sufficient β-cell reserve to maintain euglycemia with restricted diet, weight loss and medication.

Skeletal muscle is the primary tissue of insulin-stimulated post-prandial glucose disposal, where it is stored as glycogen. Insulin stimulates glycogen synthase, and is essential for maintenance of glucose homeostasis. In healthy people ~80% of glucose is taken up by skeletal muscle and stored as glycogen. Ectopic accumulation of lipid in liver and skeletal muscle leads to impairment of insulin signaling. Muscle insulin resistance due to ectopic lipid precedes liver insulin resistance and diverts ingested glucose to the liver. The rate of insulin-stimulated muscle glycogen synthesis is 70% lower in patients with T2DM and in normoglycemic offspring of patients with T2DM. By measuring the accumulation of precursors it was found that glucose transport by the GLUT4 transporter was the reason for the decreased glycogen synthesis in T2DM patients and their offspring. As muscle glycogen synthesis is the major pathway for glucose metabolism in both normal and diabetic individuals, defects in this pathway is a direct cause of insulin resistance. At the molecular level insulin signaling through IRS-1, PI3K and Akt is decreased. Ultimately this results in decreased translocation of the GLUT4 glucose transporter and impaired insulin-stimulated glucose import into muscle cells.

Hepatic insulin resistance leads to increased gluconeogenesis in the liver and release of glucose into the blood stream as well as dyslipidemia. Normally insulin suppresses gluconeogenesis and glycogenolysis, increasing hepatic glycogen synthesis, and decreasing release of glucose from the liver. However in insulin resistance the liver continues gluneogenesis and glucose release, resulting in fasting hyperglycemia. At the molecular level there is increased expression of gluconeogenic enzymes such as phosphoenolpyruvate carboxykinase and glucose 6-phosphatase, and decreased expression of enzymes that regulate glycogen synthesis and glycolysis, such as glucokinase and pyruvate kinase. Hepatic insulin response leads to high levels of circulating fatty acids and triglycerides characteristic of T2DM. Insulin increases transcription of lipogenic enzymes such as acetyl-CoA carboxylate and fatty acid synthase through activation of SREBP-1c, resulting in increased synthesis of fatty acids and triglycerides. Insulin resistance also contributes to hyperlipidemia through downregulate the LDL receptor, resulting in low LDL levels as well as low levels of apolipoprotein B, which is the main component in transport of LDL.

Glucose release from hepatocytes is also suppressed in response to insulin by the hypothalamus through the vagal nerve (Pocal 2005). Insulin also signals through the hypothalamus and from it through sympathetic nervous system signaling to adipocytes to

adipocytes in order to suppress lipolysis and increase lipogenesis in white adipose tissue (Scherer 2011).

Leptin hormone is synthesized and secreted by white adipose tissue in direct proportion to the amount of body fat, so leptin levels can represent a measurement of long-term energy stores. It is a major contributor in regulation of satiety and energy expenditure. In overfed states and obese individuals there are persistent high leptin plasma levels, indicating leptin resistance (Myers 2010). Leptin signals are integrated within the hypothalamus, as well as midbrain and brainstem, and output signals control appetite and energy expenditure by the autonomic nervous system. This neuronal output leads to appetite suppression through increased expression of anorexigenic peptide α-melanocyte stimulating hormone (α-MSH) from pro-opiomeanocortin (POMC) neurons. Decreased expression of orexigenic neuropeptide Y (NPY) and agouti-related peptide (AgRP) increases energy expenditure.

Leptin and insulin are both secreted by peripheral tissues in direct proportion to body fat stores. They are the main signals of energy status to the brain, where their signals synergize. Like leptin, insulin reduces food intake through an increase in anorexigenic (α-MSH and POMC) peptides and increases energy expenditure by increased expression of orexigenic (NPY and AgRP) peptides. However the outcome of their effects are slightly different on peripheral adipose. Whereas leptin inhibits fatty acid uptake and lipogenesis, insulin stimulates it causing weight gain.

T2DM can also be categorized as monogenic and polygenic forms. The monogenic forms are relatively rare but a number of causative genes have been characterized including mutations in insulin receptor, mutations in the peroxisome proliferator-activated receptor-γ (PPAR-γ), mutant insulin circulating as 9.39 kDa preinsulin instead of undergoing proteolytic cleavage that results in the 5.8 kDa insulin product. Several mutations that cause mature-onset diabetes of the young [MODY] have been identified, all occurring in the insulin producing pancreatic β-cells. Patients with monogenic T2DM can experience mild hyperglycemia of varying degrees or impaired glucose tolerance for years before onset of persistent hyperglycemia. Nongenetic factors that affect insulin sensitivity in other instances of T2DM do not play a significant role in the development of MODY.

The polygenic form of T2DM has a more complex pathophysiology, with both genetic and environmental factors playing a major role in development of disease. Obesity induced insulin resistance in muscle, fat and liver is present in predisposed patients for decades before development T2DM. Genetic mutations have been associated with T2DM and it is thought they synergize with the environmental factors, excess nutrition or lack of physical activity. For example, single nucleotide polymorphisms in a major negative regulator of insulin and leptin signaling, protein tyrosine phosphatase (PTP1B) have been associated with insulin resistance (Echwald 2002, Palmer 2004). Any combination of the genetic and environmental factors contributing to T2DM and obesity precede development of disease, which is precipitated when the pancreatic β-cells can no longer meet the burden from insulin resistance.

1.1.2. Complications of Diabetes

Diabetes leads to disease of macrovasculature by contributing to buildup of atherosclerotic plaques in arteries that supply the heart, brain and lower extremities. This can lead to infarcts and aneurisms. Overall, though the mechanism of macrovascular disease is different from that of hypertension, pathologically the effect of damage is the same. Importantly, it is more extensive and progresses faster in diabetics. By comparison, whereas approximately 30% of non-diabetic patients die due to atherosclerosis and this number is decreasing, an overwhelming 80% of deaths in diabetic patients are a result of atherosclerotic vascular disease, and unfortunately this number is rising. Unlike macrovascular disease, microvascular damage is specific to diabetes. Overall, risk of cardiovascular complications is up to 6 fold higher in diabetics.

The microvasculature to the retina, renal glomerulus and peripheral nerves are all affected by similar pathology. The initiating factor is chronic hyperglycemia leading to hyaline arteriolosclerosis. The extent and severity of the damage depends on the duration and the degree of uncontrolled hyperglycemia. The reason for the damage to endothelium is that these cells cannot downregulate glucose transport in the presence of high circulating glucose, and they develop intracellular hyperglycemia. Early in the course of disease hyperglycemia causes reversible abnormal blood flow and permeability in these microvessels, but progressive narrowing eventually leads to occlusion of the vascular lumina and the microvascular cells apoptose. As a consequence of the microvascular pathology diabetes mellitus is the leading cause of new blindness in people 20 years and older. Vision loss generally occurs from

persistent hemorrhage that cannot be cleared, macular edema or traction retinal detachment caused by neovascularization. More than 60% of type 2 diabetics develop some degree of retinopathy. The only effective prevention of retinopathy or its advance is intensive insulin therapy, which points to the strong need for better treatments of hyperglycemia and T2DM. Diabetes is also the leading cause of end-stage renal disease, these patients being the fastest growing group on dialysis and they constitute more than 50% of transplant recipients. Life expectancy for a diabetic with end stage renal disease is 3-4 years. Globally, most patients with diabetes are in developing countries with little access to dialysis. Diabetic nephropathy remains the major cause of morbidity and mortality for type 1 and type 2 diabetics. It is characterized by hypertension, protein in urine and ultimately impaired renal function. This is due to diabetic microvascular damage to the renal glomeruli, the basic filtration unit of the kidney.

Neuropathies are a heterogeneous group of disorders that can constitute paresis of the extremities, gastroparesis or gastroenterologic and genitourinary incontinence. Estimates for the prevalence of neuropathy indicate that about half of the patients tested had clinical symptoms such as pain or sensory/motor loss, and 90% tested positive on more specialized nerve tests, so it is a grossly underdiagnosed condition. The major morbidity associated with neuropathy is foot ulceration, a precursor to gangrene and limb amputation. In the US there are ~100,000 amputations/ year, so 1 every 10 minutes, with 87% of cases due to diabetic neuropathy.

1.1.3. Pharmacotherapy for Type 2 Diabetes

Since 1995 a revolution of sorts has started in the US as far as T2DM treatment goes. Drugs that independently target the different pathophysiologic mechanisms that contribute to diabetes have been generated. There are drugs aimed at treating hyperglycemia, which can be categorized by mechanism of action into: insulin sensitizers targeting liver, insulin sensitizers targeting peripheral tissues, insulin secretion enhancing drugs, agents that slow carb absorption. Clinically, the most commonly used drug for T2DM and the first line of therapy is a drug called metformin that sensitizes hepatic cells to insulin. If the severity of disease progresses and metformin is insufficient new drugs are added sequentially, leaving drugs with worse complications last.

1.1.3.1. Biguanide Drugs

Metformin reduces insulin resistance and causes moderate weight loss. Its main mechanism is activation of AMP-activated protein kinase (AMPK). It is thought that metformin transiently inhibits complex I of the electron chain in the mitochondria inducing a decrease in energy gradient. The resulting decrease in ATP and increase in AMP inhibits glucagon-induced cAMP synthesis and activates AMPK. AMPK is the main sensor of changes in cell energy and master coordinator of an integrated signaling network that comprises metabolic and growth pathways working in synchrony to restore energy balance in the cell. For example, AMPK increases insulin sensitivity by increasing activity of IR, IRS2 and translocation of glucose transporters in muscle. It normalizes glucose levels by inhibiting gluconeogenesis in liver. Metformin has the best tolerance among oral antihyperglycemic agents, although it does cause gastrointestinal issues such as nausea, diarrhea, abdominal cramps and taste distortion. It is cleared through renal metabolism and thus can only be used in patients that have not yet suffered irreparable damage to renal vasculature from persistent hyperglycemia. Metformin is the only biguanide available in the U.S., others have been removed as they caused fatal lactic acidosis.

1.1.3.2. Thiazolidinedione Class of Drugs

The thiazolidinedione class (TZD or glitazones) modulate the peroxisome proliferator-activated receptors (PPARs) in order to improve glycemic control, insulin sensitivity and decrease free fatty acid levels. The first TZD agent on the market was troglitazone, approved in 1997 but was withdrawn by 2000 as it was associated with fatal hepatotoxicity. Pioglitazone and rosiglitazone remained on the market although at this point a large population-based study has shown pioglitazone is associated with an increased risk of bladder cancer. Pioglitazone is associated with a 20% reduction in triglycerides, a modest improvement in HDL and LDL but also with a 63% increased risk of bladder cancer over the course of 14.5 years. The risk increases with duration of use and dose. In Europe, rosiglitazone has been taken off the market, as the benefit of treatment did not outweigh the associated risks of heart attacks and death. Although in the US this correlation was not illustrated with definitive data, the controversy has resulted in dramatic shifts away from prescribing rosiglitazone. The negative effects associated with rosiglitazone are weight gain and a slight increase in triglycerides of ~5%. The weight gain might be as a result of increased fluid retention and subcutaneous,

rather than abdominal/visceral fat, which was actually decreased, suggesting that the weight gain patients experience might not have negative health effects. Glitazones have the best track record in slowing β-cell deterioration, which is important for long-term prognosis. Their use early in disease is desirable because of the positive β-cell effects and because there is also a lower risk of heart failure due to fluid retention. However the long-term consequences are increased weight gain and possibly bone loss. Efforts to create safer agents with more selective effects continue.

1.1.3.3. Sulfonylurea Drugs

Drugs that increase insulin secretion bind to a subunit of the K_{ATP} channel, the sulfonylurea receptor (SUR1), on pancreatic β-cells. The channel normally behaves as a glucose sensor and insulin secretion trigger. Sulfonylurea binding leads to channel closure, followed by depolarization of the β-cells, opening of calcium channels causing an influx of calcium which leads to insulin secretion. Sulfonylureas have been available for over 50 years with both first- and second-generations available. They are the most cost effective and in recent trials on effects of intensive glycemic control on cardiac outcomes sulfonylureas were the only drugs without cardiovascular toxicity. Glinides have a shorter half-life and distinct binding site, producing a faster and brief increase in insulin secretion. This makes glinides a useful treatment for postprandial control of hyperglycemia. From a practical standpoint sulfonylureas are preferred because they require fewer doses and are lower cost than glinides.

1.1.3.4. Alpha Glucosidase Inhibitors

AGIs inhibit the last step of carbohydrate digestion at the intestinal brush border, shifting it more distally in the intestine, which allows for the slower insulin secretion of T2DM to catch up to absorption. One of the drugs in this class, acarbose, has been shown to improve cardiovascular outcomes more than most antihyperglycemic agents. This class of drugs has really shown only minimal effects on blood glucose reduction and as a result its use has been rather limited.

1.1.3.5. Insulin

Insulin, available since 1920, is arguably still the mainstay of therapy for most people with T2DM. Subcutaneous injection of insulin supplements endogenous production of insulin. In the basal state, long acting insulin modulates hepatic glucose production. In the postprandial state, shorter acting insulin facilitates glucose uptake into muscle and fat for storage and intraprandial metabolic needs. The main difference between the various formulations of insulin is their half-life according to which they can be used as basal or postprandial treatment. One issue with insulin treatment is that it causes weight gain and a high risk of hypoglycemia, the latter of which can be lethal.

1.1.3.6. Glucagon-Like Peptide-1 Agonists

GLP1-receptor expressed on pancreatic β-cells mediates insulin secretion in response to oral glucose. Its agonist, GLP1 is produced from the glucagon gene in intestinal L cells and secreted in response to nutrients. In addition, GLP1 slows gastric emptying, leading to slower absorption of carbohydrates and improved satiety sensing. GLP1 receptor agonists that mimic the natural effects of GLP-1 have been developed, as well as inhibitors of DPP4, the protease that degrades GLP1. The first generation was based on a naturally occurring component of the saliva of *H. suspectum* (gila monster) which has 53% sequence identity with GLP1 and is an effective agonist, but resistant to degradation by DPP4. GLP1 agonist is administered by subcutaneous injection twice-daily and results in ~1% reduction in HbA1c as well as modest weight loss of 5-10 lb/year. It is associated with nausea and hypoglycemia when co-administered with other insulin secretagogues as well as with pancreatitis. Newer generations can be administered more conveniently once daily or once per week, which has better adherence from patients. However the newer generations have been associated with medullary thyroid cancer in rodents, and as a result have not been used in patient treatment yet. DPP4 inhibitors produce a 2 fold increase in GLP, and improve glucose homeostasis as measured by an ~0.7% decrease in HbA1c and are just as well tolerated as placebo. A nice feature of these agents is weight neutrality, lack of hypoglycemia, and good tolerance. While anticipating positive effects on postprandial glucose homeostasis, β-cell survival and cardiovascular health, the reality is that their modest efficacy, cost and uncertain safety remain barriers to their clinical use.

1.1.3.7. SGLT2 Inhibitors

SGLT2 inhibitors are a novel class of T2DM drugs which in conjunction with diet and exercise can improve glycemic control. Sodium-dependent glucose co-transporters are responsible for 90% of glucose reabsorption in kidney. Inhibitors of SGLT2 increase glucose excretion and help lower circulating glucose levels. However in the short time that they have been used they have been associated with serious urinary tract infections and vaginal yeast infections, which in a diabetic with hyperglycemia can be even more difficult to cure than normal. There have also been incidents of ketoacidosis, an acute and if left untreated fatal condition normally associated with type I diabetes and rarely with type 2. There have also been associations with loss of bone density and a significant increase in bone fractures as early as 12 weeks after start of treatment, suggesting this is a severe effect.

1.1.4. Perspectives for T2DM Therapy

Diabetes and prediabetes are two of the most taxing health issues, both in the US and in the world. Overall, life expectancy is about 7-10 years shorter compared to people without diabetes due to increased mortality from diabetic complications. The rate of FDA drug approvals in response to the type 2 diabetes epidemic has been swift in recent years; just in the last 2 years as many as 9 new drugs have been approved. Yet the incidence of diabetes continues growing much faster than anyone predicted. Particularly worrisome is the increased prevalence of T2DM in children and adolescents. In this particular demographic hyperglycemia associated physiological changes could be devastating by the time they reach adulthood, and both quality of life and longevity will be negatively impacted. In spite of the treatments already available, the rise in incidence indicates that there remains a dramatic need for better treatments. Most of the current drugs are associated with serious side effects adding to the already existing concerns about T2DM symptoms. Historically drugs such as metformin, which enhance insulin signaling and glucose uptake, have been the most successful therapies of T2DM. Modulation of the kinase activity of the insulin receptor could be an alternative means to develop a treatment for T2DM. At the molecular level, insulin signaling is activated by trans-phosphorylation of the receptor in response to binding of the insulin hormone. Signaling is consequently terminated by dephosphorylation of the receptor by phosphatases. After trans-phosphorylation, it is the activity of phosphatases that controls the duration and amplitude of the cellular response to insulin. As such, control of the phosphatase activity would allow for

regulation of insulin signaling, and inhibition of the phosphatase would potentiate insulin signaling, essentially helping sensitize the cell to insulin. Most of the focus with drug development has been on kinases such as the insulin receptor and AMP-kinase, through which drugs such as metformin and insulin enhance glucose uptake. Inhibition of phosphatases that negatively regulate insulin signaling, such as PTP1B, is an alternative approach that would increase insulin sensitivity, thus targeting the primary cause of T2DM, insulin resistance.

1.2. Signal Transduction

Since its discovery in the 1950's, phosphorylation of proteins has been characterized as an important signaling mechanism involved in regulation of all aspects of cellular function including cell growth, differentiation, motility and proliferation (Krebs 1955). Meanwhile, abnormalities in phosphorylation due to mutations in phosphatases or kinases leading to signaling defects have been shown to underlie many disease processes. Fischer and Krebs identified reversible protein phosphorylation as a regulatory mechanism when they discovered that phosphorylation activates glycogen phosphorylase, the rate-limiting enzyme of glycogenolysis (Fischer and Krebs 1955). Protein phosphorylation is a reversible process that is controlled by two classes of enzymes: protein kinases and protein phosphatases, which carry out their functions in as coordinate manner to regulate the outcome of physiological stimulation as illustrated in Figure 1.1 (Cheng 2002). Kinases are enzymes that catalyze the transfer of a phosphate moiety from the γ-phosphate of adenosine triphosphate (ATP) onto target substrates. Phosphatases catalyze the hydrolysis of phosphate groups from phospho-protein substrates through a nucleophilic attack reaction. Phosphate removal by a phosphatase from a substrate can result in increase or decrease of the substrate's biological activity and the same is true for phosphate addition (Cohen 2002). Importantly, kinases and phosphatases are not simply antagonists to each other, but rather their mechanisms of catalysis, substrate recognition, regulation and kinetics of catalysis are precisely coordinated in order to achieve specificity.

1.2.1. Insulin signaling

Insulin signaling is initiated upon binding of the insulin hormone to the insulin receptor. The insulin receptor belongs to a subfamily of receptor tyrosine kinases that also includes the insulin-like growth factor (IGF-1R) and the insulin receptor-related receptor (IRR) (Patti 1998). The insulin receptor is a heterotetrameric complex, consisting of 2 extracellular α subunits that

bind insulin hormone and 2 transmembrane β subunits with tyrosine kinase activity. Insulin binding to the α subunits induces transphosphorylation of the β subunits on tyrosine residues in the activation loop. Following transphosphorylation by the β subunits on tyrosine 1162 and 1163, the receptor undergoes autophosphorylation of other tyrosine residues in the juxtamembrane regions and C-terminal tail.

The activated insulin receptor phosphorylates tyrosine residues on the insulin receptor substrate proteins 1-4 (IRS1-4) and others such as Gab-1, $p60^{dok}$, Cbl, APS and Shc isoforms. These phospho-tyrosine substrates then serve as docking sites for proteins that contain Src homology 2 (SH2) domains, many of which are adaptor molecules such as Grb2 and the p85 regulatory subunit of PI3K. Taking into consideration the divergent pathways downstream of the insulin receptor and the number of genes and protein isoforms for the substrates, it is reasonable to think of insulin signaling as a cascade that contains critical nodes. Activation of IRS proteins is a critical node, which leads to activation of the phosphatidylinositol 3-kinase (PI3K), followed by generation of phosphatidylinositol-3,4,5-triphosphate (PIP3) and activation of Akt/protein kinase B (PKB) which ultimately leads to control of metabolic function. The adaptor molecule Grb2 associates with son-of-sevenless, SOS, to activate Ras-mitogen-activated protein kinase (MAPK) pathway resulting in insulin-mediated control of cell growth and differentiation.

Generation of PIP_3 upon activation of PI3K activates other critical regulators of insulin signaling, and thus PI3K is another regulatory node in the insulin pathway. Proteins with pleckstrin homology (PH) domains such as the AGC superfamily of Ser/Thr kinases, guanine-nucleotide exchange factors of the Rho family and the TEC family of tyrosine kinases bind to PIP_3 and become activated. One of the most critical members of the AGC superfamily for insulin signaling is the 3-phosphoinositide-dependent protein kinase 1 (PDK1), as it phosphorylates Akt/PKB on Thr308 and activates it. Akt has been suggested to further propagate the insulin signal by phosphorylation of the enzyme Gsk-3, the forkhead transcription factors and cAMP response element-binding protein.

A second important pathway for insulin-stimulated glucose uptake is activated through tyrosine phosphorylation of Cbl which associates with the adapter protein CAP, and upon phosphorylation recruits the adapter protein CrkII to lipid rafts. CrkII forms a guanyl nucleotide-exchange protein, leading to activation of its substrate TC10, which serves as a second signal

to GLUT4 protein in parallel with PI3K (Saltier 2001). The ability of both the insulin receptor and IRS proteins to mediate cellular signaling in response to insulin is negatively regulated by the action of tyrosine phosphatases and by phosphorylation of serine residues as mentioned in the section on pathogenesis of diabetic disease.

1.2.2. Protein Tyrosine Phosphatases

Unlike the protein kinases, which are derived from a common ancestor, the protein phosphatases have evolved in structurally and mechanistically distinct families. Based on substrate specificity, protein tyrosine phosphatases (PTPs) are broadly divided into two groups: classical phosphatases, which remove phosphate groups from tyrosine residues and dual specificity phosphatases, which are able to accommodate, at least *in vitro,* phosphorylated tyrosine, serine and threonine residues in their active site, although *in vivo* their might be selective for just 2 of the 3 residues. Besides the protein phosphatases there are other phosphatases with different structural and functional features such as lipid phosphatases, alkaline phosphatases and acid phosphatases. The PTP superfamily shares a common, evolutionarily conserved signature amino acid motif HCX_5R in the catalytic site, in which the invariant cysteine and arginine residues are essential for catalysis. The classical PTPs recognize phosphotyrosyl residues exclusively as their substrate and can be further sub-classified on the basis of cellular localization as transmembrane and cytosolic PTPs (Figure 1.2). The transmembrane PTPs control phosphorylation in response to extracellular stimuli. The activity and specificity of non-transmembrane PTPs is controlled by subcellular localization and by regulatory domains.

In light of the prevalence of tyrosine kinases with oncogenic function, and the role of phosphatases to reverse the phosphorylation modification of kinases, it was long thought that tyrosine phosphatases would be identified as tumor suppressors. Protein tyrosine phosphatases have been shown to function as both inhibitors and positive regulators of phospho-tyrosine dependent signaling (Figure 1.3). Inactivating and missense mutations of PTPs with tumor suppressor role have been detected in several cancers. Some phosphatases such as PTEN and DEP1 have been characterized as bonafide tumor suppressors that function as negative regulators of signaling. There are also some PTPs that act as positive, signal-enhancing, regulators. For example, the phosphatase SHP2 has been characterized to play an oncogenic role in leukemia through a gain of function mutation (Mohi 2007). Overall, the PTP

superfamily coordinates regulation of phosphorylation with tyrosine kinases to control numerous signaling pathways in physiological processes.

1.2.3. Therapeutic Targeting of Kinases and Phosphatases

Efforts to therapeutically modulate disease processes have targeted both kinases and phosphatases. At this point in time there are more kinase than phosphatase inhibitors in clinical use, although a large part of the lag in the development of drugs that target phosphatases is simply timing. The first phosphorylation of a protein was described in 1954, whereas the first phosphatase was not published until 1988 (Tonks 1988a, Cohen 2002). By 1980 the oncogenic role of some protein tyrosine kinases had been identified and rational drug discovery efforts started. During the last 35 years the field of research for both kinases and phosphatases has advanced in strides. On the kinase side, there are over 30 kinase inhibitors in clinical use and over 100 in phase 2 and 3 clinical trials. Dysfunction of tyrosine kinases as a result of mutations is a molecular event that frequently contributes to initiation or progression of cancer and other diseases. At this point kinase domains have been targeted and successfully drugged. Initially there was doubt as to the feasibility of successfully targeting kinases due to a high degree of similarity in their active site. The expectation was that inhibitors would not be selective enough and they would be associated with too many unwanted side effects. There have been selective inhibitors generated, such as Ruxolitinib, which selectively targets JAK1 and JAK2 (Cervantes 2013). However, the majority of kinase inhibitors used clinically are relatively unselective and can target several kinases (Karaman 2008). For example imatinib, the first small molecule kinase inhibitor was approved by the FDA as an inhibitor of the Bcr-Abl kinase in chronic myelogenous leukemia. The lead compound for imatinib was actually a hit from a screen for inhibition of PKC. Chemical modification generated an inhibitor of Bcr-Abl, which in the last 25 years has also been approved for the treatment of diseases with underlying mutations in c-Kit and PDGF receptor. The poly-selectivity of kinase inhibitors has actually become more a benefit rather than a detriment. Lessons from kinases can be useful in the phosphatase field, particularly in the search for small molecule inhibitors. Considerable interest and effort has been dedicated to PTP inhibition, with several PTPs validated as causes of disease and potential drug targets. PTP1B in particular has been targeted in the development of therapeutics for diabetes and obesity based on its role in mediating insulin and leptin signaling. Thus far investigations have yielded high affinity inhibitors targeting the active site of PTP1B, but because they target the active site they are phosphotyrosine-mimetics and therefore highly

charged. Charged molecules have reduced ability to permeate membranes and to be absorbed intestinally, resulting in poor oral bioavailability which is the required standard in industry for treatment of T2DM. Developing inhibitors with better physical and chemical properties will allow for clinically effective phosphatase inhibition, and if targeting the active site is difficult, finding alternative mechanisms or sites of inhibiting phosphatases is necessary. This is an area of the phosphatase field that our lab has been actively working on.

1.2.4. PTP1B

PTP1B was the first protein tyrosine phosphatase to be purified to homogeneity; it was isolated from human placenta tissue as a 37 kDa catalytic domain (Tonks 1988a, Tonks 1988b). The purified protein demonstrated specificity and high affinity for phosphotyrosyl substrates and showed no phosphatase activity on phosphoseryl and phosphothreonyl substrates (Tonks 1988b). Determination of its amino acid sequence led to isolation of cDNA, which indicated that PTP1B contains 435 amino acid residues, an ~ 50 kDa protein (Charbonneau 1989, Brown-Shimer 1990, Chernoff 1990, Guan 1990). The N-terminal 321 residues compose the catalytic domain, which is then followed C-terminally disordered region and by a membrane localization domain, which anchors it on the cytoplasmic side of the ER membrane (Frangioni 1992).

The crystal structure of the 37 kDa catalytic domain of PTP1B shows that it forms a single globular domain consisting of 8 α-helices and 12 β-strands, with the majority of the β-sheets forming the core of the molecule and the surface exposed α-helices connecting between the β-sheets (Figure 1.4) (Barford 1994a, Barford 1994b). This structural arrangement of the catalytic domain is conserved within the PTP family. A comparison of the primary sequences indicates that most of the conserved residues are found closer to the core of the molecule, whereas the less conserved are found on the surface of the protein on the loops connecting the secondary structure motifs.

The catalytic site is located within a crevice on the molecule as marked by the essential cysteine residue. The main feature of the catalytic site is the presence of the signature motif [I/V\HCXAGXXR[S/T]G, conserved throughout the classical PTPs, that forms a rigid structure which coordinates the aryl-phosphate moiety of the substrate (Barford 1994a, Tonks 2003). The cysteine at residue 215 is part of the catalytic cleft and carries out a nucleophilic attack reaction on the phospho-substrate (Barford 1994a). Three other motifs are important in defining

the sides of the catalytic cleft. The WPD loop, composed of tryptophan179, proline180 and aspartic acid181, and the Q loop contribute to the catalytic process (Tonks 2006). Tyr46 in the pTyr loop contributes to substrate selectivity by defining the depth of the active site cleft as 8-9Å, so only tyrosine residues are long enough to reach the Cys215 buried in the catalytic cleft compared to the shorter serine and threonine residues (Tonks 2006).

1.2.5. Catalytic Mechanism of PTP1B

Crystallographic studies into substrate recognition revealed insights into the catalytic mechanism of PTP1B and its open and closed conformations (Barford 1994a, Jia 1995). In the open conformation the binding pocket is accessible to substrate. Substrate binding leads to induced fit with the WPD loop closing around the phospho-Tyr residue and over the active-site binding pocket. In the first step, Cys215 at the base of the active site cleft acts as a nucleophile and attacks the phosphate on the pTyr-substrate (Jia 1995). As the phosphate is captured by the PTP1B thiol, the tyrosine of the substrate is protonated by Asp181 of the WPD loop, which behaves as a general acid in this reaction (Jia 1995). In the second step, the phosphate group is hydrolyzed off the cysteinyl of PTP1B, mediated by Gln262, which coordinates a water molecule for nucleophilic attack and Asp181, which now functions as a general base (Jia 1995, Pannifer 1998). Substrate hydrolysis also regenerates the enzyme back to its active conformation, such that it can dephosphorylate again.

1.2.6. Redox Regulation of PTP1B

Redox regulation has been demonstrated as a mechanism for the modulation of PTP function in response to physiological stimuli (Meng 2004, Salmeen 2005). Under basal conditions when ROS levels are low, PTP1B suppresses the tyrosine phosphorylation and activation of the receptor PTK and acts as negative regulator of signaling. As illustrated in the model in Figure 1.6, insulin stimulation and activation of the insulin receptor tyrosine kinase triggers generation of a burst of intracellular H_2O_2 through Rac-dependent NADPH oxidase assembly at the membrane in insulin-sensitive cells. This H_2O_2 leads to transient and reversible oxidative inhibition of phosphatase activity of PTP1B, thereby promoting tyrosine phosphorylation (Mahadev 2001, Meng 2004). The presence of ROS in response to insulin signaling is transient with production tightly controlled by NOX enzymes and degradation regulated by peroxiredoxins (Mahadev 2004). Chronic production of reactive oxygen species

(ROS) is a common feature of several diseases, including diabetes and obesity (Newsholme 2007). A natural product of mitochondrial oxidative phosphorylation, superoxide ($O_2^{\bullet -}$) is normally converted by superoxide dismutase to hydrogen peroxide (H_2O_2). H_2O_2 is subsequently converted to water by antioxidant enzymes such as glutathione peroxidase, peroxiredoxins or catalase. The chronic uptake and oxidation of fatty acids and glucose that occurs in obesity is thought to result in increased mitochondrial generation of superoxide and hydrogen peroxide. Oxidative stress has been linked to promotion of insulin resistance in humans and rodents (Anderson 2009).

Localization of PTP1B at the ER-membrane contributes to regulation of its function by subcellular location and restricts the spectrum of substrates to which it has access. Proteolytic cleavage of PTP1B with calpain generates a 42 kD form of the enzyme by cleaving a 75-residues C-terminal peptide (Frangioni 1993). This truncated for of PTP1B exhibits enhanced phosphatase activity, suggesting the C-terminal portion serves a regulatory role, either through subcellular localization or through manipulation of catalytic activity. Studies have shown that PTP1B anchored in the ER-membrane comes into contact with the activated receptor tyrosine kinases such as EGFR, PDGFR as well as IR when they are internalized, a prerequisite for the interaction (Haj 2002, Cromlish 2006). This mechanism indicates that RTK inactivation by PTP1B is spatially and temporally partitioned within cells with the IR being dephosphorylated at perinuclear patches, presumably on the endocytotic compartment (Romsicki 2004, Haque 2011). Unpublished data from the Tonks lab shows that the peptide anchoring PTP1B to the ER-membrane is required for redox regulation of PTP1B in response to insulin stimulation. Expression of full length PTP1B and the truncated catalytic domain (1-321) with an ER-anchoring peptide (C-terminal 35 residues of PTP1B) are both oxidized in response to insulin and both forms of the protein are bound by scFv45. Very little interaction was observed between cytoplasmic PTP1B (1-321) expressed without an ER-membrane anchoring peptide and scFv45, even if the cells were treated with H_2O_2.

Cysteine has a normal pKa of ~ 8, however in the active site cleft of PTP1B the surrounding charged residues create a low pKα of 4.5-5.0 that renders the cysteinyl predominantly in the thiolate form (Lohse 1997). The thiolate form makes the active site cysteine a strong nucleophile in catalysis, but it also renders it susceptible to oxidation. It has been reported that several PTPs are transiently oxidized by H_2O_2, and that this is important for optimal tyrosine phosphorylation in response to physiological stimuli (Lee 2002, Meng 2002,

Savitsky 2002). Mild oxidation of the active site cysteine of PTP1B produces a sulphenic acid intermediate that is inactive and rapidly converts to a 5-atom cyclic sulphenyl-amide that is reversible under reducing conditions. In order to maintain reversibility, the active-site cysteine can be oxidized no further than to sulphenic (SOH), as higher oxidation to sulphinic (SO_2H), or sulphonic (SO_3H) acid is irreversible (Figure 1.7) (Sundaresan 1995, Denu 1998, Meng 2002).

Formation of the cyclic sulphenyl-amide breaks critical hydrogen bonds that stabilize Cys215 and Ser216 and triggers residues to flip out from the cleft of the active site and become solvent exposed. This causes a profound conformational change in the active site, which protects PTP1B from irreversible oxidation and exposes the oxidized Cys215 closer to the protein surface, facilitating reactivation by cellular reducing agents (Figure 1.8) (Salmeen A 2003, Van Montfort 2003). Exposure of alternate residues to the surface in the context of the conformational change also exposes new surfaces that we can attempt to target therapeutically. If we could stabilize PTP1B generated by reversible oxidation in the transiently inactive conformation, signaling can be potentiated in PTP1B substrates. A mutant form of PTP1B containing Cys215 to Ala and Ser216 to Ala mutations (PTP1B-CASA) was generated for crystallographic analysis and as expected it adopted a stable conformation identical to that of reversibly oxidized PTP1B since the 2 hydrogen bonds that normally stabilize the active site were disrupted (Haque 2011).

1.2.7. PTP1B in Signaling and Disease

PTP1B has been characterized as an enzyme that can play both a negative and positive role in diverse signaling pathways-which is to say that substrate dephosphorylation can have either an inactivating or an activating effect, depending on the substrate and signaling pathway (Figure 1.3). Biochemical studies have implicated PTP1B in multiple signaling pathways, through the dephosphorylation of several receptor kinases, including IR, EGFR, PDGFR, IGF1R (Ahmad 1995, Kenner 1996, Flint 1997, Elchebly 1999, Buckley 2002, Haj 2002). PTP1B also rephosphorylates non-transmembrane tyrosine kinases such as Src, p210Bcr-Abl, JAK2, TYK2 and transcription factor STAT5 (LaMontagne 1998, Bjorge 2000, Myers 2001, Cheng 2002, Zabolotny 2002, Gu 2003).

Table 1: A Summary of Validated Substrates of PTP1B

Receptor Tyrosine Ki	Cytoplasmic Tyrosine Ki	Transcription Fa
Insulin Receptor β	IRS-1	STAT5a
EGF Receptor	c-Src	Stat6a
PDGF Receptor	p210Bcr-Abl	
IGF1 Receptor	JAK2	
	TYK2	
	Fak	

PTP1B plays an important role in the regulation of both insulin and leptin signaling (Elchebly 1999, Cheng 2002, Zabolotny 2002). Due to this role as a negative regulator in type 2 diabetes and obesity, and its positive role in cell proliferation as a positive effector in ErbB2 signaling in breast cancer, the development of inhibitors of PTP1B has become a high priority in the pharmaceutical industry for the treatment of diabetes and obesity as well as an adjuvant therapy in breast cancer. Through its role as a negative regulator of metabolism PTP1B has recently been implicated as a therapeutic target in the treatment of Rett syndrome, a MECP2 linked neurological disorder (Krishnan 2015). The gene for PTP1B (PTPN1) is a target of MECP2, an epigenetic factor that regulates chromatin structure and therefore expression, and its mutation in Rett syndrome, leads to increased levels of PTP1B protein.

PTP1B has been shown to be a specific regulator of multiple tyrosine phosphorylation-dependent pathways in a context dependent manner. PTP1B behaves as a tumor suppressor in limiting transformation with certain kinases, with PTP1B overexpression diminishing v-src, Bcr-abl and Neu induced transformation in cells (Brown-Shimer 1992, Woodford-Thomas 1992, LaMontagne 1998). By comparison PTP1B does not behave as a suppressor of tumorigenesis in cells infected with v-fms or v-ErbB (Lammers 1993). This suggests that PTP1B exerts its suppressive effects by targeting *specific* oncogenic pathways. In the context of ErbB2 cancers, mouse models expressing the activated ErbB2 and PTP1B-null exhibited significant delay in tumor development and decreased incidence of lung metastases (Bentires-Alj 2007, Julien 2007). These studies illustrated a positive effect for PTP1B in ErbB2 tumorigenesis. In normal breast cells PTP1B attenuates the Ras/MAP kinase pathway via the adaptor protein p62Dok.

1.3. PTP1B Signaling in Diabetes

1.3.1. PTP1B in Insulin Signaling

The physiological role of insulin is to promote anabolic metabolism. As such it promotes synthesis and storage of lipids, protein and carbohydrates, and inhibits their breakdown and release in circulation. Insulin induces activation of the insulin receptor tyrosine kinase through autophosphorylation of the β subunit in the activation loop and subsequently in the juxtamembrane and the tail regions (Saltiel 2002). Recruitment and phosphorylation of insulin-receptor substrate (IRS) proteins induces activation of phosphatidylinositol 3-kinases (PI3K). PI3K activation triggers downstream effectors, such as phosphatidylinositol-dependent kinase 1 (PDK1) and protein kinase B (PKB/Akt), leading to translocation of glucose transporter 4 (GLUT4) and glucose uptake in muscle and adipose as well as inactivation of glycogen-synthase kinase 3 (GSK3) (Bryant 2002). PTP1B dephosphorylates membrane-bound or endocytosed insulin receptors, therefore playing a negative, inhibitory role in the signaling events downstream of the insulin receptor (Haj 2002).

The first report of insulin signaling regulation came with experiments in which microinjection of PTP1B into *Xenopus* oocytes inhibited insulin-induced kinase activation and cell transition through G2/M phase checkpoint (Cicirelli 1990). Osmotic loading of neutralizing antibodies to PTP1B into hepatoma cells increased insulin induced phosphorylation and activation of IRβ and IRS-1 substrate (Ahmad 1995). Ultimately it was the phenotype of PTP1B knockout mice that demonstrated its major role in modulating insulin sensitivity and metabolism, establishing PTP1B as a therapeutic target in T2DM and obesity. Importantly, the PTP1B knock out mice indicated that inhibiting PTP1B therapeutically would not be associated with harmful effects as the mice are healthy and fertile. Elchebly *et al*. was the first to report that PTP1B-null and heterozygous mice are resistant to development of T2DM and obesity when fed a high-fat diet compared to wild type mice, which gain weight and develop insulin resistance (Elchebly 1999). The PTP1B -/- and +/- mice have lower blood glucose concentrations and 50% the insulin concentration of wild type littermates, indicating enhanced insulin sensitivity. Insulin and glucose tolerance tests also indicated improved tolerance in PTP1B -/-, with sustained phosphorylation of IRβ in liver and increased phosphorylation of IRβ and IRS1 in muscle tissue compared to wild type mice. Subsequently Klaman *et al.* showed that PTP1B-/- mice have increased basal metabolic rate and energy expenditure leading to protection from diet-induced

obesity. These PTP1B-/- mice are also leaner and have smaller fat deposits, which is due to reduced adipocyte mass, rather than a change in adipocyte number. To analyze the effect of PTP1B inhibition in mouse models of obesity induced T2DM antisense oligonucleotides were used to knock down PTP1B (Zinker 2002). Similar to the PTP1B -/-, antisense mediated knockdown of PTP1B improved insulin sensitivity, glucose homeostasis and HbA_{1c}. Each of these mouse model experiments of PTP1B elimination contributed to establishing PTP1B as a major therapeutic target in diabetes and obesity.

Hamster models fed a fructose diet developed insulin resistance and increased expression of hepatic PTP1B, whereas PTP1B expression is reduced in fasted mice (Taghibiglou 2002, Gu 2003). Notably, enhanced PTP1B expression has been reported in studies of insulin-resistant patients (Cheung 1998). A decrease of PTP1B expression in adipose tissue was observed following weight loss in obese patients accompanied by improved insulin sensitivity (Ahmad 1997). Tissue specific knockouts of PTP1B in brain, liver, and skeletal muscle indicate that while they all improve insulin sensitivity and glucose tolerance, weight gain is primarily controlled in the brain, specifically in pro-opiomelanocortin neurons in the hypothalamus with contributions from the rest of the body (Bence 2006, Delibegovic 2007, Delibegovic 2009, Banno 2010). Crystallographic and kinetic studies provided clear evidence that PTP1B preferentially dephosphorylates tyrosine residue 1162 of the insulin receptor β subunit (Salmeen 2000). Due to its role as a major negative regulator of insulin signaling in both diabetes and obesity PTP1B is a desirable target for therapeutic development. Animal studies also helped establish PTP1B inhibition as a therapeutic approach in T2DM that could avoid all the negative effects associated with current treatments such as weight gain, hypoglycemia, nausea or other GI symptoms.

1.3.2 Role of PTP1B in Leptin Signaling

Leptin signaling is initiated when leptin, a hormone mostly secreted by white adipose, binds to the leptin receptor leading to a conformational change followed by association and phosphorylation with its co-activator JAK2. The signal is then propagated through phosphorylation of the transcription factors STAT3 and STAT5 and their translocation into the nucleus where they activate transcription of POMC and inhibit the agrp promoter. The physiological effects of POMC expression and AgRP suppression are reduction of food intake, increased energy expenditure and decreased body weight; the role of leptin translates to

maintenance of energy balance. Like insulin signaling, leptin also activates PI3K and Akt through IRS, resulting in control of POMC expression through ATP-sensitive channels. The main mechanism of leptin signaling at the molecular level is tyrosine phosphorylation of JAK2. PTP1B and TCPTP are both negative regulators of leptin signaling. PTP1B-null and heterozygous mice established PTP1B as major negative regulator of leptin signaling as they are resistant to diet-induced obesity (Elchebly 1999, Klaman 2000, Zinker 2002).

The resistance of PTP1B-null mice to obesity on a high-fat diet was the first indication that PTP1B is a negative regulator of leptin signaling. PTP1B substrate-trapping mutants bound to JAK2, and not to the leptin receptor or STAT3, and PTP1B overexpression induced dephosphorylation of JAK2, a co-activator of the leptin receptor (Myers 2001, Ahima 2004). Conversely, PTP1B deletion is associated with hypersensitivity to leptin hormone in mice, as well as increased phosphorylation of JAK2, and its downstream substrate STAT3 (Cheng 2002, Zabolotny 2002). Mouse models containing double knock-out alleles of the leptin receptor and PTP1B weighed less than the leptin receptor-deficient mice, indicating that the substrate of PTP1B in this signaling pathway was JAK2 and STAT2, rather than the receptor, as it is in the case of insulin signaling (Cheng 2002, Zabolotny 2002). Leptin hormone administration was never considered as therapy because circulating leptin is high in obesity and because it is thought very little would cross the blood brain barrier to reach the hypothalamus, which is where leptin signaling is most prominent. Instead inhibition of PTP1B, the negative regulator of leptin signaling became of greater interest as an alternative or a supplement to leptin treatment of obesity.

The PTP1B-/- mouse model established PTP1B as a valid therapeutic target. Characterization of its role as a negative regulator in both insulin and leptin signaling validated the benefits of finding a small molecule inhibitor. As the initial approach to develop inhibitors to the active site had been difficult due to poor oral bioavailability our lab sought to take an alternative approach. This alternative approach harnessed the redox regulation of PTP1B in response to insulin signaling. In order to explore mechanisms by which oxidized PTP1B may be selectively targeted our lab used phage display to identify an antibody that specifically recognized the reversibly oxidized conformation of PTP1B.

1.4. Phage Display Approach to a PTP1B Inhibitor

Avian antibodies were generated by immunization of a chicken with PTP1B-CASA, which adopts the same conformation as oxPTP1B (Haque 2011). One benefit of using avian species is that PTP1B is less conserved than in mammalian species increasing the chances of a strong immune response. The RNA encoding the functional antibodies was subsequently used to generate a phage display library which was screened for an antibody that is conformation sensitive and selectively binds PTP1B-CASA and oxPTP1B over reduced PTP1B (Haque 2011).

1.4.1. Antibody Structure and Function

The physiological function of antibodies involves specific binding to antigens and activation of other components of the immune system to fight pathogens. Antibodies are immunoglobulin glycoproteins, consisting of four polypeptide chains: two identical heavy chains and two identical light chains (Figure 1.9). They can be classified into different types on the basis of their constant domains, such as IgM, IgD, IgA, IgE and IgGs in mammals. Disulfide bonds and non-covalent interactions hold the structure together. In the tertiary structure the variable domains are in the N-terminal portion of both the light and the heavy chains and form the antigen-binding region, called the paratope. In a N to C-terminal direction each antibody contains variable (V), diverse (D), joining (J) and constant (C) regions. Within each variable domain there are six hypervariable regions, which are known as the complementarity determining regions (CDRs); these portions and the frame-work regions around them are mainly responsible for antigen recognition. C-terminally, the constant domains typically mediate activation of effectors after antigen recognition and binding.

In normal immune response a process of molecular diversification occurs through somatic recombination that rearranges the cassettes in the CDR of both light and heavy chains. Typically the V(D)J cassettes recombine to create the diversity in the CDR which is then tested for optimal antigen binding by the immune cells. Antibody maturation in avian species in addition undergo multiple gene conversion events in which blocks of sequences from pseudogenes upstream are inserted into the V(D)J cassette essentially increasing sequence diversity (Reynaud 1987, Reynaud 1989).

Antibodies are modular molecules that can be separated into domains by proteolytic digestion or expressed recombinantly. There are two Fab fragments within an antibody, containing the entire light chain (V_L) and one variable and one constant domain of the heavy chain (V_H and C_H); notably it maintains antigen-binding properties of the full-length antibody (Figure 1.9). The Fc is formed by the C_H chains connected by disulfide bonds and has no antigen binding sites; it normally plays an important role in stabilizing the antibody and activating the immune response such as complement and other immune cells. The smallest functional antigen-binding fragment is a fragment variable, Fv, and it contains the variable light and the variable heavy globular domains. This molecule is difficult to generate by proteolytic cleavage, but can be recombinantly generated from cDNA through ectopic expression. A single chain variable fragment, scFv, contains the 2 variable regions artificially joined with a flexible peptide linker, of varied length. The length of the linker can favor a diabody if as short as ~7 residues or a monomer with 15 or more residues.

Antibody fragments can be expressed readily in *E.coli,* which is fast growing and produces considerable amounts of protein. However scFv expression can be difficult, as most scFvs tend to form inclusion bodies in *E.coli.* Strategies to maintain their solubility include optimization of growth conditions, secretion to the periplasmic space via N-terminal signal peptide, co-expression with chaperones, or solubility-enhancing tags such as maltose binding protein (MBP).

1.4.2. Phage Display Identification of scFv45, a Conformation-Sensing Antibody

In phage display a gene is introduced through a phagemid, which results in expression of a polypeptide onto the surface of the phage, linked to a surface protein. This technique, therefore, links the phenotype with the genotype. The phage library tested for conformation-sensing antibodies to oxPTP1B was a collection of phage particles each representing a distinct recombinant antibody fragment (scFv) expressed in fusion with a phage surface protein (pIII). To increase the diversity of the antibody library two types of scFv constructs were generated, one with a short linker sequence (GGSSRSS) and one with a longer linker (GGSSRSSSSGGGGSGGGG) and mixed together generating a library of $2x10^7$ total clones. These linkers became important in the process of expressing the scFvs for crystallography as described in Chapter 2.

The first rounds of selection were to enrich for scFvs that bound epitopes only present on oxPTP1B, and sought to eliminate scFvs that bound epitopes common to both reduced and oxidized PTP1B. Five rounds of subtractive panning were performed using N-terminally biotinylated PTP1B-CASA in the presence of increasing molar excess of non-modified PTP1B-WT in a reducing environment. The presence of reduced PTP1B-WT ensured selection against scFvs that bound epitopes common to the reduced and oxidized forms of PTP1B. Sequencing demonstrated selective enrichment of phage expressing scFvs specific for PTP1B-CASA, with the diversity among sequences decreasing from 70% to 20 % over 5 rounds of panning. In the second round of panning the phage clones that bound were tested for functional ability to inhibit reactivation of oxidized PTP1B. First, scFvs were tested to ensure they had no inhibitory effect against PTP1B-WT under reducing conditions. Secondly, scFvs were screened for their ability to stabilize oxPTP1B and prevent its reactivation by reducing agent. ScFv45 was characterized to inhibit reactivation of oxPTP1B by ≥70% (IC_{50} 19nM), reflecting its ability to stabilize and inhibit the activity of PTP1B. In response to insulin stimulation, expression of scFv45 in mammalian cells such as 293T potentiated insulin signaling by increasing the phosphorylation of IR and downstream effectors IRS, PI3K, PDK1 and Akt (Haque 2011). This indicated that scFv45 is able to find the pool of PTP1B that negatively regulates insulin and leptin signaling, and which is redox regulated in the context of insulin and leptin receptor activation.

1.5. Rationale of Project

There has been considerable interest in harnessing PTP1B as a therapeutic target for diabetes and obesity after its important role as a negative regulator of insulin and leptin signaling had been elucidated. Drug development has particularly focused on small molecule inhibitors that bind the active site pocket identified by *in vitro* screens (Combs 2010). Since the active site is highly charged, the candidate inhibitors are also polar, charged molecules with poor oral bioavailability. Furthermore, as the active site is highly conserved among PTPs, including PTP1B and TCPTP, it has speculated that it would be difficult to design a specific PTP1B inhibitor that selectively targets the active site to the exclusion of other PTPs.

Reversible oxidation causes profound conformational change at the active site of PTP1B, generating a form of PTP1B in which unique potential binding surfaces for inhibitors are presented. Our lab has demonstrated that conformation-sensor antibodies are able to distinguish between the reduced and oxidized forms of PTP1B, and specifically bind and

stabilize oxPTP1B. If the interface of interaction between scFv45 and oxPTP1B is elucidated, it will guide development of scFv45-mimetic molecules, either by de-novo design, optimizing lead compounds from screens or compounds from in silico screens.

The prevalence of type 2 diabetes has increased at a fast rate in the last 50 years, in large part in a direct relationship to increase in body mass index and obesity. The consistent increase in prevalence highlights that our current therapies, dietary and lifestyle interventions alone are not effectively combating what is becoming an epidemic. From a healthcare perspective, the most striking are the comorbidities associated with diabetes ultimately leading to reduction of functional status in patients due to physical and cognitive disability. The most common complications associated with T2DM consist of cardiovascular disease, stroke, peripheral neuropathy, vision loss, kidney failure, amputation of limbs and cognitive loss. In addition, the incidence of childhood obesity has overcome that of T2DM in developing countries, which will only worsen the epidemic. These increases in prevalence emphasize a need for new and more effective therapeutic approaches. Current treatments focus on glycemic control and minimizing vascular complications, as well as attempts at lifestyle changes. An alternative approach, targeting PTP1B, a key negative regulator of insulin signaling at the level of the insulin receptor and insulin receptor substrate proteins would provide a much needed therapy that targets the root of the disease: insulin resistance. Inhibition of PTP1B would potentiate insulin signaling, possibly completely eliminating the need for therapeutic glycemic control and revolutionizing the treatment of type 2 diabetes.

The first line of therapy, metformin, enhances insulin sensitivity in muscle and fat, while inhibiting hepatic glucose release. If metformin at a maximum tolerated dose does not maintain glucose homeostasis a 2nd line drug is added, such as a sulfonylurea, thiazolidinedione, dipeptidyl peptidase inhibitor, sodium-glucose co-transporter inhibitor or glucagon-like peptide receptor agonist are added. Each of these medications has their own side effects, such as hypoglycemia, edema, heart failure, fractures, gastrointestinal or genitourinary problems and weight gain. If in spite of lifestyle changes, metformin and 2nd line therapies patients are still unable to achieve good glucose homeostasis insulin or another of the 2nd line therapeutics listed above is added depending on the patient's risks. The treatment cocktail and dose can be altered, however in reality the risk of hypoglycemia and other side effects make treatment difficult, and often it is further complicated by obesity.

Insulin signaling is terminated by PTP1B and TCPTP dephosphorylating the insulin receptor and some of its downstream substrates. PTP1B knock out mice are hypersensitive to insulin and normalize blood-glucose levels at lower insulin concentrations. We have shown that scFv45 binding to oxPTP1B potentiates insulin signaling. Identifying small molecules that mimic the effects of scFv45 on oxPTP1B would prolong insulin signaling and thus sensitize cells to insulin. They could constitute a sought after novel inhibitor of PTP1B and importantly a needed treatment for T2DM and obesity.

The overall aim of my project was to characterize the mechanism of interaction between scFv45 and oxPTP1B. I proposed to co-crystallize scFv45 and oxPTP1B to analyze the molecular interaction between the two molecules. Alternatively I proposed to use mutagenesis and binding assays to dissect the molecular basis of recognition between the two proteins. Ectopic expression of scFv45 in 293T cells led to potentiation of insulin signaling. I proposed to investigate alternative cell systems, which are physiologically relevant to insulin.

The specific aims of my thesis are as follows:

1. To determine the molecular mechanism for recognition of oxPTP1B by scFv45
2. To determine the functional effect of PTP1B inhibition via scFv45 stabilization on insulin signaling in a physiologically relevant cell model.

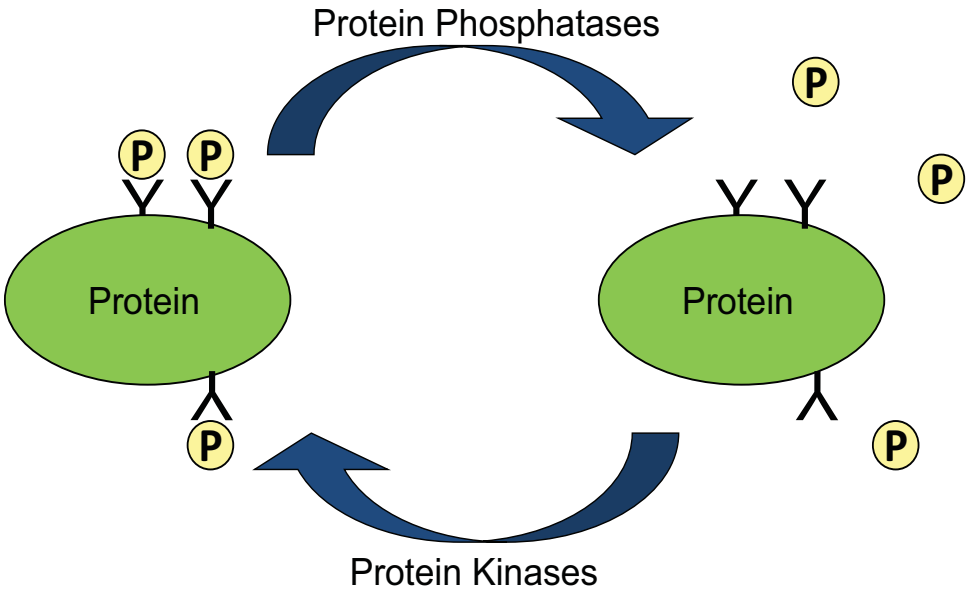

Figure 1.1 Reversible Phosphorylation of Proteins. Protein phosphorylation is one of the major signal transducing mechanisms in cells. Two groups of enzymes control the protein phosphorylation staes: the protein kinases and the protein phosphatases. The kinases transfer phosphate groups from ATP to protein and the protein phosphatases catalyze the removal of phosphate groups.

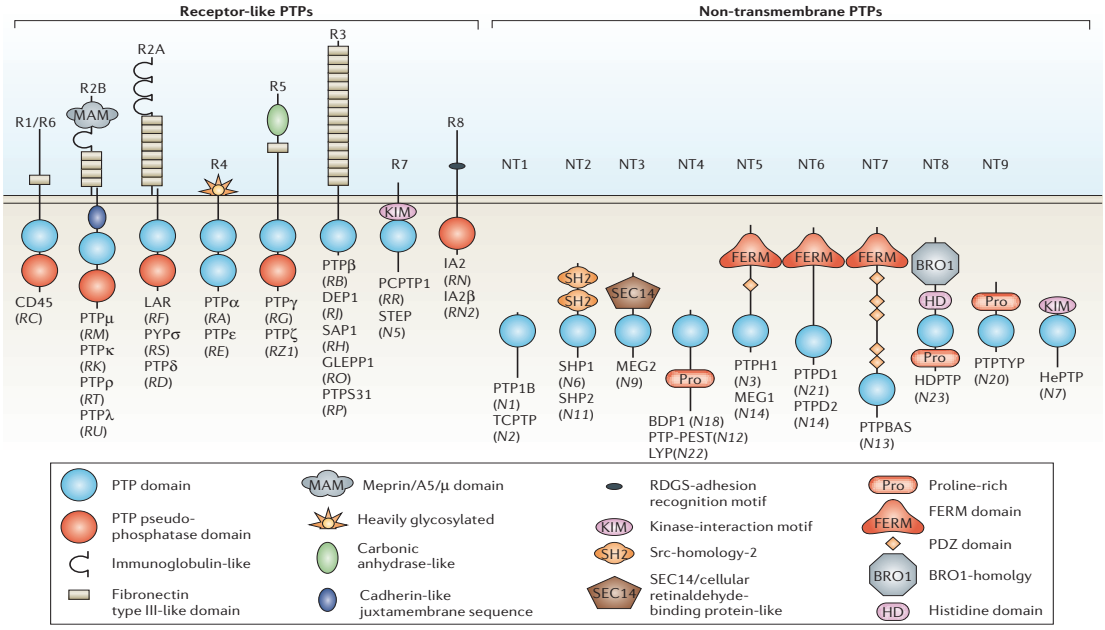

Figure 1.2 The Classical Protein Tyrosine Phosphatases (PTPs). The classical PTPs are divided into 2 broad groups-the transmembrane receptor-like proteins (RPTPs) and the non-transmembrane (NT) cytoplasmic proteins (Tonks 2006). The PTPs are structurally and functionally different from the Ser/Thr phosphatases. They are defined by the presence of a signature motif in the catalytic core, in which Cys and Arg are essential for catalysis. Receptor-like PTPs can regulate cellular signaling by ligand-controlled dephosphorylation of tyrosine residues on substrate proteins whereas non-transmembrane PTPs dephosphorylate their substrates at specific locations in the cytoplasm.

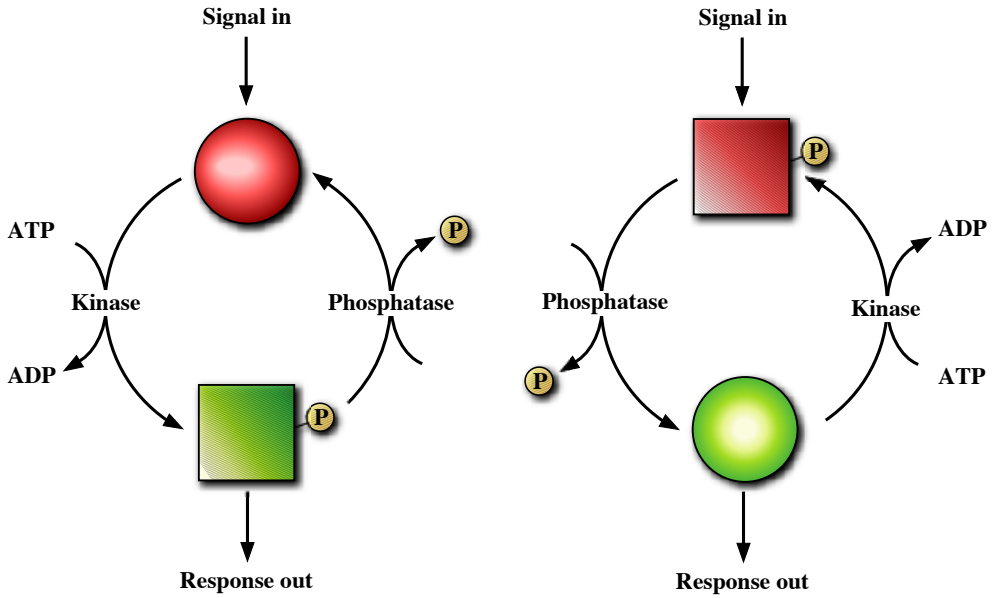

Figure 1.3 Alternative Function of PTPs in Signaling. PTPs have been shown to function as both inhibitors and positive regulators in the contexts of phospho-tyrosine dependent signaling. Dephosphorylation of phospho-substrates can lead to either a stimulatory or an inhibitory response, depending on the substrate and the signaling pathway.

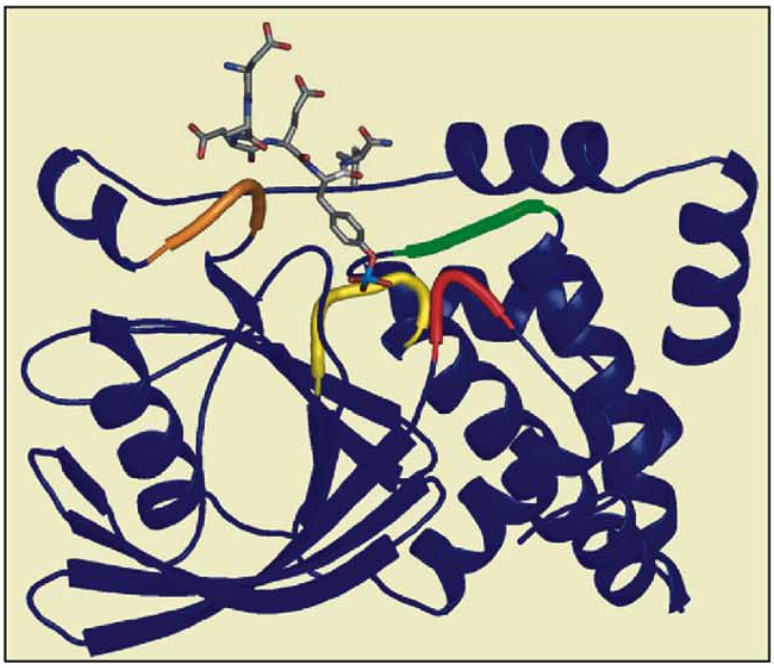

Figure 1.4 Structure of Catalytic Domain of PTP1B. Ribbon representation of the crystal structure of the catalytic domain of PTP1B, 37 kDa in complex with a hexapeptide substrate, modeled on an autophosphorylation site of the EGF receptor (Jia 1995). The catalytic site is in the center of the molecule. The secondary structure elements of the catalytic domain are show in blue. Critical elements that comprise the catalytic site are highlighted in yellow for the signature motif, red for the WPD loop and green for the pTyr loop(Tonks 2003).

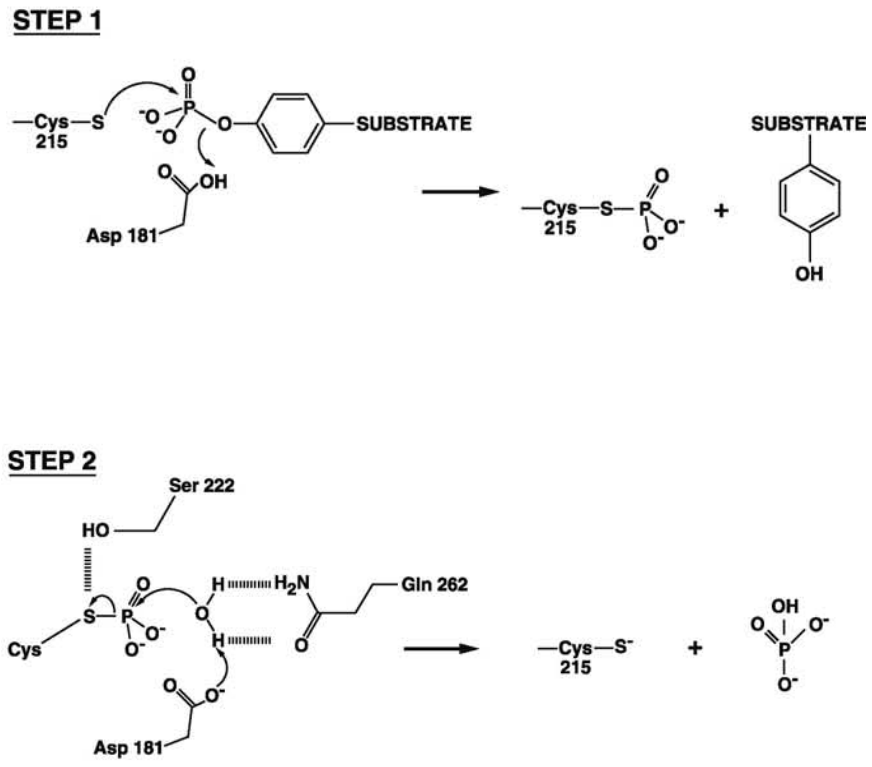

Figure 1.5 PTP Catalytic Mechanism The catalytic mechanism of PTP1B involves a two-step process. In the first step the cysteine in the active site acts as a nucleophile and attacks the phosphate on the pTyr-substrate, with the aspartate (Asp181) in the WPD loop functioning as a general acid. This first reaction yields a phospho-cysteinyl intermediate PTP1B and release of the dephosphorylated Tyr-substrate. In the second step, the phosphate group is hydrolyzed off the cysteine residues of PTP1B and released to restore the active form of the enzyme (Tonks 2003).

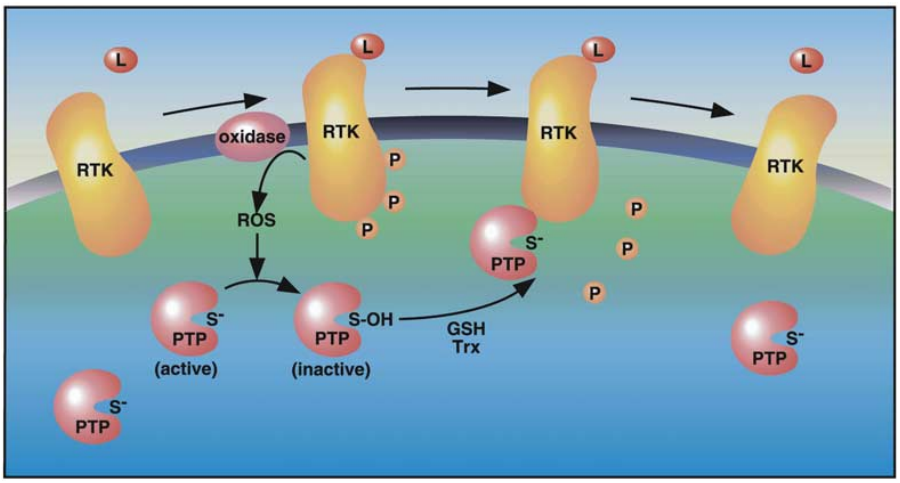

Figure 1.6 Model for Regulation of PTP1B activity by Reversible Oxidation in context of PTK signaling. A ligand dependent activation of the receptor tyrosine kinase triggers the production of ROS through Rac-dependent NADPH oxidase assembly at the membrane. ROS oxidize the active site Cys residue of PTP1B, converting it from its active (thiolate ion) form to its inactive form (sulphenic acid). This reversible oxidation and inhibiton of PTP1B activity promotes tyrosine phosphorylation and signaling into the cell through the activated signaling pathway. The sulphenic acid form of Cys is rapidly converted to sulphenyl amide, protecting it from irreversible oxidation and eventually restored to its active form by thioredoxin or glutathione (Tonks 2003).

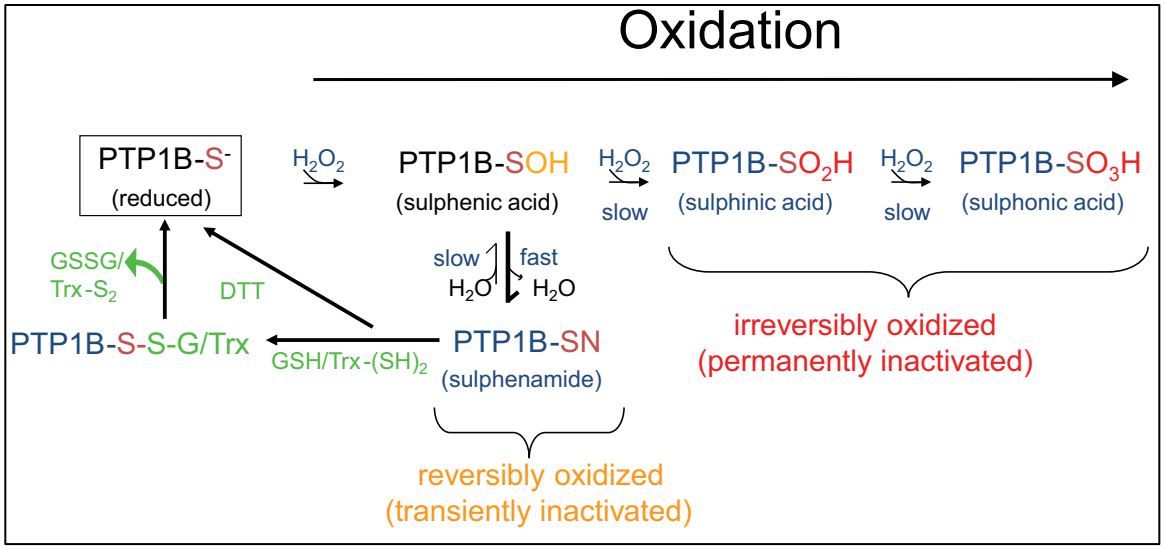

1.7 PTP1B Function is Regulated by Reduction and Oxidation. The overall regulation of PTP1B function by oxidation is illustrated here. Reactive oxygen species can oxidize and modify the active site cysteine rendering it inactive. With mild oxidation the cysteine is converted to a sulphenic acid form, which is reversible; it quickly proceeds to a sulphenyl-amide intermediate, which protects it from irreversible modification and exposes the sulphenyl closer to the surface aiding reduction and conversion to the active form. The sulphenic form can also be further oxidized to a sulphenic and sulphenic acid, which are irreversible.

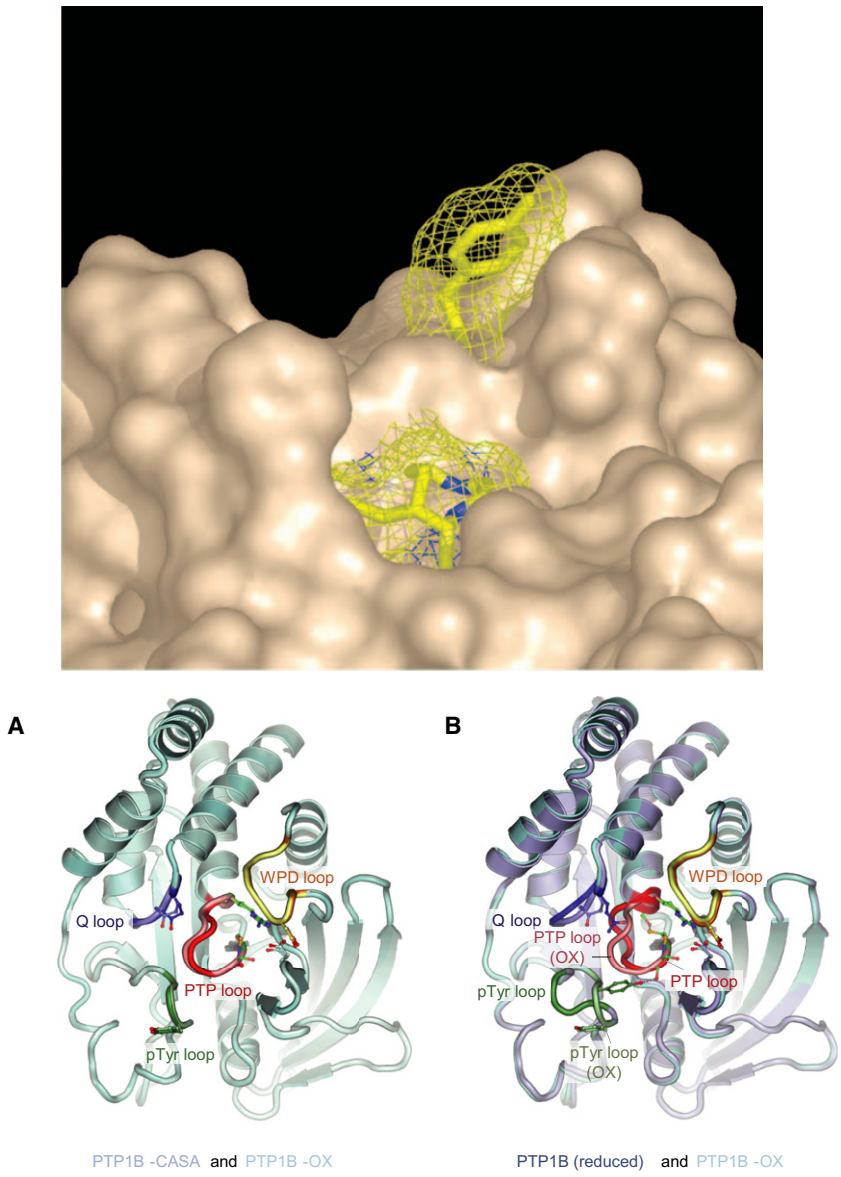

1.8 Structural Consequences of oxidation at the PTP1B active site. Incubation of PTP1B crystals with stoichiometric quantities of H_2O_2 induced formation of the cyclic sulphenamide and a profound conformational change at the active site of the enzyme, which no change was observed in other regions (Haque 2011). The 2 elements of the active site that changed position in the oxidation process are highlighted in yellow: the PTP loop containing the signature motif and catalytic Cys and Tyr46 from the pTyr loop which defines the depth and specificity of the catalytic cleft. PTP1B-C215AS216A crystal superimposed onto PTP1B-ox (sulphenyl-amide species) illustrates the similarity in structure.

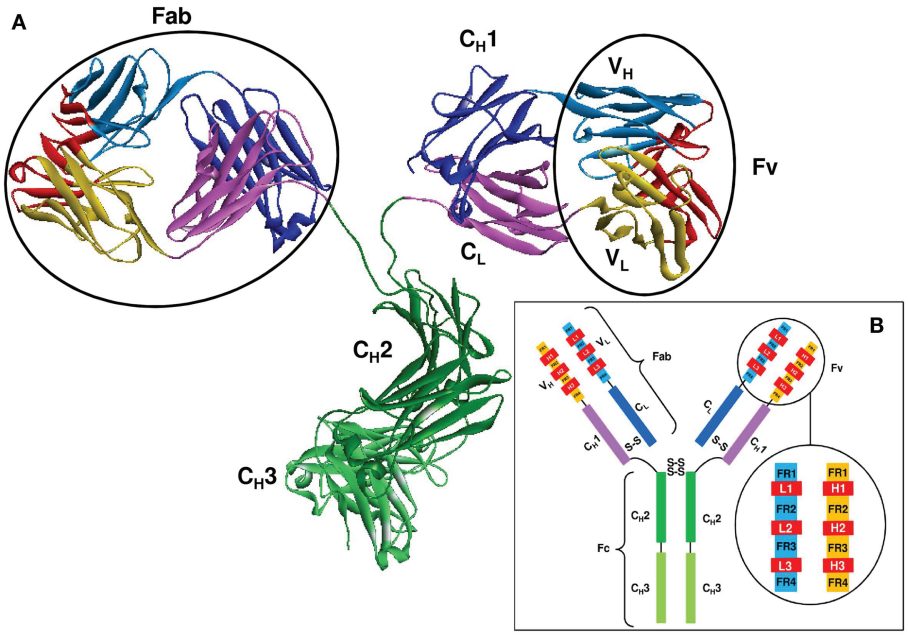

1.9 Basic Antibody Structure and Subunit Composition. Structure of an antibody molecule published by Sela-Culand *et al.* in Frontiers in Immunology, 2013. A schematic representation of the full length antibody in (B) illustrates the arrangement of the constant heavy chain (CH) constant light chain (CL) and the variable light (VL) and variable heavy (VH) domains. In (A) corresponding colors illustrate the domains in tertiary structure. The Fc portion, which is located in the C-terminal portion of the antibody typically confers structural support, stability and activates the immune response. A small fragment variable (Fv) composed of VL and VH domains can be expressed as a single polypeptide by joining the two domains with a neutral linker in an expression construct. A Fab fragment is formed by a VL and VH and two CH domains as illustrates in (A) and (B).

Chapter 2

Crystallographic Screening of PTP1B-CASA in complex with scFv45

2.1 Introduction

As described in the introduction, PTP1B is a validated target for treatment of diabetes and obesity as it is a major regulator of signaling by the insulin and leptin receptors. Consequently, there have been industrial efforts to develop small molecule inhibitors of PTP1B to promote insulin signaling in resistant states. These inhibitors are highly charged and have not been developed for clinical due to a clinical requirement for T2DM therapeutics to be orally bioavailable. Our lab took a novel approach to the development of PTP1B inhibitors by harnessing its physiological mechanism of regulation by reversible oxidation - a mechanism of fine tuning pTyr-dependent signaling. Regulated production of ROS, in the context of receptor tyrosine kinase stimulation, oxidizes the active site cysteine and inactivates PTP1B (oxPTP1B) resulting in a profound conformational change occurs at the catalytic site (Salmeen A 2003). The Tyr46 and the PTP loop adopt a solvent accessible position as illustrated in Figure 1.8 in the introduction. The new surfaces provide unique potential binding sites, which are not found in the reduced, active enzyme.

Phage display was used to identify a conformation-sensor scFv antibody that selectively binds oxPTP1B. Expression of scFv45 in cells increases their insulin sensitivity, indicating stabilization of oxPTP1B. The ability to modulate the insulin and signal transduction pathways through inhibition of oxPTP1B holds tremendous therapeutic potential in the treatment of diabetes and obesity. In anticipation of ultimately developing small molecule inhibitors a major focus of our research has been defining the mechanism of recognition between scFv45 and oxPTP1B. We have pursued crystallographic studies in collaboration with Dr. Leemor Joshua Tor's lab at CSHL. We used the PTP1B-CASA mutant form, which is identical in conformation of oxPTP1B, and it circumvents the reversible oxidation step, which would be logistically more difficult to perform.

Historically, antibody fragments such as Fabs and scFvs have been used as adjuvants in crystallography, in particular for stabilization of membrane proteins. More recently scFvs conjugated to nanoparticles or liposomes containing cytotoxic drugs have been developed. The epitope binding properties of antibodies are used to target chemotherapeutics to tumors overexpressing aberrant receptors and for internalization. The smaller scFv and Fab in particular are preferred to full-length antibodies as they lack the Fc receptor that that activates

immune response and they are smaller and might penetrate deeper into the tumor Zhang and Nielsen (2015).

Co-crystals of scFv45 and PTP1B-CASA would provide important information for optimization of therapeutic molecules that mimic the effects of scFv45 on oxPTP1B in insulin signaling. Our approach to inhibit PTP1B, by stabilizing the oxidized, inactive form of the enzyme is a novel therapeutic strategy. In addition, using phage display as a tool in the future development of inhibitors is a unique and challenging approach with potential to offer a new model for protein directed drug development.

2.2 Methods

2.2.1 Cloning of Constructs into Cleavable Tag Vectors

We used sequence ligation independent cloning (SLIC) to subclone both the scFv45 and PTP1B-CASA into bacterial vectors containing protease removable affinity tags. This method makes use of bacterial DNA repair mechanisms to recombine 2 linearized DNA fragments that contain single-stranded complementary overhangs of at least 15 nucleotides. First the vector and insert were linearized by PCR with a high fidelity polymerase; we used Phusion Polymerase (Thermo Scientific). After the PCR product was verified on agarose gel and DpnI digestion of template DNA was carried out the PCR product was purified with Qiagen PCR cleanup kit. We used the 3' → 5' single stranded exonuclease activity of T4 DNA polymerase to generate overhangs. The T4 polymerase reaction was quenched by addition of one of the dNTPs (dCTP). The vector and insert concentrations were quantified by determining the absorption at 260 nm using a nanodrop instrument. We mixed vector and insert based on their size and concentration and co-transformed into *E. coli* strain DH5α. Positive clones were confirmed by DNA sequencing.

2.2.2 Expression and Purification of Recombinant PTP1B

The catalytic domain, 37kDa, of human PTP1B-CASA was expressed in BL21-RIPL *E.coli* cells from a pET19b vector, which contains no affinity tag, and from a pET28 vector, that contains a cleavable N-terminal His_6-sumo-tag. Colonies harboring the expression plasmid were grown in a starter culture of LB + Kanamycin (50 µg/ml) at 37°C for 4 hours. The starter culture

was expanded to 1L and expression of recombinant protein was induced with 1mM IPTG at the optimal growth phase as indicated by an OD_{600nm} of 0.7. Protein was expressed overnight, at 18°C, shaking at 200 rpm. Cells were harvested by centrifugation, at 3000 x g for 30 min, and resuspended in lysis buffer. For storage cells were flash frozen in liquid nitrogen and stored at -80°C. Frozen cells were thawed and lysed by sonication on ice and lysates were cleared by centrifugation at 35,000 x g at 4°C, for 50 min.

For purification of the untagged PTP1B from pET19b we resuspended and flash froze cell pellets in lysis buffer (25 mM NaH_2PO_4, pH 6.5, 10 mM NaCl, 1 mM EDTA, 5 mM DTT, 1 mM PMSF, 1 mM benzamidine and protease inhibitor cocktail). The cleared lysates were first passed through a cation exchange column (SP Sepharose HP, GE Life Science) using 25 mM NaH_2PO_4, pH 6.5, 10 mM NaCl, 1 mM EDTA, 5 mM DTT as the binding buffer and the protein was eluted by a gradient elution with 10-500 mM NaCl. Fractions containing PTP1B were pooled together and passed through an anion exchange column (Q Sepharose HP, GE Life Science) using 25 mM Tris-HCl, pH 7.5, 1 mM EDTA, 5 mM DTT as the binding buffer. The purified PTP1B was eluted with a 0-500 mM NaCl gradient.

For affinity tag purification with Ni-NTA the cleared lysate in the first wash buffer/lysis buffer (50 mM HEPES, pH 7.4, 100 mM NaCl, 20 mM Imidazole, 5mM βME) was incubated with 1mL of Ni-NTA resin (Qiagen) per 1.5 L of culture for 1 hour at 4°C on a rolling shaker. The resin was applied to a gravity flow column and washed extensively with 10 column volumes of lysis buffer, a high salt concentration wash buffer (50 mM HEPES, pH 7.4, 500 mM NaCl, 20 mM Imidazole, 5mM βME), and lysis buffer again. The His-sumo tag was removed by cleavage with ULP1 protease on-column, in lysis buffer of equal volume to the beads with the enzymatic reaction carried out overnight at 4°C. Ulp1 recognizes the tertiary structure of the SUMO tag rather than amino acid sequence and leaves no residues behind. The protein was eluted off the column with several more additions of wash buffer and the cleavage efficiency and purity was verified by SDS-PAGE. Fractions containing PTP1B-CASA were pooled together, concentrated and then purified with a HiLoad 16/60 Superdex200 size exclusion column (GE Life Science) equilibrated with 50mM HEPES pH 7.4, 150 mM NaCl and 5 mM DTT. The fractions containing PTP1B-CASA protein as indicated by absorbance at 280 nm were verified via SDS-PAGE and pooled and concentrated. They were used to form a complex as described in 2.2.3 with recombinant scFv45 purified as described below in section 2.2.2.

2.2.3 Expression and Purification of Recombinant scFv45

The purification scheme of scFv45 (sequence in Fig. 2.1) is similar to that described for PTP1B-CASA above. The protein was expressed in BL21-RIPL *E.coli* cells from a pET21b vector with a C-terminal His tag initially and from a pET22 vector that contains a C-terminal TEV-His tag for the crystallography studies. Colonies harboring the expression plasmid were grow in a starter culture of LB + Kanamycin (50 µg/ml) at 37°C for 4 hours. The starter culture was expanded to 1L and expression of recombinant protein was induced with 1mM IPTG at the optimal growth phase as indicated by an OD_{600nm} of 0.7. Protein was expressed overnight, at 18°C, shaking at 200 rpm. Cells were harvested by centrifugation, at 3000 x g for 30 min, and resuspended in lysis buffer (50 mM HEPES, pH 7.4, 100 mM NaCl, 20 mM Imidazole, 5mM βME). For storage cells were flash frozen in liquid nitrogen and stored at -80°C. Frozen cells were thawed and lysed by sonication on ice and lysates were cleared by centrifugation at 35,000 x g at 4°C, for 50 min. The cleared lysate was incubated with 1mL of Ni-NTA resin (Qiagen) per 1.5 L of culture for 1 hour at 4°C on a rolling shaker. The resin was applied to a gravity flow column and washed extensively with lysis buffer, a high salt concentration wash buffer (50 mM HEPES, pH 7.4, 1000 mM NaCl, 20 mM Imidazole, 5mM βME), followed by a wash with lysis buffer again. The His-TEV tag was removed by cleavage with TEV protease on-column, in lysis buffer of equal volume to the beads with the enzymatic reaction carried out overnight at 4°C. The protein was eluted off the column with several more additions of wash buffer and the cleavage efficiency and purity was verified by SDS-PAGE. Fractions containing scFv45 were pooled together, concentrated and then purified with a HiLoad 16/60 Superdex75 size exclusion column (GE Life Science) equilibrated with 50mM HEPES pH 7.4, 150 mM NaCl and 5 mM DTT. The fractions containing PTP1B protein as indicated by absorbance at 280 nm were verified via SDS-PAGE and pooled and concentrated. We used absorbance at 280nm, extinction coefficient and molecular mass on a nanodrop instrument. The pure scFv45 protein was used to form a complex as described in 2.2.3 with recombinant PTP1B-CASA purified as described below in section 2.2.1.

2.2.4 Complex formation and Crystal Screening

For crystallization a complex of PTP1B-CASA and scFv45 was formed. We have optimized complex formation ratio and observed that a 1 : 1.1 molar ratio at 20°C for 30 minutes were appropriate for a stable complex to form. After excess, unbound scFv45 was resolved from the

stable complex on a HiLoad 16/60 Superdex200 size exclusion column (GE Life Science) equilibrated with 10mM HEPES pH 7.4, 100 mM NaCl and 2 mM DTT. SDS-PAGE was used to analyze the fractions. Only the fractions containing complex, at the center of the complex peak, were pooled, concentrated and used for crystal screening.

2.3 Results and Discussion

2.3.1 PTP1B Protein Quality and PTP1B-CASA Crystals

PTP1B purification had been well established when the enzyme was first identified (Barford 1994a). I initially started with this protocol, which involved passing the protein sequentially through a cation exchange column, followed by an anion exchange column and finally through a Superdex200 size exclusion column. In order to speed up the purification process, but also to avoid flowing lysate through the chromatography system we subcloned PTP1B-CASA for purification using a protease removable affinity tag. We purified PTP1B-CASA as described in the methods section. We were able to obtain large amounts of homogenous PTP1B-CASA protein (~1-2mg/L of culture) after the final purification step (Figure 2.2). We tested the quality of the protein by generating crystals of PTP1B-CASA. We were able to reproduce the previously published condition by Barford et al. setting up drops manually in a grid screen around the central condition of 0.1M HEPES, pH 7.5, 0.2M magnesium acetate, and 16% PEG 8000. We also obtained crystals with PTP1B-CASA from drops set up with an automated robot in a previously unpublished condition of 0.1M MES, pH 6.5, 0.2M Magnesium Acetate and 16% PEG 8000. The 2 different methods contain different volumes of protein and buffer, 4 µL versus 300 nL, with the components mixed in a 1:1 ratio, which results in a different rate of diffusion. We planned to use the automated system in the Joshua-Tor lab to set up drops for screening of a co-crystal of scFv45 and PTP1B-CASA as it enables trial of hundreds of conditions with smaller protein drops. As such it was reassuring to see that PTP1B-CASA is able to crystalize in such conditions. We were reassured that the purification process was adequate and that we could proceed with the purification of scFv45 and ultimately screening for a complex.

2.3.2 Optimization of scFv45 Expression and Purification

Initially we worked with a scFv45 construct in which the VL and VH domains were connected with a 7 residue linker as this had previously been used for characterization studies published in Haque *et al*. The purification required some optimization of protein induction. After affinity purification with Ni-NTA the scFv45 protein resolved on SDS-PAGE as 2 bands, one at ~25 kDa as expected but also a slight smaller band migrating faster (Figure 2.3A). We analyzed the protein sample from the gel with mass spectrometry to determine whether there might be site of proteolytic cleavage that we could prevent by mutating the site in scFv45 or by using a protease specific inhibitor. We did not find a readily identifiable site, and we were not able to prevent cleavage by increasing the number and amount of protease inhibitors. We used a protease inhibitor cocktail to inhibit proteases such as thermolysin, chymotrypsin, trypsin, papain and thrombin. We proceeded to optimize induction temperature and IPTG and we eliminated the faster migrating band, observing a homogenous scFv45 protein after affinity purification. We believe that shorter species was a truncated expression product rather than the result of proteolytic cleavage. We have since found that the scFv45 molecule is in fact not readily cleaved by proteases, which I will discuss in chapter 3.

Optimization of induction allowed us to obtain robust expression of a homogenous scFv45 protein as illustrated in Figure 2.3b and in reasonable quantities (~2mg/L of culture) that would allow for screening. The protein expressed from the scFv45 construct had a 7 residue linker connecting the V_L and V_H domains, so we named it scFv45-SL, for short linker. We tried to purify the fractions from affinity chromatography by anion exchange but we were not able to separate the scFv45 protein from bacterial impurities proteins as they co-eluted. We obtained better scFv45 protein purity with size exclusion chromatography. The scFv45-SL protein eluted in 2 peaks, first an oligomer, likely a dimer, and later a monomer with some overlap between the peaks as seen in Figure 2.3B. We wanted to form a complex with the monomer species of scFv45 and PTP1B-CASA, and to avoid working with the dimer if possible.

2.3.3 Optimization of scFv45 for Crystallographic Studies

2.3.3.1 Studies with scFv45-SL

We formed the complex with fractions of scFv45-SL eluting as a monomer. We were able to form a stable complex with PTP1B-CASA as shown in Figure 2.4. For complex formation we tried a range of temperatures from 4°C to 37 °C, and saw evidence that some precipitation was occurring at 37°C so we used 20°C with shaking. We tried to set up drops to co-crystallize the complex and in the process of concentrating the sample we observed the protein aggregated at concentrations above 5mg/mL. Since PTP1B was crystalized in drops set up with 10 mg/mL of protein, we planned to set up drops with the complex with a minimum of 10 mg/mL, but preferably higher. In regards to concentration the closer it is to supersaturation for a particular protein sample the higher the chances that it will crystalize. We tested the sample for homogeneity by dynamic light scattering (DLS), a method that determines the size distribution profile of a sample from a scattered monochromatic light source passed through the sample. The measurements are an estimation of the radius of molecules dispersed in the sample. In the case of complex with scFv45 and PTP1B-CASA they varied by more than 50% indicating the sample was aggregating at >5mg/mL. Centrifugation of the sample formed a white precipitate in the tube and the supernatant had no absorbance at 280 nm so we could conclude the sample aggregated.

Reports in literature suggest scFv molecules aggregate more readily than other antibody fragments or full-length molecules with others using solubility increasing tags or adjuvants to increase solubility. However whereas adjuvants that prevent aggregation are helpful during protein expression or purification, they will likely interfere with the process of crystal formation. The expression construct for scFv45 contains an ompA secretory sequence as suggested by Barbas *et al.* in the phage display laboratory manual, which was used when the library containing scFv45 was generated. The ompA signal targets scFv45 for periplasmic secretion after which it is cleaved off by proteases in the periplasmic space (Thie 2008). During affinity purification scFv45 has a His tag which could help with solubility. Solubility issues only arose with scFv45-SL when it was concentrated for crystallographic screening in complex with PTP1B-CASA.

2.3.3.2 Studies with scFv45-LL

When setting up drops for crystallization we want to set up a homogenous protein population without tags that interfere with crystallization by increasing solubility or interfere with molecule packing. In considering other alternatives we first tried a scFv45 construct in which the V_L and V_H globular domains are linked by an 18 residue peptide, which we called scFv45-LL. The phage library contained scFvs with both 7 and 18 residues, as it provided greater diversity, and we tested this linker length as it already provided functional scFv45 molecules. The levels of protein obtained from bacterial expression and affinity chromatography were comparable to that of the short linker construct. The affinity purification step also yielded similar amounts of protein, which then resolved on size exclusion with a Superdex75 column much better than the short linker and better than we had expected. We still observed two peaks, but they resolved from each other so the monomeric peak could be isolated without overlap as illustrated in Figure 2.4. The final step of purification yielded milligram amounts of homogenous protein, which could be concentrated as high as 30mg/mL without compromise in solubility. Fractions from both peaks from size exclusion chromatography (SEC) resolved on SDS-PAGE a single band of approximately 27 kDa, so the higher molecular weight peak likely consists of scFv45-multimersfirst eluting peak is an oligomer by electrostatic interaction between scFv45-LL multimers.

We proceeded to form a complex with scFv45-LL and PTP1B-CASA by incubation for 30 min, at 20°C with shaking. The complex formed with scFv45-LL and PTP1B-CASA illustrated on the SEC profile in Figure 2.5 eluted as a symmetric peak on Superdex200 indicating homogeneity of this sample. The complex elutes first with a symmetric peak indicating the homogeneity of the sample, and excess scFv45 elutes later. Using multiangle light scattering (MALS) we determined the mass of the complex was ~64 kDa, which confirmed binding in a 1:1 ratio. MALS is a method that independently calculates mass of a protein relative to a reference such as BSA, based on measurements of radius. It uses precise measurements of light scattering intensity and concentrations without considering conformation or shape, an for this reason it works best for globular proteins. Because the short linker scFv45 aggregated we wanted to confirm that was not the case with the long linker species. DSL of the complex with scFv45LL confirmed the polydispersity of the sample was <20%, and although each sample is different, it is generally thought that proteins with polydispersity <30% behave well enough to proceed with screening for crystals.

2.3.4 Crystallographic Trials

At this point we had optimized the purification protocol to obtain pure and homogeneous protein complex that we could systematically test in various crystallization conditions. We carried out extensive crystal screening as described in this section, in hopes that we could obtain some type of crystal or a lead that we could optimize to a crystal. We used matrix screens in 96 well plates that consist of conditions that vary pH, ionic strength, buffer conditions, precipitant, additives or salt concentration. These screens are based on a compilation of conditions in which proteins have previously successfully crystallized. We probed the solubility of the protein complex by incrementally varying it within a range of 5-25 mg/mL, and did so in response to the degree of precipitation we observed. The appropriate concentration of protein to use for screening is considered to be one at which precipitation occurs in ~50% of the wells. The protein screens are typically incubated at 20°C and 4°C. PTP1B has only been crystallized at 4°C, but the proteins in complex are essentially a new species, that has not been crystallized before, so we set screening plates at both temperatures. There are also several ways in which the drop of protein and buffer are set up for diffusion, the two most popular being a hanging drop and a sitting drop. The differences are in the support for the drop, top if it is hanging or bottom if sitting and the geometry of the setup. Any subtle change in geometry, for example tilt, will affect the rate of equilibration between the drop and the surrounding environment in the well. Based on previous crystals with PTP1B-CASA, we started the screens using the hanging drop format.

After testing an exhaustive combination of parameters that could affect crystallization success we concluded that the scFv45-LL was unlikely to crystalize. We considered what other changes we could make to improve the possibility of crystallization and we decided to focus next on trying to alter the solubility of the protein.

2.3.5 Further Protein Optimization

Empirically we observed that the complex formed with scFv45LL was stable at concentrations as high as 30 mg/mL, in contrast to scFv45SL, which aggregated at higher than 5mg/mL. As the scFv field has developed, issues with solubility have highlighted the importance of the artificial linkers on biophysical properties (Chen 2013). The length and amino acid composition can improve stability, biological activity and expression yield. The length of

the scFv45 linker had dramatic effects on the solubility of the protein. The longer linker, GQSSRSSSGGGSSGGGGS, contains several more serine residues than the short linker, GQSSRSS. Their nucleophilic nature significantly increased solubility of scFv45-LL. Based on their solubility, we generated a series of constructs with linkers of 12, 14, 15 and 16 residues connecting the V_H and V_L domains. Based on conversations with Dr. Bryce Nelson the director of the phage display facility at CSHL and his work with scFvs in Dr. Sidhu Sachdev's lab we also introduced some alanine and threonine residues in these constructs because these residues have been shown to help maintain flexibility (Figure 2.6).

We purified the scFv45 containing the linker mutants and observed that the length of the linker did not correlate to better resolution of monomer on Superdex75 SEC as shown in Figure 2.8. The scFv45-12aa construct did not purify as a homogeneous population and in fact upon incubation with PTP1B-CASA the protein precipitated – so this particular linker, whether it was the length or introduction of an alanine and threonine residue was the worst construct we had tried. Of the remaining constructs, scFv45-16aa purification yielded the most homogenous monomer population on SEC with the peaks of oligomer and monomer completely resolved and had a Gaussian shape indicating homogeneity. However, complex of scFv45-16aa and PTP1B-CASA actually resolved on SEC as 3 peaks, one for complex, an intermediate peak and one for excess scFv45-16aa. The SEC profile for scFv45-15aa looked similar to that of scFv-SL (Figure 2.2), while scFv45-14aa seemed to resolve the monomer and oligomer peaks much better, which indicates that there is an optimal length for the linker, but increasing its length does not necessarily increase stability and improve folding. Overall after incubation of PTP1B-CASA with the scFv45 linker mutants, the complex formed with scFv45-14aa demonstrated the best binding on SEC (Figure 2.8). We had expected that the longer linkers would behave better, but the linker with 14 residues, seemed to be the optimal for scFv45. We suspect that changes in the sequence of the linker would also lead to changes in the folding of the scFv if they change the steric hindrance between the functional domains.

2.3.6 scFv45 Does Not Bind PTP1B-WT in Reducing Conditions

We show by SEC and SDS-PAGE that incubation of PTP1B-WT and scFv45 under reducing conditions does not result in complex formation. Whereas oxPTP1B and scFv45 form a complex visible on SEC this was not the case for PTP1B-WT. Incubation of the wild type protein (Alonso 2002) with scFv45 (27 kDa) results in elution of the two proteins as two

separate, but adjacent peaks, due to their similar size. If a complex had formed we would expect to see a larger peak eluting first representing the complex, and a small peak for excess scFv45. However we see a smaller peak for PTP1B-WT and a larger peak for scFv45. There is minor broadening of the PTP1B-WT peak, suggesting minor nonspecific binding. SDS-PAGE analysis indicates co-elution of PTP1B-WT and scFv45 as scFv45 is distributed throughout the fractions rather than being concentrated in the complex fractions and a smaller amount in the excess peak. This indicates scFv45 and PTP1B-WT co-elute due to their size similarity and not to binding. SDS-PAGE of the oxPTP1B : scFv45 complex shows scFv45 protein is present only in fractions from complex and in fractions from the excess scFv45 peak, with no protein in the intermediate fractions between the two peaks.

2.4 Figures

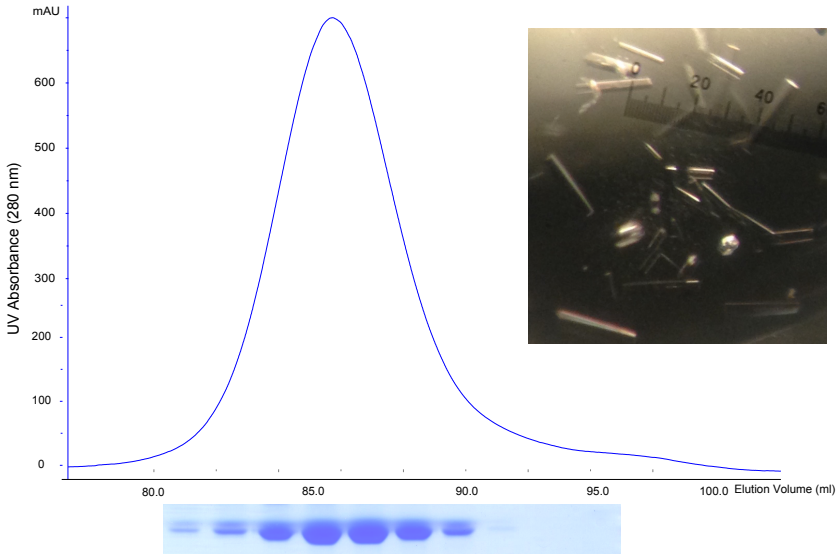

Figure 2.1 Purification of PTP1B-CASA. Size exclusion chromatography of PTP1B-CASA on a HiLoad Superdex 200 and its resolution on SDS-PAGE illustrate that the final protein sample is pure and homogeneous. High amounts of protein (1-2mg/mL) could be purified to homogeneity in a two-step purification process, a Ni-NTA affinity step and size exclusion chromatography. The quality of the protein was confirmed by replicating crystals, which grew as long hexagonal rods.

```
   1 ATGAAAAAGACAGCT ATCGCGATTGCAGTG GCACTGGCTGGTTTC GCTACCGTGGCCCAG GCGGCCCTGACTCAG
   1  M  K  K  T  A   I  A  I  A  V   A  L  A  G  F   A  T  V  A  Q   A  A  L  T  Q
  76 CCGTCCTCGGTGTCA GCGAACCCGGGAGGA ACCGTCAAGATCACC TGCTCCGGGAGTAGC AGTGCCTATGGTTAT
  26  P  S  S  V  S   A  N  P  G  G   T  V  K  I  T   C  S  G  S  S   S  A  Y  G  Y
 151 GGCTGGTATCAGCAG AAGTCACCTGGCAGT GCCCCTGTCACTGTG ATCTATAACAACAAT AAGAGACCCTCAAAC
  51  G  W  Y  Q  Q   K  S  P  G  S   A  P  V  T  V   I  Y  N  N  N   K  R  P  S  N
 226 ATCCCTTCACGATTC TCCGGTTCCAAATCC GGCTCCACGGGCACA TTAACCATCACTGGG GTCCAAGCCGAGGAC
  76  I  P  S  R  F   S  G  S  K  S   G  S  T  G  T   L  T  I  T  G   V  Q  A  E  D
 301 GAGGCCGTCTATTTC TGTGGGAGTGAAGAC AGCAGCACTGATGCT ATATTTGGGGCCGGG ACAACCCTGACCGTC
 101  E  A  V  Y  F   C  G  S  E  D   S  S  T  D  A   I  F  G  A  G   T  T  L  T  V
 376 CTAGGTCAGTCCTCT AGATCTTCCACCGTG ACGTTGGACGAGTCC GGGGGCGGCCTCCAG GCGCCCGGAGGAGCG
 126  L  G  Q  S  S   R  S  S  T  V   T  L  D  E  S   G  G  G  L  Q   A  P  G  G  A
 451 CTCAGCCTCGTCTGC AAGGCCTCCGGGTTC ACCTTCAGCAGTTAC GACATGGGTTGGATA CGACAGGCGCCCGGC
 151  L  S  L  V  C   K  A  S  G  F   T  F  S  S  Y   D  M  G  W  I   R  Q  A  P  G
 526 AAGGGGCTGGAATAC GTTGCGGGTATTACC GATAATGGTAGATAC GCATCATATGGGTCG GCGGTGGATGGCCGT
 176  K  G  L  E  Y   V  A  G  I  T   D  N  G  R  Y   A  S  Y  G  S   A  V  D  G  R
 601 GCCACCATCTCGAGG GACAACGGGCAGAGC TCAGTGAGGCTGCAG CTGAACAACCTCAGG GCTGAGGACACCGGC
 201  A  T  I  S  R   D  N  G  Q  S   S  V  R  L  Q   L  N  N  L  R   A  E  D  T  G
 676 ACCTACTACTGTGCC AGAGATGACGGTAGT GGTTGGACTGGTAAT AGTATCGACGCATGG GGCCACGGGACCGAA
 226  T  Y  Y  C  A   R  D  D  G  S   G  W  T  G  N   S  I  D  A  W   G  H  G  T  E
 751 GTCATCGTCTCCTCC ACTAGTGGCCAGGCC GGCCAG
 251  V  I  V  S  S   T  S  G  Q  A   G  Q
```

Figure 2.2 Sequence of scFv45. DNA and amino acid sequences are shown for scFv45-SL. The sequential order it contains the V_L, followed by the short 7 residues linker, ending with the V_H domain.

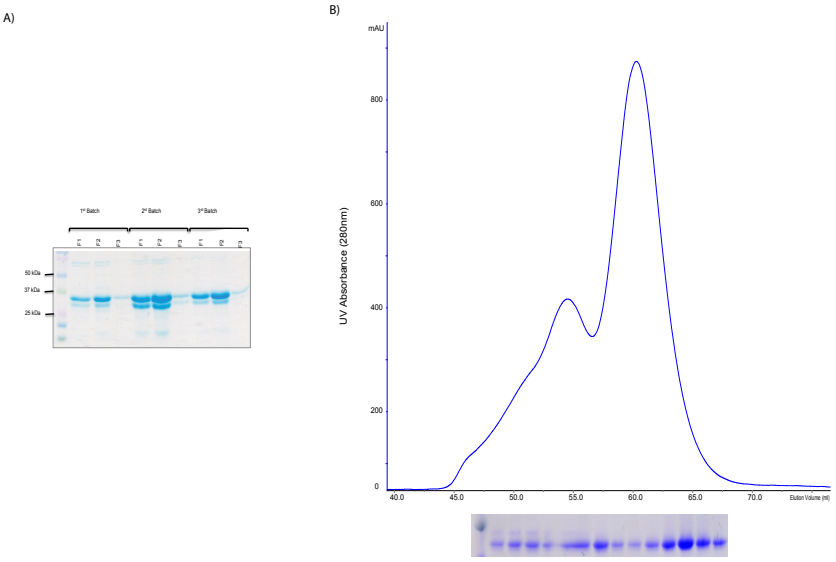

Figure 2.3 Purification of scFv45-SL (A) Ni-NTA affinity purification of ScFv45-SL expressed from a pET21b vector containing a His_6-tag resolved on SDS-PAGE after Ni-contained a fraction of a truncated protein species. (B) Size exclusion chromatography of scFv45-SL expressed in the pET22-TEV-Hix_6 vector. Sequential 2-step purification of affinity purification, tag-cleavage and size exclusion chromatography on a HiLoad Superdex75 column yield two protein populations, the larger molecular weight peak is an oligomer and the smaller molecular weight represents a monomer. The scFv45 protein eluting as a monomer is what the proceeded to try to co-crystallize. As observed on SDS-PAGE samples from fractions throughout the elution resolve to the same molecular size of 25kDa, and this was the case both in the presence and absence of reducing agent.

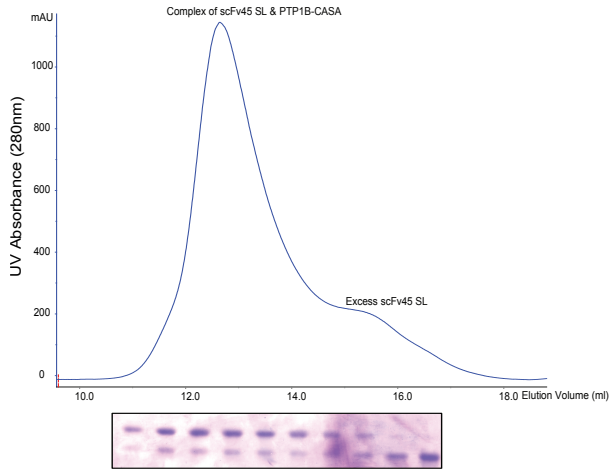

Figure 2.4 Complex Formation with scFv45-SL and PTP1B-CASA A stable complex formed between scFv45-SL and PTP1B-CASA, which could be resolved on a Superdex200 size exclusion column although excess scFv45-SL could not be fully resolved from the complex. The protein in complex was collected and concentrated for crystallographic screening but aggregation was observed.

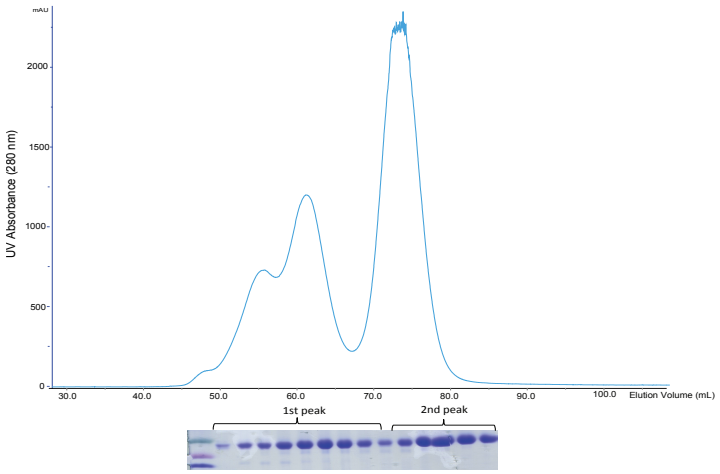

Figure 2.5 Purification of scFv45 LL. After affinity purification with a Ni-NTA column, scFv45-LL was further purified on a HiLoad Superdex 75 size exclusion column resulting in homogeneous monomeric population of scFv45-LL that could be resolved from the larger molecular mass oligomeric species. This purification yielded ~2 mg of protein per liter of bacteria culture.

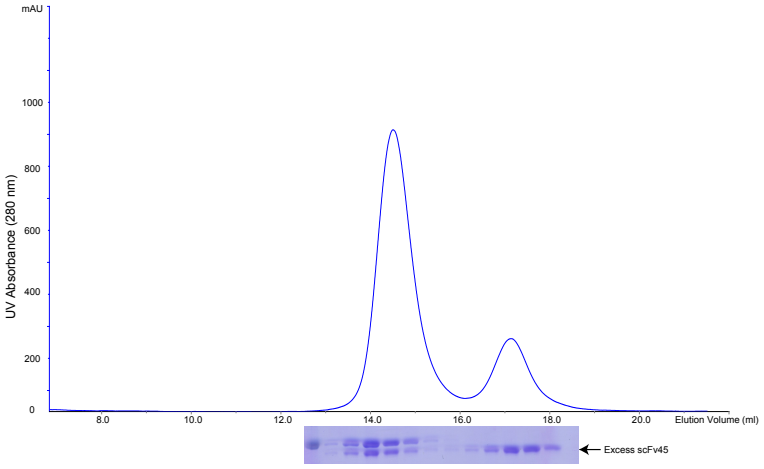

Figure 2.6 Complex of scFv45 LL and PTP1B-CASA. A stable complex formed between scFv45-LL and PTP1B-CASA could be resolved on a Superdex200 column to separate from excess scFv45-LL. The protein in complex was collected and used for crystallographic screening.

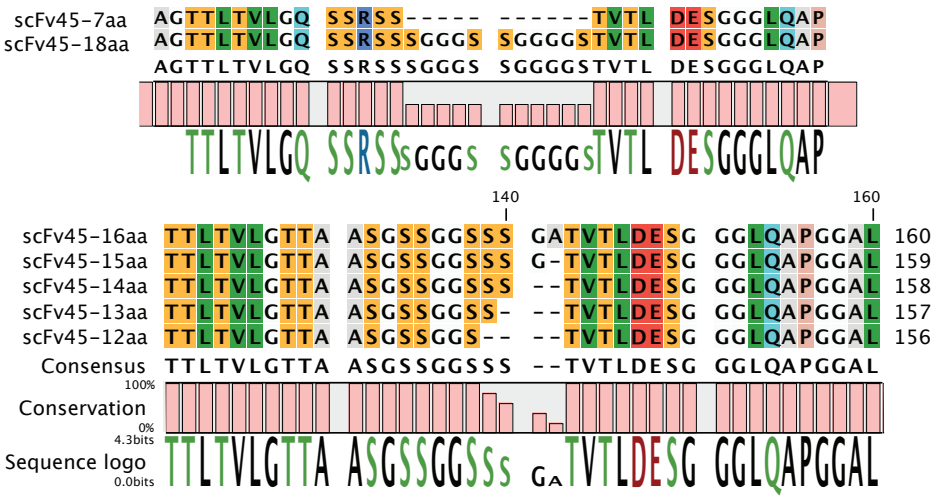

Figure 2.7 Alignment of Linker Clone Sequences. Alignment of the linker sequences of scFv45-SL, with a 7 residues linker and scFv45-LL with an 18 residues linker is illustrated in the top panel. The sequences of linkers with 12, 14, 15 and 16 residues are illustrated in the lower panel. The sequences for these artificial linkers generated based on the Phage Manual by Barbas *et al.* as well as studies of naturally occurring multi-domain proteins and the residues normally found in the naturally occurring linkers that connect those domains.

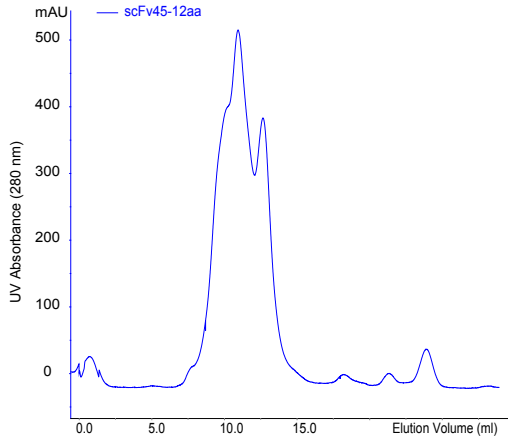
mAU
scFv45-12aa
500
400
300
200
100
0
UV Absorbance (280 nm)
0.0
5.0
10.0
15.0
Elution Volume (ml)

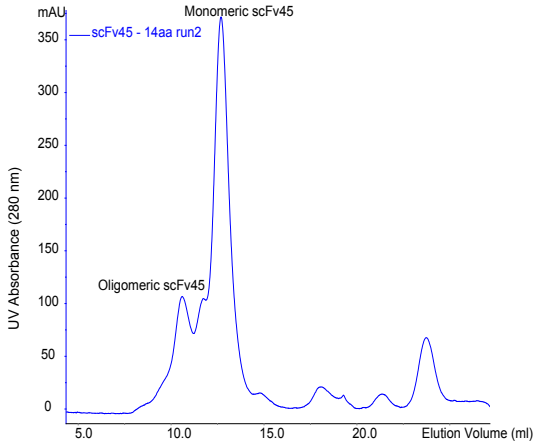
mAU
scFv45 - 14aa run2
Monomeric scFv45
Oligomeric scFv45
350
300
250
200
150
100
50
0
UV Absorbance (280 nm)
5.0
10.0
15.0
20.0
Elution Volume (ml)

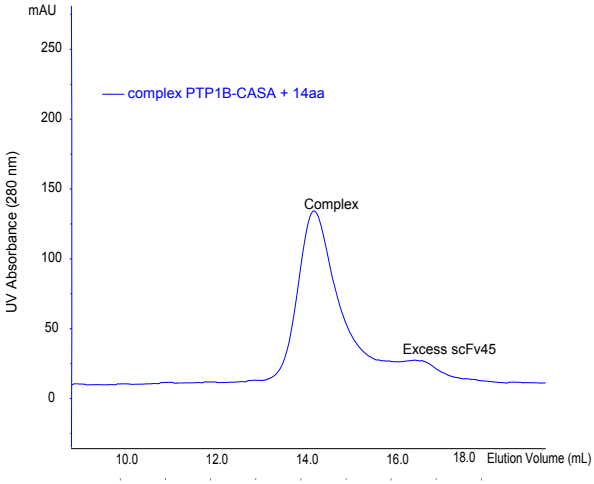
mAU
complex PTP1B-CASA + 14aa
Complex
Excess scFv45
250
200
150
100
50
0
UV Absorbance (280 nm)
10.0
12.0
14.0
16.0
18.0
Elution Volume (mL)

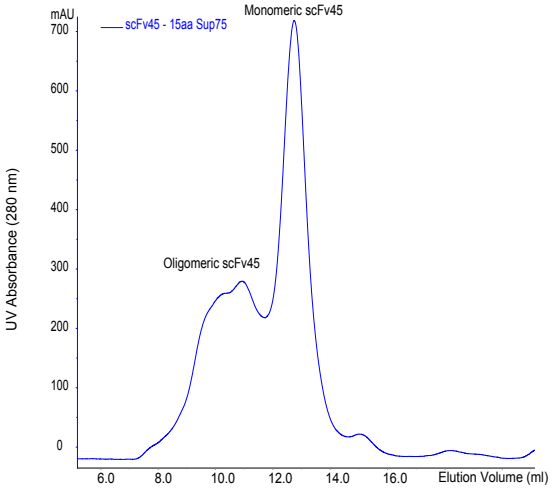
mAU
scFv45 - 15aa Sup75
Monomeric scFv45
Oligomeric scFv45
700
600
500
400
300
200
100
0
UV Absorbance (280 nm)
6.0
8.0
10.0
12.0
14.0
16.0
Elution Volume (ml)

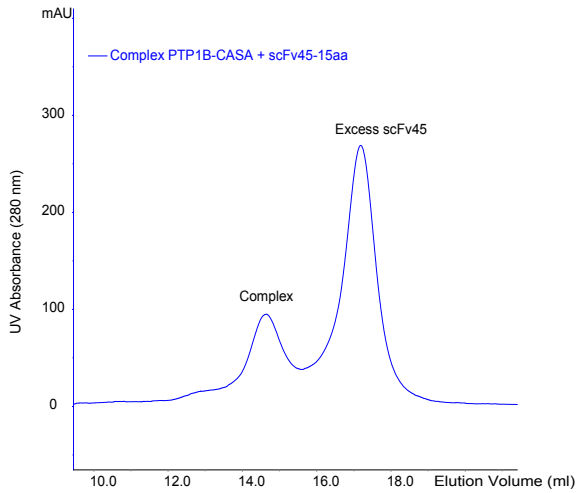
mAU
Complex PTP1B-CASA + scFv45-15aa
Excess scFv45
Complex
300
200
100
0
UV Absorbance (280 nm)
10.0
12.0
14.0
16.0
18.0
Elution Volume (ml)

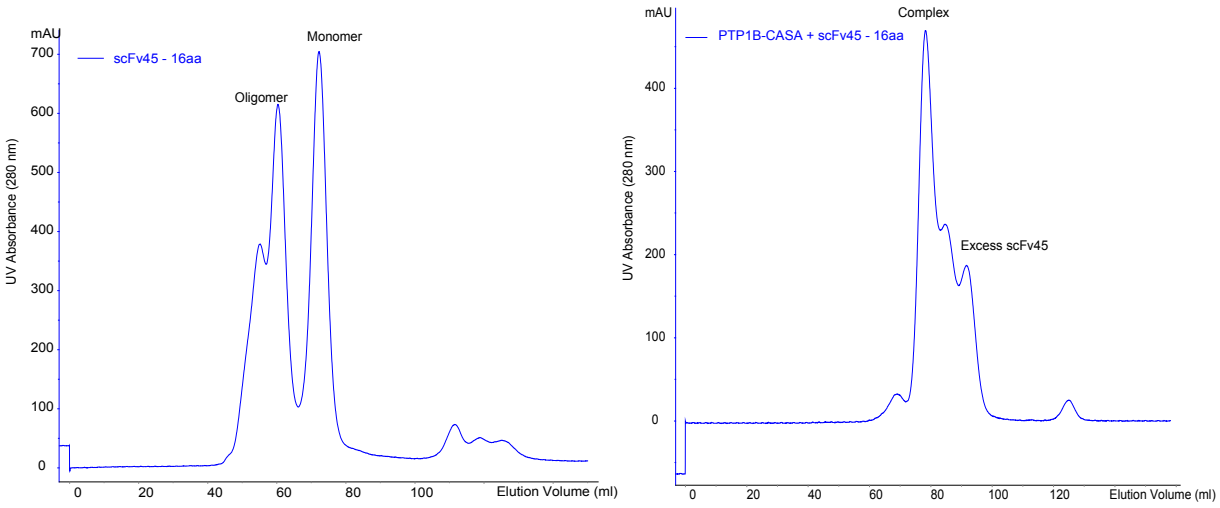

Figure 2.8 Purification of scFv45 Linker Mutants. We tested the purification of scFv45 proteins containing a series of linker lengths connecting their V_L and V_H domains in order to search for a construct that does not aggregate as scFv45-SL does, forms a complex with PTP1B-CASA and has lower solubility than scFv45-LL, which has a very nucleophilic linker. We systematically cloned linkers of 12, 14, 15 and 16 residues and analyzed their homogeneity by their profile on size exclusion chromatography with a SuperDex75 column. We compared their purification profile with that of scFv45-SL and scFv45-LL as an indicator of our ability to isolate a pure monomer protein population.

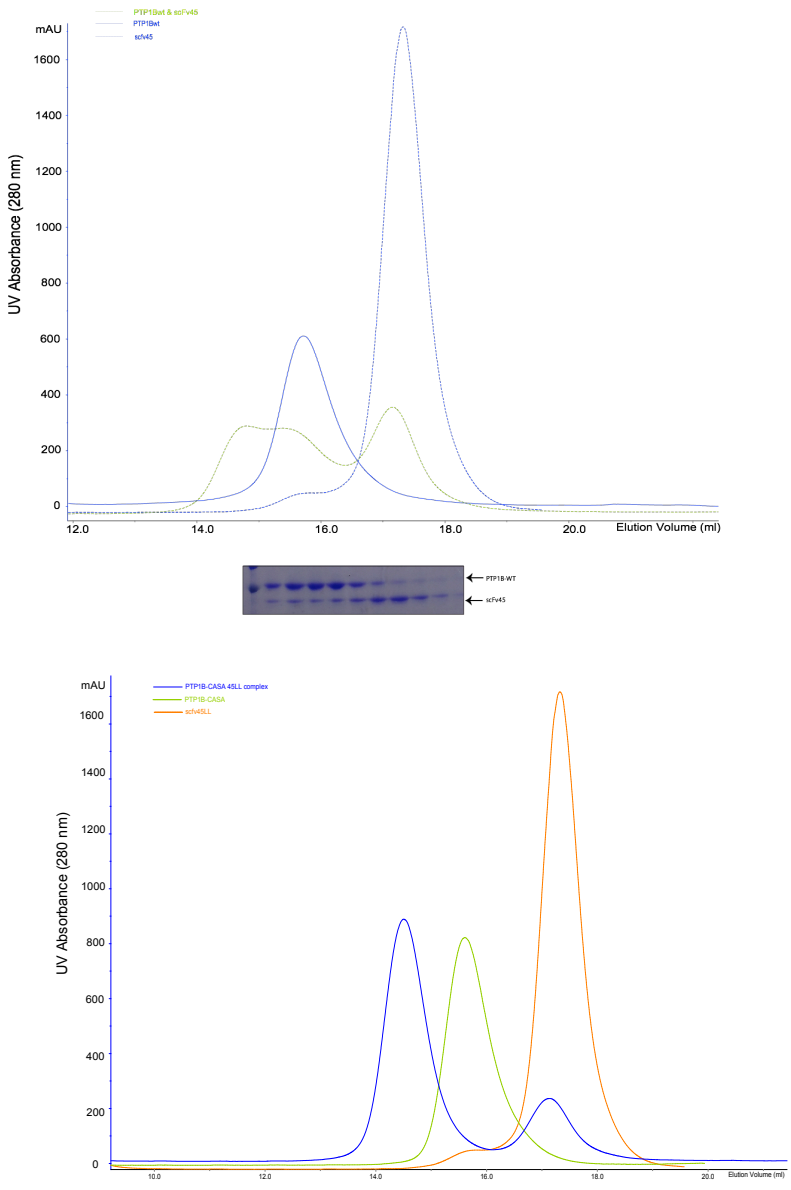

Figure 2.9 Reduced PTP1B-WT is not bound by scFv45-LL. (A) We tested the lack of binding between scFv45-LL and PTP1B-WT under reducing conditions (green line). The two proteins were incubated for binding in the same manner PTP1B-CASA is, for 30 min, at 20°C. Instead of a large peak for the complex and second peak for excess scFv45 as in Figures 2.5 and 2.9 we observe a broadened peak representing elution of reduced PTP1B-WT and a small amount of nonspecific binding. PTP1B-WT is 37 kDa and elutes first. Essentially all the scFv45 protein, which is 27 kDa elutes immediately after PTP1B-CASA; if a complex was formed we could expect to see a larger complex peak and a small excess peak. (B) PTP1B-CASA and scFv45-LL complex is illustrated for comparison. In this case there is a peak with Gaussian distribution for the complex, which elutes earlier than the PTP1B-CASA and scFv45 proteins.

Chapter 3

Defining the Binding Specificity of scFv45 to oxPTP1B

3.1 Introduction

When PTP1B was initially sequenced, it was observed that it shared 75% sequence identity in the catalytic domain with TCPTP as illustrated in Figure 3.1 (Charbonneau 1989, Cool 1989). In their reduced state the crystal structures of the enzymes are similar, with differences appearing primarily in loop areas exposed to the surface (Figure 3.1) (Iversen 2002). Nevertheless, both biochemical studies and knock-out mouse models have illustrated that they serve distinct biological functions.

TCPTP is ubiquitously expressed in all tissues and cell types and at all developmental stages. Two variants of TCPTP are expressed through alternative splicing of the gene: a 48 kDa form, which is targeted to the ER by a hydrophobic C-terminal sequence, and a 45 kDa variant that is targeted to the nucleus via a bipartite nuclear localization sequence. Despite this nuclear localization sequence, the 45 kDa form of TCPTP can exit the nucleus in response to stimuli such as insulin/EGF and dephosphorylate substrates in the cytoplasm and at the plasma membrane (Lam 2001, Galic 2003). TCPTP substrates include both receptor tyrosine kinases such as IR, EGFR, PDGF and non-receptor tyrosine kinases such as c-Src, Fyn, Lck, JAK-1, -3 as well as transcription factors STAT-1, -3, -5, -6 (Tiganis 1998, Simoncic 2002, Yamamoto 2002, Galic 2003, Persson 2004, Shields 2008, Wiede 2011).

TCPTP and PTP1B exhibit a high degree of substrate selectivity in a cellular context as illustrated in the distinct phenotypes of mouse models of knockout PTP1B and TCPTP. In contrast to PTP1B-deficient mice, which exhibit improved insulin and leptin signaling, TCPTP -/- mice, physically normal at birth, by 2 weeks of age develop systemic inflammatory disease and succumb to severe anemia by 5 weeks of age (You-Ten 1997, Heinonen 2004). Molecular studies have also illustrated their differential preference for a number of specific substrates. Whereas TCPTP dephosphorylates JAK1/3, PTP1B has a preference for JAK2, the leptin receptor co-activator. An elegant example of their specificity was highlighted by their roles in the regulation of Src. PTP1B dephosphorylates the inhibitory Y529 site to activate Src, and TCPTP dephosphorylating Y418 on the activation loop, to inactivate Src (Bjorge 2000, van Vliet 2005). In the context of insulin signaling, PTP1B and TCPTP dephosphorylate the tandem pTyr 1162/1163, not redundantly, but rather in a coordinated manner regulating the intensity and duration of phosphorylation (Galic 2005). In cells that are either PTP1B -/- or TCPTP -/- the

phosphorylation of PI3K/Akt was prolonged, compared to wild type cells. In PTP1B and TCPTP double knock out cells the phosphorylation was prolonged even further. PTP1B-/- cells showed increased levels of IR phosphorylation at Y1162/1163 compared to control, but dephosphorylation occurred within the same time frame for both. Meanwhile in TCPTP-/- cells, IR Y1162/1163 phosphorylation was sustained for an extended period of time, suggesting the timing of dephosphorylation by TCPTP and PTP1B are different.

Both TCPTP and PTP1B attenuate CNS insulin and leptin signaling. In hypothalamic neurons leptin hormone signals via JAK2/STAT3 and JAK2/IRS2/PI3K, whereas insulin signals via IR/IRS2/PI3K to promote expression of anorexigenic neuropeptide POMC and repress expression of orexigenic neuropeptides AgRP and NPY. Overall the physiologic effect of insulin and leptin signaling into the hypothalamus is of increasing energy expenditure and reduction of eating, by signaling satiety. The hypothalamus is critical in coordinating glucose homeostasis and energy balance in response to peripheral signals from insulin and leptin. Inhibitors of PTP1B would potentiate both insulin and leptin signaling and increase their normal physiologic roles.

Due to their structural similarity, it is likely that highly potent inhibitors targeting the catalytic site of PTP1B would show some degree of inhibition of TCPTP activity as well. Our lab's approach to generating scFvs that can stabilize oxPTP1B and inhibit its reactivation has thus far produced scFv45, which is highly selective for oxPTP1B over TCPTP. ScFv45 did not bind oxTCPTP *in vitro* or in 293T cells stimulated with insulin. This is remarkable as both phosphatases are reversibly oxidized upon insulin stimulation (Meng 2004). Although the crystal structures of reduced PTP1B and TCPTP overlap significantly, there are distinct sequence and structural differences, particularly in the surface exposed loops. In our quest for defining the binding interface between scFv45 and oxPTP1B, and absent any crystals, we tried to use sequence and structural differences between the two enzymes for comparative studies. We generated mutant constructs of PTP1B and TCPTP in which residues surrounding the active site were swapped between the two enzymes as listed in Figure 3.1.

We used chimeric mutants of PTP1B and TCPTP to analyze changes in their interaction with scFv45. First we pursued systematic *in vitro* binding assays between scFv45 and each of the mutants in a reversibly oxidized state. We wanted to corroborate our findings with an alternative approach, and preferably one that involved some structural information. We

have validated our observation from the binding assays with proteolysis protection coupled with mass spectrometry. These assays can convey a broader interaction interface where scFv45 binds to PTP1B-CASA by indicating which PTP1B peptides are protected from proteolysis.

3.2 Methods

3.2.1 Recombinant Protein Preparation

The catalytic domain, 37kDa, of human PTP1B-WT was expressed in BL21-RIPL *E.coli* cells from a pET21b vector, which contains a C-terminal His-tag. Colonies harboring the expression plasmid were grown in a starter culture of LB media and ampicilin (50 µg/ml) at 37°C for 4 hours. The starter culture was expanded to 1L and expression of recombinant protein was induced with 1mM IPTG at the optimal growth phase as indicated by an OD_{600nm} of 0.7. Protein was expressed overnight, at 18°C, shaking at 200 rpm. Cells were harvested by centrifugation, at 3000 x g for 30 min, and resuspended in lysis buffer (50 mM HEPES, pH 7.4, 100 mM NaCl, 20 mM Imidazole, 5mM βME). For storage cells were flash frozen in liquid nitrogen and stored at -80°C. Frozen cells were thawed and lysed by sonication on ice and lysates were cleared by centrifugation at 35,000 x g at 4°C, for 50 min. The cleared lysate was incubated with 1mL of Ni-NTA resin (Qiagen) per 1.5 L of culture for 1 hour at 4°C on a rolling shaker. The resin was applied to a gravity flow column and washed extensively with 10 column volumes of lysis buffer, a high salt concentration wash buffer (50 mM HEPES, pH 7.4, 500 mM NaCl, 20 mM Imidazole, 5mM βME), and lysis buffer again. The bound protein was finally eluted with 3 column volumes of elution buffer (50 mM HEPES, pH 7.4, 100 mM NaCl, 250 mM Imidazole, 5 mM βME). Fractions containing PTP1B-CASA were pooled together and buffer exchanged into storage buffer (50mM HEPES pH 7.4, 150 mM NaCl, 5 mM DTT and 50% glycerol)

3.2.2 Activity Assays

Reduced carboxamidomethylated and maleylated lysozyme (RCML) was labeled with ^{32}P using recombinant GST-FER kinase to stoichiometry up to 0.8 mol ^{32}P incorporated/mol of protein. PTP1B (1-321)-WT and PTP1B-mut 1-6 purified as described in section 3.2.1 above were mixed with varying concentrations of ^{32}P-RCML (0-100nM) in phosphatse assay buffer (50 mM HEPES, pH 7.0, 100 mM NaCl, 0.1% BSA, 5 mM TCEP) and incubated at 30°C for 10min.

The reaction was stopped with 10 %TCA (final) with 2.5% (w/v) BSA, incubated at -80°C for 30 min, and thawed at room temperature. The supernatant was collected and the CPM was determined by scintillation counting. Specific activity of the mutant proteins was compared with that of wild type protein.

3.2.3 Reversible Oxidation and Reactivation PTP Assays

PTP1B and TCPTP (100nM) were oxidized with a range of H_2O_2 concentrations for 10 min, at 20°C. From the oxidation reaction 10 nM of protein (PTP1B and TCPTP) were collected and subsequently used for a reduction/reactivation reaction carried with addition of TCEP (5 mM) in assay buffer (50 mM HEPES, pH 7.0, 100 mM NaCl, 5mM DTT, 0.1 mg/mL BSA, 2mM EDTA). The reactivation was monitored with activity assays performed with the fluorogenic substrate DiFMUP (5 μM, Molecular Probes). Recovery of activity constitutes reactivation of the enzyme from reversible oxidized form of sulphenic acid to the reduced, active thiolate form. The fraction of activity recovered is normalized relative to wild-type phosphatase that was not treated with H_2O_2 and expressed in parallel with oxidized enzyme (no TCEP samples).

3.2.4 *In vitro* binding assay for scFv45 with PTP1B and TCPTP mutants

In order to test interaction between scFv45 and mutants of PTP1B and TCPTP we performed an *in vitro* binding assay using recombinant protein purified as described in section 3.2.1 above. Purified phosphatase (50 nM) was reversibly oxidized with 250 μM H_2O_2 followed by buffer exchange to removed excess H_2O_2. Purified scFv45 was incubated in molar excess (50x) with oxPTP1B-WT and oxPTP1B-muts1-6 and we tested their binding by immunoprecipiation. For mut1 and mut2 we tested binding with a range of scFv45 concentrations, from 0.5-50 times molar excess. Immunoprecipitation was carried out at 4°C, overnight, in binding buffer (20 mM HEPES, pH 7.4, 300 mM NaCl, 0.05% BSA, 0.05% Tween-20 and protease inhibitor [Complete Protease Inhibitor Cocktail from Roche]). Protein complex bound to HA-affinity matrix (Roche, clone 3F10) was pulled down and washed 3 times, at 4°C. The complex was resolved by SDS-PAGE and we used anti-PTP1B (FG6 clone) antibodies to detect PTP1B-WT and PTP1B-mutants.

In parallel recombinant TCPTP (50nM) –WT and –muts1-6 was reversibly oxidized with 250 μM H_2O_2 and an immunoprecipitation assay was carried out after excess H_2O_2 was removed. Binding was detected with anti-TCPTP (R&D, MAB1930).

3.2.5 Proteolysis Protection of PTP1B by scFv45 Coupled with Mass Spectrometry

These experiments were conducted in collaboration with Dr. Chris Bonham, a postdoctoral fellow with expertise in mass spectrometry who has joined the Tonks lab a year ago. We conducted digestion of PTP1B-CASA alone, scFv45 alone and a complex of PTP1B-CASA or PTP1B-CASA-mut2 with scFv45 in order to detect any proteolytic changes that the binding of scFv45 might protect from. The complex was formed by incubation of PTP1B-CASA or PTP1B-CASA-mut2 with scFv45 on ice for 20 min. We used 1:1.1 PTP1B to scFv45, 300 ng/μL and 240 ng/μ, respectively. We tested several proteases based on the amino acids available in the first 60 residues of PTP1B. As such we have tested enzymes that cleave C-terminal to lysine and glutamic acid, N-terminal to aspartic acid as well as trypsin, which cleaves C-terminal to arginine and lysine residues. We initially conducted a pilot experiment where we used a broad range of protease concentrations from 1: 1000-1:50, for a range of time periods from 0-16 hours. The data was collected from samples digested with 1:500 AspN and 1:750LysC, for 0-480 min. The proteolytic reaction was split into 2 equal volumes for analysis. Half was used for SDS-PAGE analysis, and for this purpose proteolysis was stopped with 2.5x protease inhibitor (Roche). For MALDI/MS analysis we stopped the reaction by addition of 65% ACN and 0.1% TFA and used ~700 fmol protein for optimal sensitivity and spectral quality.

3.3 Results and Discussion

3.3.1 scFv45 Does Not Bind oxTCPTP or Inhibit Its Reactivation

It has been shown in our lab that although TCPTP and PTP1B are both reversibly oxidized in mammalian cells, scFv45 only binds oxPTP1B, and does not bind oxTCPTP (Figure 3.2) (Haque 2011). Binding assays *in vitro* show that for a range of scFv45 concentrations, using as much as 50 times molar excess scFv45 did not result in an interaction with reduced or oxidized TCPTP. By comparison oxPTP1B is immunoprecipitated with as little as 0.5 molar equivalent of scFv45, as the two proteins form a complex in equimolar ratio.

We compared the reversible oxidation profile of TCPTP and PTP1B with a range of H_2O_2 concentrations and reactivating with TCEP as a reducing agent. Monitoring their recovery of phosphatase activity with the fluorogenic substrate DiFMUP we observed that TCPTP (10nM) is reactivated within a narrower range of H_2O_2 compared to PTP1B (Figure 3.3). Importantly we see that TCPTP is reversibly oxidized and can be reactivated. It also suggests that scFv45 binding to oxPTP1B is selective for the enzyme, more so than for example simple recognition and binding of sulphenic acid or sulphenamide conformation. Using in vitro activity assays we also tested whether introducing scFv45 to oxTCPTP would inhibit the reactivation of TCPTP. As scFv45 binds oxPTP1B we see loss of reactivation in a dose response manner. However with oxTCPTP, there is no binding by scFv45 and phosphatase activity is regained (Figure 3.2).

3.3.2 PTP1B Residues that Confer Specificity to scFv45 Binding

As described in the results section 3.3.1, although PTP1B and TCPTP are similar in tertiary structure, scFv45 binds oxPTP1B selectively and does not bind oxTCPTP. Comparison of the catalytic domain primary sequence of PTP1B and TCPTP illustrated several regions containing residues that varied between the two enzymes, whereas the vast majority of the sequence is identical on alignment (Figure 3.1). Several of the regions containing different residues between the 2 enzymes map around the catalytic site based on the tertiary structure. Prior characterization of scFv45 also showed that it only binds oxPTP1B, and not reduced PTP1B. Given that the major conformation changes between the oxidized and reduced forms of PTP1B occur in the catalytic cleft, with the Tyr46 and the loop containing Cys215 splaying out from the cleft and onto the surface as illustrated in Figure 1.8 it suggests that scFv45 is likely binding in the region that becomes surface exposed when the conformation changes. Mutants generated wherein the residues in these regions are substituted from PTP1B into TCPTP and vice versa were used for binding analysis with scFv45 (Figure 3.4). Binding analysis of scFv45 and reversibly oxidized PTP1B mutants indicated that when 3 particular residues are mutated, it leads to loss of binding between PTP1B and scFv45 (Figure 3.4). PTP1B-mut2, containing L37F/K39E/K41R is no longer co-immunoprecipitated by scFv45 as PTP1B-WT and PTP1B mut1 (S28H/F30Y/C32H) and mut3 (F52Y) are. Even more striking, introducing the F39L/L41K/R43K residues in TCPTP introduced binding between oxTCPTP-mut2 and scFv45 (Figure 3.4). Although scFv45 bound oxTCPTP-mut2 it did not bind reduced TCPTP-mut2, indicating that the oxidation induced conformational change is important to the binding.

We tested the binding of wild type enzyme, both PTP1B and TCPTP, as well as -mut1 and -mut2 with a broad range of scFv45 concentrations with a representative image show in Figure 3.4. PTP1B-mut2 abrogates binding to scFv45, and the protein is found in the supernatant. Meanwhile, oxPTP1B-mut1 exhibited a slight increase in binding to scFv45 compared to oxPTP1B-wt. Even at low concentrations of scFv45 it binds oxTCPTP-mut2.

We tested whether any of the 3 residues in –mut2 were more important than the others. We generated mutants wherein 1 or 2 parental residues were re-introduced in PTP1B-mut2 and TCPTP-mut2 (Figure 3.5). PTP1B binding assays with scFv45 suggest that leucine 37 and lysine 39 are both important for the interaction as the protein regains binding when they are reintroduced into PTP1B-mut2. Conversely when leucine and lysine residues are mutated in TCPTP-mut2 back to parental phenylalanine and glutamic acid they abrogate binding between scFv45 and oxTCPTP-mut2. Binding was also lost under reducing conditions just as it was with the binding assays of the original mutant. Therefore both the conformational change that occurs with oxidation and at least 2 of the residues in –mut2 are important for mediating the interaction.

Oxidation and reactivation assays of PTP1B-mut2 in the presence of scFv45 showed no functional inhibition of reactivation. Reactivation of PTP1B-mut1 was actually inhibited with a lower IC_{50} than PTP1B-WT Figure 3.6. Activity assays using the artificial substrate ^{32}pTyr-RCML have indicated that all the mutant enzymes have retained their enzymatic activity. The specific activity of each of the mutants of PTP1B is comparable to that of the wild type enzyme. Similarly, the mutants of TCPTP showed activity similar to that of the wild type enzyme. PTP1B-mut1 and PTP1B-wt have similar oxidation/reactivation profiles (Figure 3.6). Activity of PTP1B-mut1 and PTP1B-WT after oxidation with a range of H_2O_2 and addition of reducing agent was recovered in a similar pattern. By comparison, activity of oxPTP1B-mut 2 could be recovered within a lower narrower range of H_2O_2 treatment, which interestingly is a pattern similar to oxidation and reactivation of TCPTP-WT.

3.3.3 Proteolysis Protection Coupled with Mass Spectrometry Analysis

We have used proteolysis coupled with mass spectrometry to corroborate the binding observations from the co-immunoprecipitation assays. We hypothesized that as scFv45 and oxPTP1B bind with high affinity (15-20 nM), the presence of bound scFv45 would hinder

proteolysis of PTP1B by sequence specific proteases around the respective surface of PTP1B. Mass spectrometry (MALDI-TOF) was used to detect the PTP1B peptides produced by proteolysis with proteases specifically chosen to target sequences in the N-terminal 60 residues of PTP1B. We observed there was a specific difference in the MS analysis of peptides from PTP1B-CASA treated with proteases as compared to PTP1B-CASA in complex with scFv45 (Figure 3.7).

3.3.4 Digestion with Enzyme cleaving N-terminal to Aspartic Acid (AspN)

There are two cleavage events upon treatment with AspN enzyme that can occur within the N-terminal region that was also highlighted by PTP1B-CASA-mut2 in binding assays previously described. There are two peptides that appear on the MS profile that are located in the N-terminal region of interest in PTP1B (Figure 3.8). One peptide with a mass of ~2520 m/z corresponding to N-terminal cleavage at the aspartic acid residue 22 results in a peptide of residues 22 residues. The other peptide of mass ~827 m/z, corresponds to N-terminal cleavage at residues 22 and 29, yielding a 6 residue peptide. Both of these peptides appear on the spectra for PTP1B-CASA cleaved with AspN (Figure 3.8A).

The complex of PTP1B-CASA and scFv45 by comparison gave rise to the peptide 1-21, 2520 m/z, but the peptide 22-28 could not be observed even when proteolytic digestion was allowed to occur for as long as 30 minutes (Figure 3.8A). This indicates that aspartic acid 29 is not accessible for proteolysis by AspN enzyme when scFv45 has bound to PTP1B-CASA, and thus that scFv45 protects from proteolysis within a peptide region that starts after residue 22 and contains residue 29 within it.

Binding of oxPTP1B-mut2 and scFv45 was abrogated by substitution of just 3 residues from TCPTP. We repeated the AspN proteolysis experiment with PTP1B-CASA-mut2 in the presence and absence of scFv45 and observed the same digestion pattern regardless of scFv45 presence (Figure 3.8B). As scFv45 did not bind PTP1B-mut2 in co-IP assays (Figure 3.4), and did not bind and inhibit its reactivation (Figure 3.7) we expected that it would also not protect from AspN cleavage N-terminal to aspartic acid 29. There is a 3rd aspartic acid in this sequence, residue 11, which did not appear on any of the spectra. We do not expect this was due to protection but rather to optimal length of a peptide that would be required for binding of the protease in order to cleave.

3.3.5 Digestion with Enzyme Cleaving C-terminal to Lysine (LysC)

Complementary to the AspN cleavage experiments I described above we also used an enzyme that cleaves C-terminal to lysine residues. There are several lysine residues in PTP1B within the first 60 residues as highlighted by blue arrows in Figure 3.9. MS analysis of peptides from LysC proteolysis of PTP1B-CASA in complex with scFv45 indicates protection around a peptide extending from Lys42 to Lys58, (2163 m/z). This peptide appears in the MS profile by 30 min and in the case of PTP1B-CASA, without scFv45, it continues to grow in intensity faster than any other peptides observed on the spectra. Digestion of PTP1B-CASA in complex with scFv45 also produced the 2163 m/z peptide, however its intensity is much lower at the 30min time point than in the spectra for PTP1B-CASA without scFv45. MS analysis at several time point illustrates the progression in proteolysis illustrates: in PTP1B-CASA the Lys42-Lys58 peptide that appears at 2163 m/z increases from the earliest time point at 30 to the last time point at 240min.

Comparison to a C-terminal peptide, representing cleavage at Lys293 and Lys314, mass ~ 2511 m/z, can be used to estimate the extent of scFv45 protection. The C-terminal peptide is equally accessible to proteases whether scFv45 is present or not, and therefore its intensity will be constant. Comparison of the intensity of the C-terminal peak (2511 m/z) and N-terminal peak (2163 m/z) shows that without scFv45 the N-terminal peak at 2163 m/z is much more prominent than the C-terminal peak at 2511 m/z. In the presence of scFv45 the intensity of the N-terminal peak decreases. This indicates that the presence of scFv45 hinders access of the protease to the N-terminal peptide containing Lys42-Lys58, and less of this peptide is produce and detected by MS.

3.4 Figures

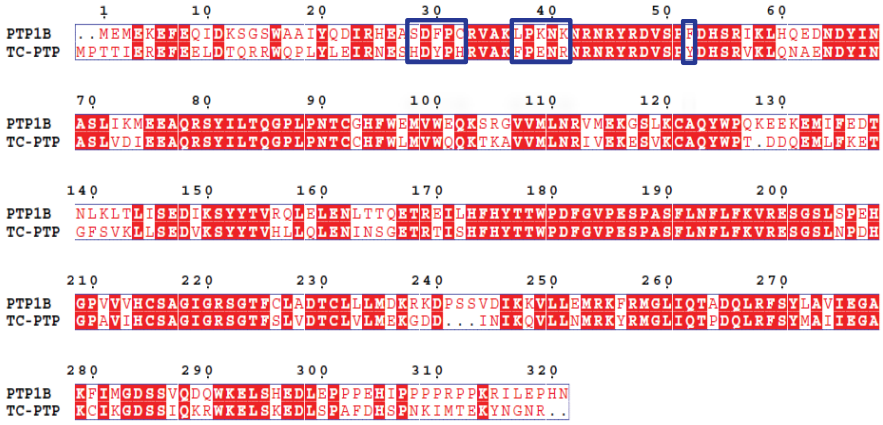

PTP1B → TCPTP mutants	TCPTP→ PTP1B mutants
1B-mut 1 → S28H/F30Y/C32H	TC-mut 1 → H30S/Y32F/H34C
1B-mut 2 → L37F/K39E/K41R	TC-mut 2 → F39L/E41K/R43K
1B-mut 3 → F52Y	TC-mut 3 → Y54F
1B-mut 4 → mut 1/mut 2	TC-mut 4 → mut 1/mut 2
1B-mut 5 → mut 1/mut 3	TC-mut 5 → mut 1/mut 3
1B-mut 6 → mut 2/mut 3	TC-mut 6 → mut 2/mut 3

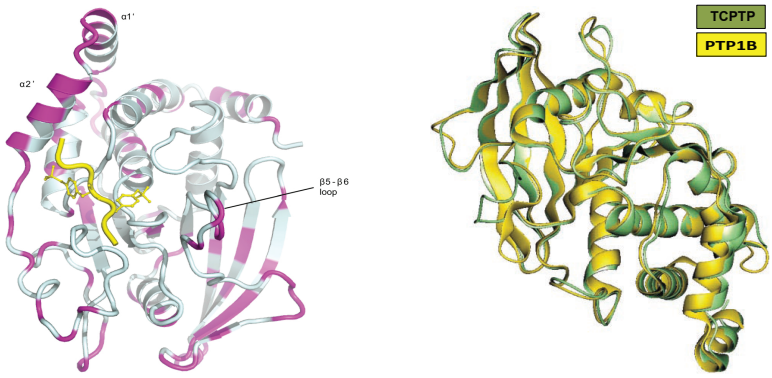

Figure 3.1 Chimeric Mutants Informed by Comparison of PTP1B & TCPTP. Amino acid sequence alignment of the catalytic domains of PTP1B (1-321) and TCPTP (1-317) shows a high degree of similarity. Three regions potentially important in the binding of scFv45 to oxPTP1B are highlighted. Chimeric mutants of TCPTP and PTP1B were generated in which amino acids were swapped between the 2 phosphatases. These residues map on α-helices located around the catalytic site. Tertiary structure of PTP1B (reduced) in which the silver color denotes residues that are identical between TCPTP and PTP1B and magenta highlights residues that are different. Adjacent are structures of both TCPTP and PTP1B showing the highly similar tertiary structure, with difference mainly observed in the loops that are surface exposed.

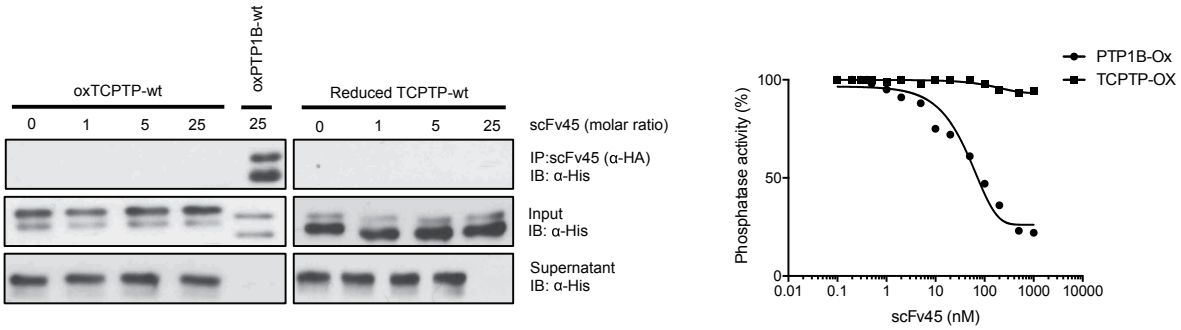

Figure 3.2 scFv45 binds specifically to oxPTP1B *in vitro,* and does not bind oxTCPTP
Reversibly oxidized wt-PTP1B (1-321) and wt-TCPTP (1-317) were assayed for immuno-precipitation with scFv45 using a HA-tag at the C-terminal end of scFv45 and anti-HA antibodies coupled to matrix. Quantification using ImageJ software indicates 1.5-fold increase in binding of oxPTP1B relative to input.

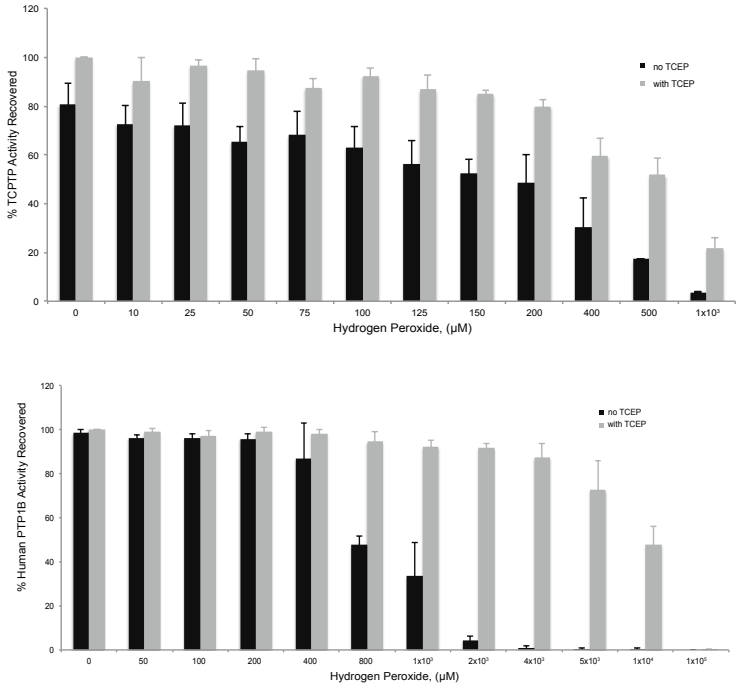

Figure 3.3 Oxidation and Reactivation Profile of PTP1B-wt and TCPTP-wt Recombinant PTP1B-wt (1-321) and TCPTP-wt (1-317) (100nM) were treated with a range of H_2O_2 concentrations as illustrated on the x-axis. Reactivation by TCEP (5mM) was assayed with DiFMUP (5 μM), a fluorogenic substrate.

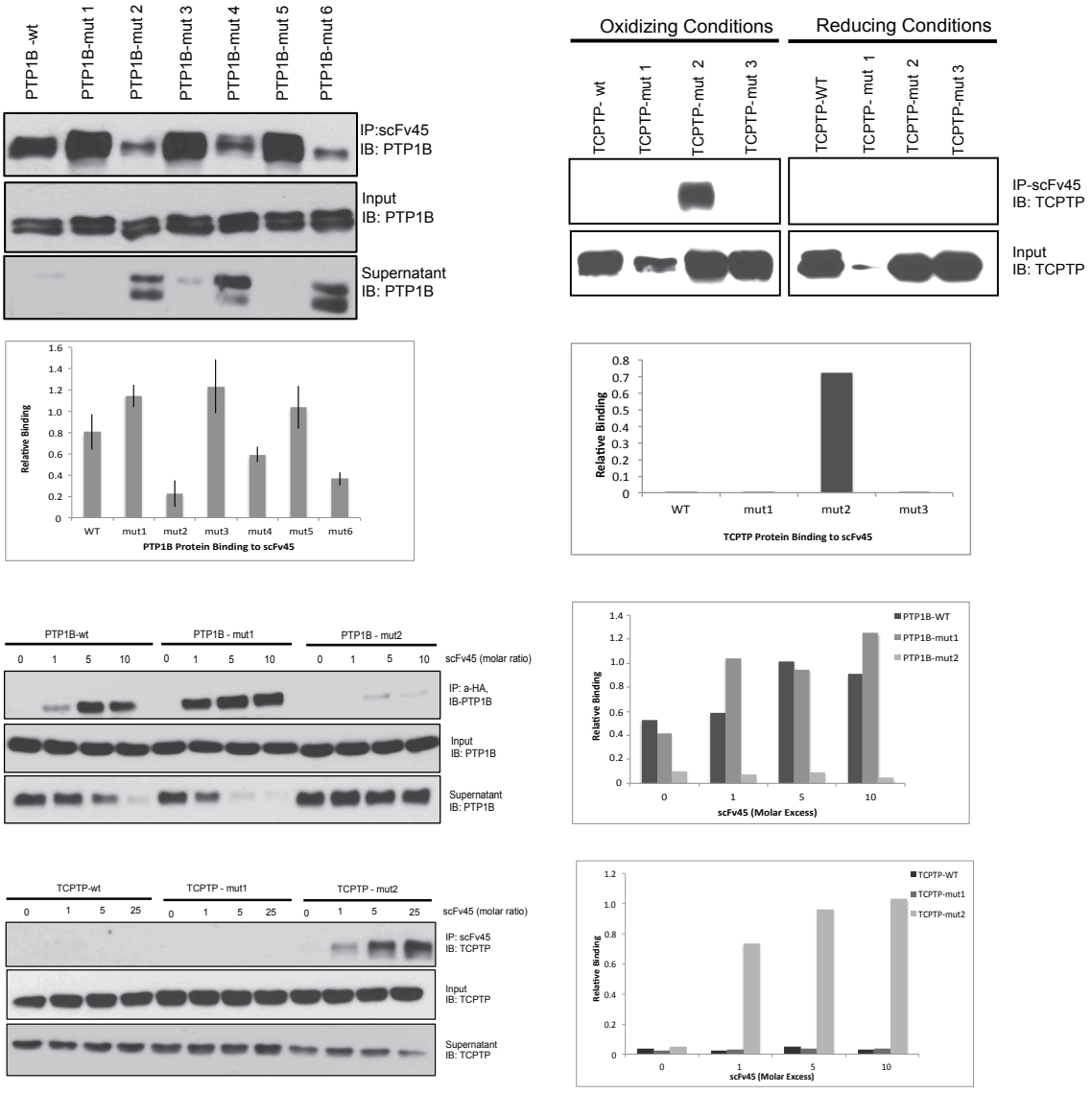

Figure 3.4 Three key residues in PTP1B are important in mediating binding of scFv45
Amino acid sequence alignment of the catalytic domains of PTP1B (1-321) and TCPTP (1-317) shows a high degree of similarity; 3 potential regions of interest are highlight. Chimeric mutants of TCPTP and PTP1B were generated, wherein the residues that map around the catalytic site and are different are swapped between PTP1B and TCPTP.

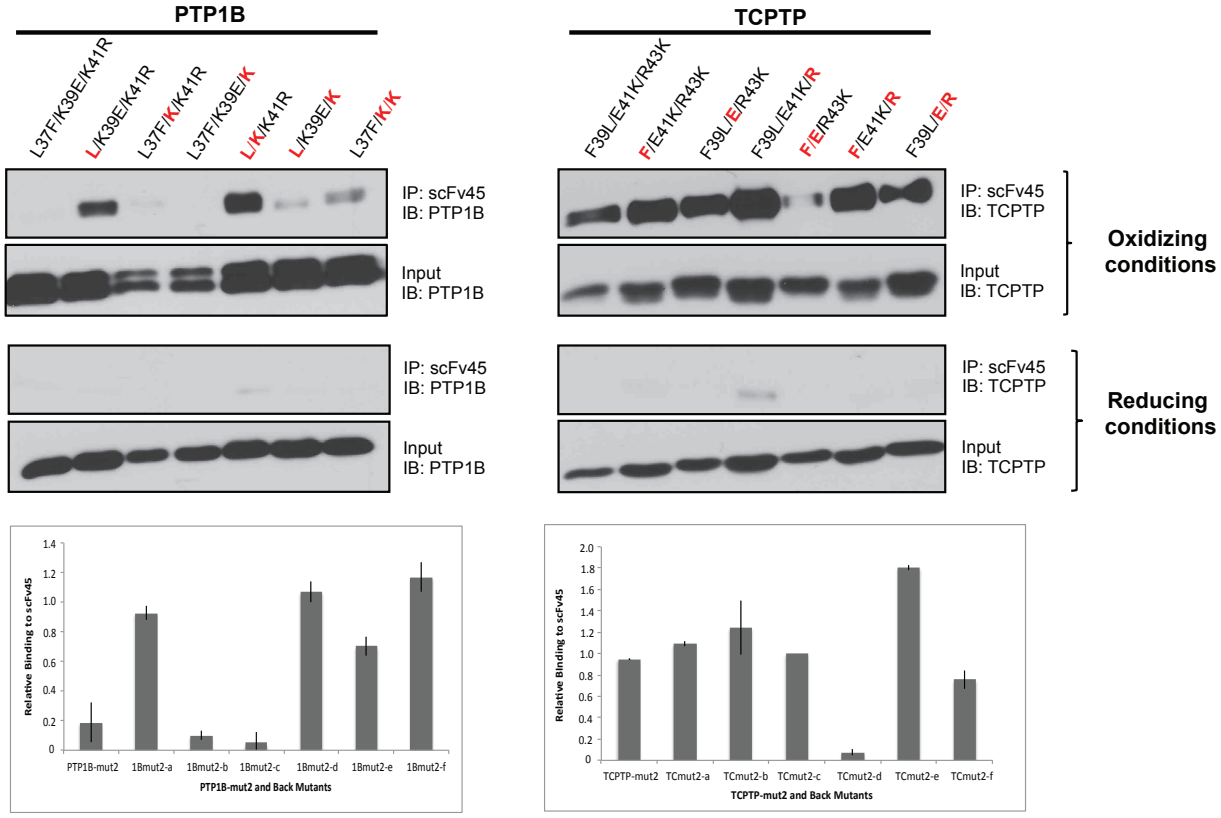

Legend of mutants as abbreviated in the quantification graphs above:

PTP1Bmut2	L37F/K39E/K41R
TP1Bmut2	L37F/K39E/K41R
1Bmut2-a	L/K39E/K41R
1Bmut2-b	L37F/K/K41R
1Bmut2-c	L37F/K39E/K
1Bmut2-d	L/K/K41R
1Bmut2-e	L/K39E/K
1Bmut2-f	L37F/K/K

TCPTPmut2	F39L/E41RK/R43K
TCmut2-a	F/E41K/R43K
TCmut2-b	F39L/E/R43K
TCmut2-c	F39L/E41K/R
TCmut2-d	F/E/R43K
1Bmut2-e	F/E41K/R
1Bmut2-f	F39L/E/R

Figure 3.5 Back-mutation of the residues in PTP1B-mut2 and TCPTP-mut2 key residues in PTP1B are important in mediating binding of scFv45 Mut2 of the chimeric mutants generated by swapping residues between PTP1B and TCPTP indicated that 3 residues were able to abrogate binding in PTP1B and to introduce binding in TCPTP. In order to investigate further whether any of these residues are more important than others I mutated both PTP1B-mut2 and TCPTP-mut2 back to the parental sequence.

	PTP1B-WT	PTP1B-mut1	PTP1B-mut2	PTP1B-mut3	PTP1B-mut4	PTP1B-mut5	PTP1B-mut6	PTP1B-mut7	PTP1B-CASA
Vmax	2885	2579	2546	2642	2452	2399	2726	2045	249.8
Km	196.1	215.1	148.4	254.0	546.6	260.7	291.3	242.9	201.2

	TCPTP-WT	TCPTP-mut1	TCPTP-mut2	TCPTP-mut3	TCPTP-mut4	TCPTP-mut5	TCPTP-mut6	TCPTP-mut7	TCPTP-mut8
Vmax	2832	3028	2842	2788	2803	2610	2788	2445	124.3
Km	205.0	227.9	214.9	206.0	241.1	177.3	196.7	258.4	256.7

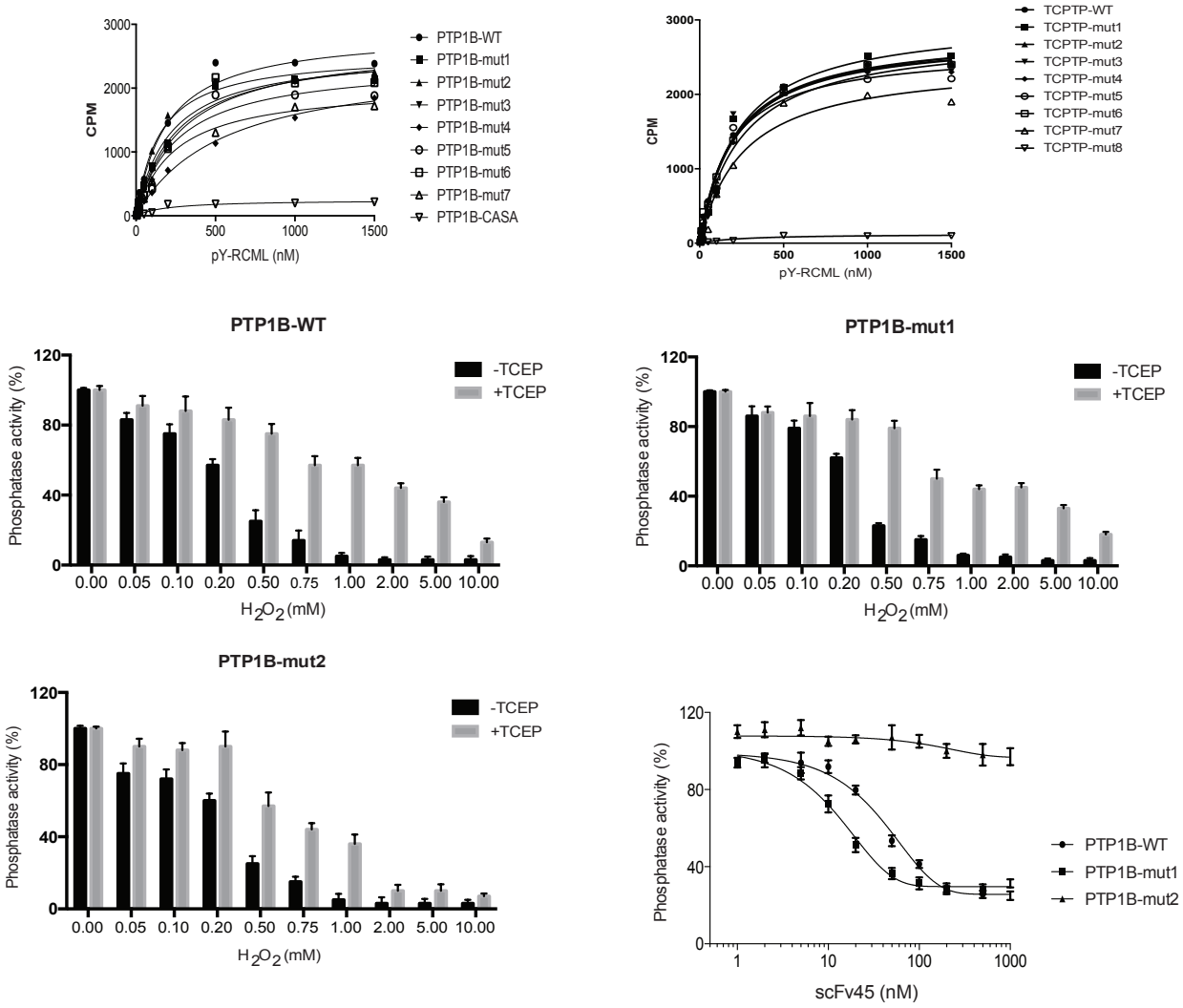

Figure 3.6 (A) PTP Activity Assays of the Mutants. All 7 mutants of PTP1B had comparable activity with wild-type enzyme and similarly all 7 TCPTP mutants have activity similar to wild-type TCPTP. PTP activity was measure using ^{32}P-RCML as the substrate as described in the methods section. **(B) Activity and Oxidation and Reactivation profiles of PTP1-wt, -mut1 and –mut2.** PTP1B-mut1 and PTP1B-wt have similar oxidation/reactivation profiles. Activity was recovered to almost 100% at low concentrations of H_2O_2, and the range of H_2O_2 at which activity could be recovered was similar. PTP1B-mut 2 activity was recovered but within a narrower range of H_2O_2 treatment than PTP1B-wt. The activity of PTP1B-mut2 was also not recovered to 100% even at low concentrations of H_2O_2, which is a pattern similar to TCPTP.

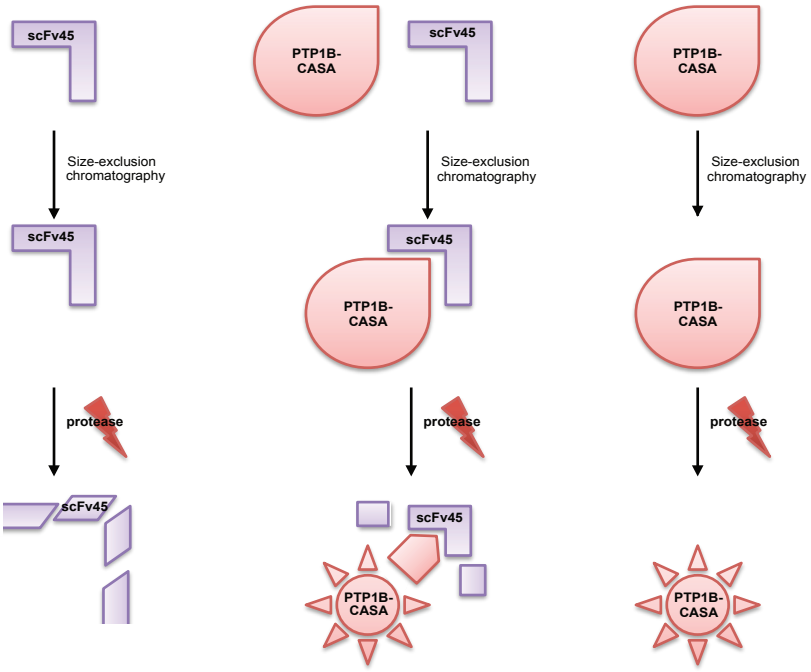

Figure 3.7 Protection Proteolysis Experimental Model Treatment of PTP1B-CASA should lead to proteolysis of the protein, which can be observed by MS analysis. By comparison treatment of PTP1B-CASA in complex with scFv45 as expected yielded a different pattern of digestion based on protection from protease activity around the binding site between the 2 proteins.

A)

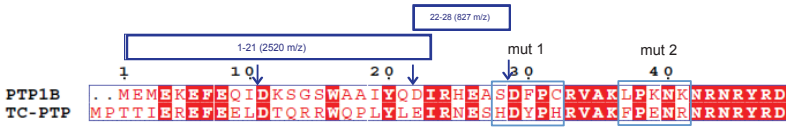

m/z (mi)	m/z (av)	N-terminal residue	C-terminal residue	MSMS	Original Data	Sequence
827.4006	827.8772	22	28	Y	N	(Q) DIRHEAS(D)
1171.538	1172.247	289	297	Y	Y	(Q) DQWKELSHE(D)
1262.66	1263.407	53	62	N	N	(E) DHSRIKLHQF(D)
2067.186	2068.488	300	317	Y	N	(L) EPPPEHIPPPPRPPKRIL(E)
2295.297	2296.738	298	317	N	N	(E) DLEPPPEHIPPPPRPPKRIL(E)
2375.299	2376.812	29	47	N	Y	(S) DFPCRVAKLPKNKNRNRYR(D)
2520.142	2521.845	1	21	Y	Y	(-) MEMEKEFEQIDKSGSWAAIYQ(D)
2772.494	2774.218	298	321	N	N	(E) DLEPPPEHIPPPPRPPKRILEPHN(-)
2901.537	2903.334	297	321	N	N	(H) EDLEPPPEHIPPPPRPPKRILEPHN(-)
3183.682	3185.667	22	47	N	Y	(Q) DIRHEASDFPCRVAKLPKNKNRNRYR(D)
3328.525	3330.699	1	28	N	Y	(-) MEMEKEFEQIDKSGSWAAIYQDIRHEAS(D)
3447.817	3449.962	289	317	N	N	(Q) DQWKELSHEDLEPPPEHIPPPPRPPKRIL(E)
3925.014	3927.442	289	321	N	Y	(Q) DQWKELSHEDLEPPPEHIPPPPRPPKRILEPHN(-)
PTP1B-CASA mut2						
3840.844	3843.296	6	38	N	N	(K) EFEQIDKSGSWAAIYQDIRHEASDFPCRVAKFP(E)

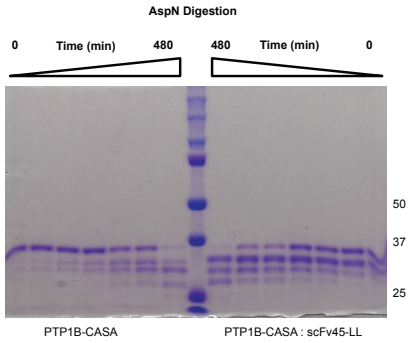

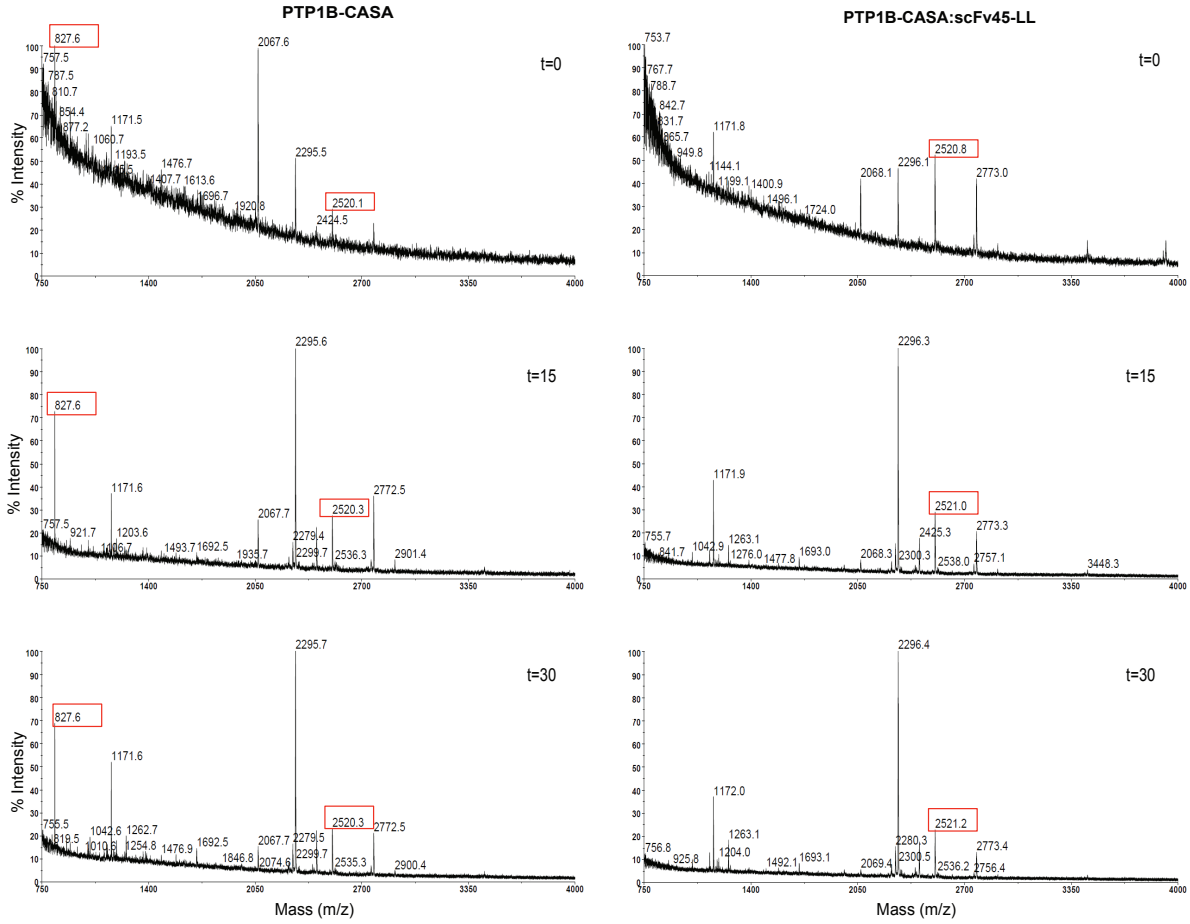

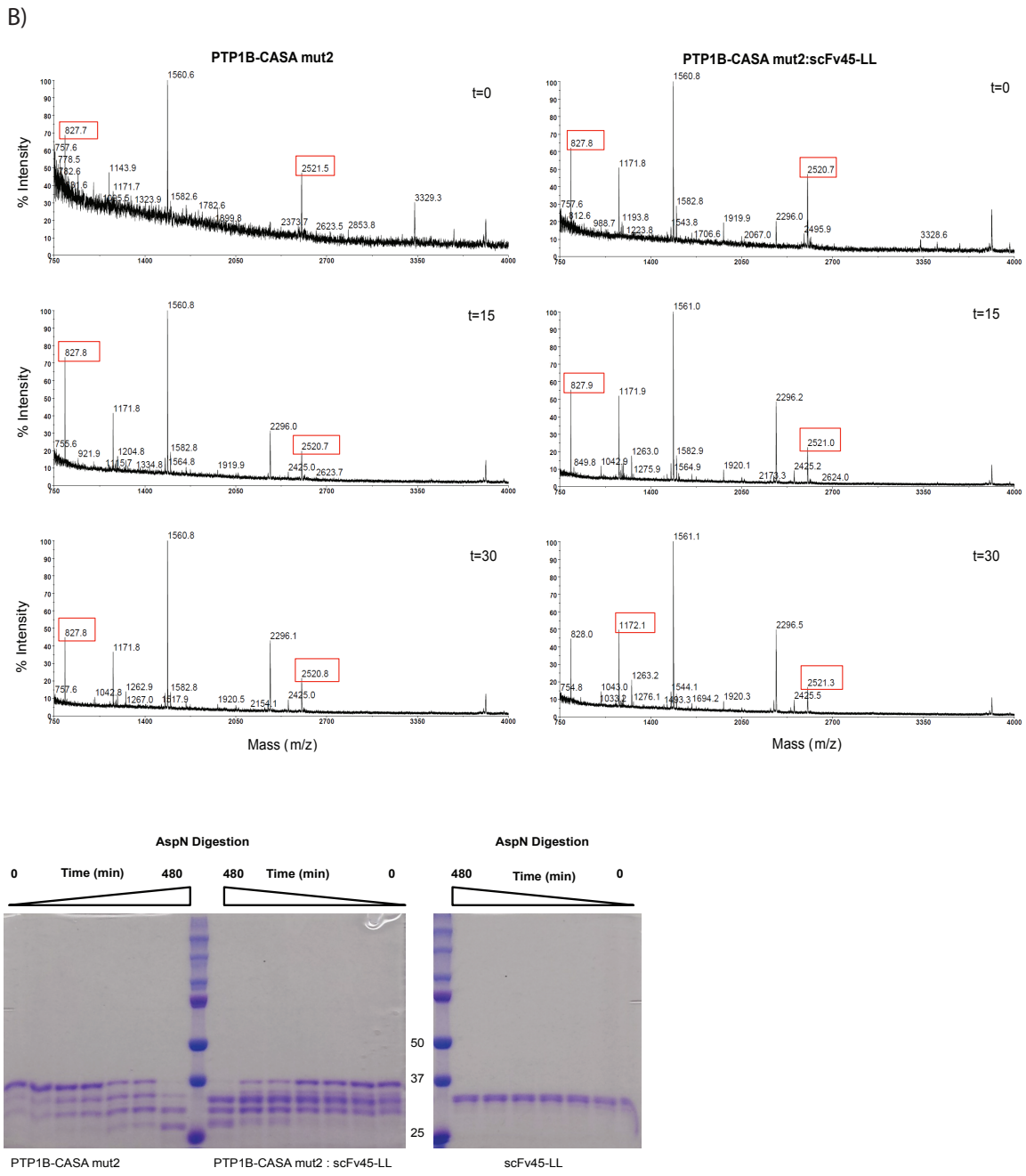

Figure 3.8 Protection Proteolysis with AspN **(A)** Treatment of PTP1B-CASA with proteases led to proteolysis of the protein, which can be observed by MS analysis in the panels on the left. By comparison treatment of PTP1B-CASA in complex with scFv45 as expected yielded a different pattern of digestion based on protection from protease activity around the binding site between the 2 proteins as is observed in the panels on the right. **(B)** Treatment of PTP1B-CASA-mut2, which had abrogated binding to scFv45 by IP, exhibits the same mass spectra whether scFv45 is present, as there is no protection from antibody binding.

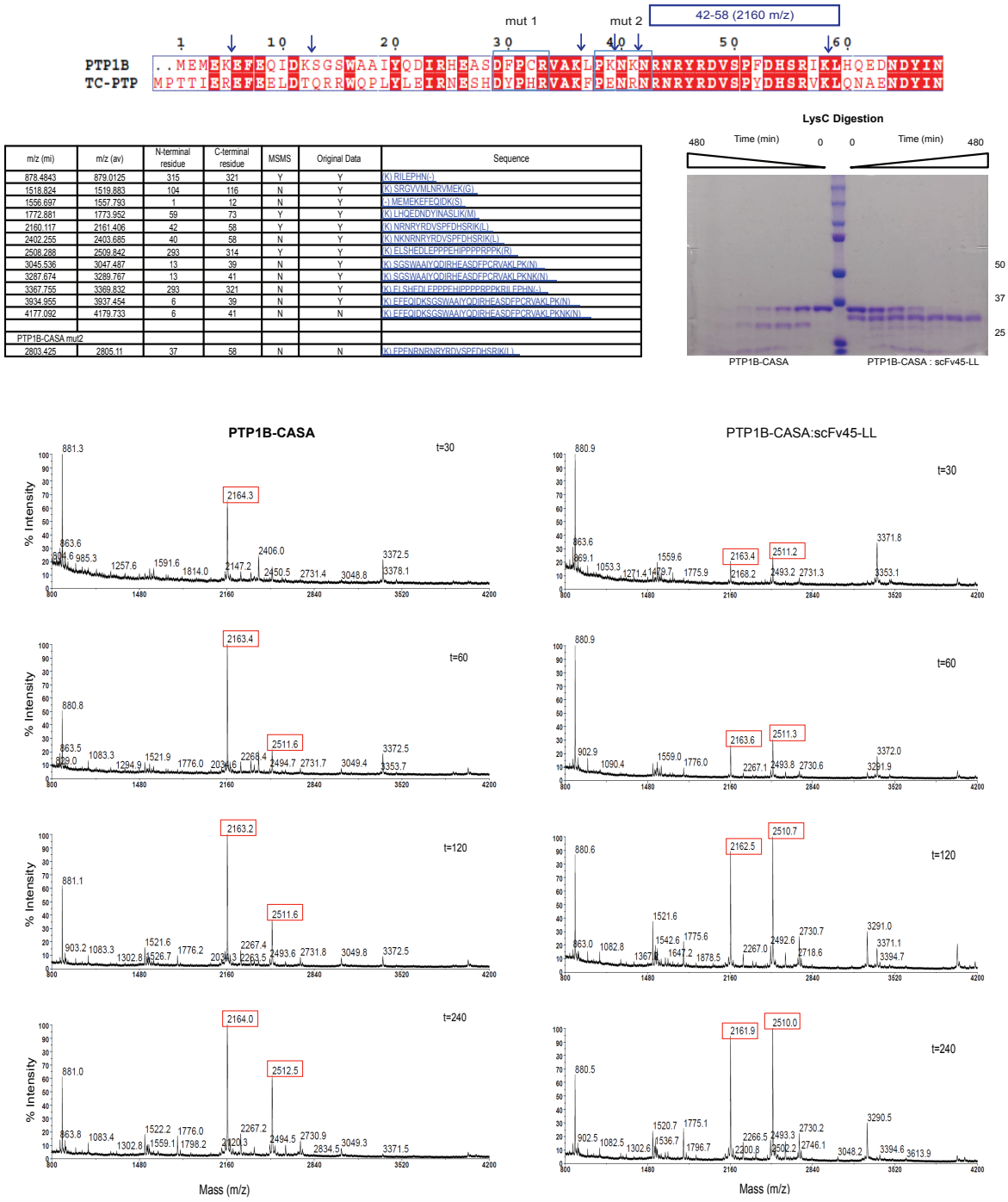

m/z (mi)	m/z (av)	N-terminal residue	C-terminal residue	MSMS	Original Data	Sequence
878.4843	879.0125	315	321	Y	Y	(K) RILEPHN(-)
1518.824	1519.883	104	116	N	Y	(K) SRGVVMLNRVMEK(G)
1556.697	1557.793	1	12	N	Y	(-) MEMEKEFEQIDK(S)
1772.881	1773.952	59	73	Y	Y	(K) LHQEDNDYINASLIK(M)
2160.117	2161.406	42	58	Y	Y	(K) NRNRYRDVSPFDHSRIK(L)
2402.255	2403.685	40	58	N	Y	(K) NKNRNRYRDVSPFDHSRIK(L)
2508.288	2509.842	293	314	Y	Y	(K) ELSHEDLEPPPEHIPPPPRPPK(R)
3045.536	3047.487	13	39	N	Y	(K) SGSWAAIYQDIRHEASDFPCRVAKLPK(N)
3287.674	3289.767	13	41	N	Y	(K) SGSWAAIYQDIRHEASDFPCRVAKLPKNK(N)
3367.755	3369.832	293	321	N	Y	(K) ELSHEDLEPPPEHIPPPPRPPKRILEPHN(-)
3934.955	3937.454	6	39	N	Y	(K) EFEQIDKSGSWAAIYQDIRHEASDFPCRVAKLPK(N)
4177.092	4179.733	6	41	N	N	(K) EFEQIDKSGSWAAIYQDIRHEASDFPCRVAKLPKNK(N)
PTP1B-CASA mut2						
2803.425	2805.11	37	58	N	N	(K) EPENRNRNRYRDVSPFDHSRIK(L)

Figure 3.9 Protection Proteolysis with LysC Treatment of PTP1B-CASA with LysC in the absence of scFv45 lead to a change in mass spectra (left panels) compared to treatment of PTP1B-CASA in complex with scFv45 (right panels). Comparison of the intensity of a N-terminal peptide (2160m/z) indicates more prominent proteolysis at early time points of PTP1B-CASA in the absence of scFv45 than in its presence, and thus protection of cleavage by the antibody. We have used a reference peptide for this relative quantitation.

Chapter 4

Understanding the mechanism of PTP1B redox regulation in a cell model relevant to insulin signaling

4.1 Introduction

Redox regulation of PTPs in response to physiological stimuli and RTK activation is emerging as a regulatory mechanism for controlling PTP-mediated signaling responses and subsequently for regulation of pTyr-mediated signaling. Several labs have demonstrated that PTPs are an important target of ROS in the induction of an optimal response to physiological stimuli, such as insulin, EGF and PDGF (Mahadev 2001, Meng 2002, Meng 2004, Boivin 2008). Stimulation of cells with insulin causes rapid and transient oxidation and reversible inactivation of PTP1B, thus facilitating increased phosphorylation of insulin receptors. The scFv45 molecule identified in our lab recognizes the conformation of oxPTP1B and selectively binds it rather than reduced PTP1B. Our group has demonstrated that transient expression of conformation-sensing scFv45 as an intrabody stabilizes oxPTP1B in insulin stimulated 293T and COS-1 cells and shifts the balance towards tyrosine phosphorylation of IRβ and its downstream targets such as IRS-1 and Akt (Haque 2011). In this context scFv45 functions as an insulin-sensitizer, and illustrates how a small molecule that mimics the effects of scFv45 binding to oxPTP1B could function as a treatment in type 2 diabetes. Importantly, scFv45 potentiates insulin signaling in response to stimulation with the hormone, indicating that it binds only the pool of oxPTP1B generated in the context of oxidation by ROS species generated by the activation of the insulin receptor kinases. Unpublished data from out lab indicates that as a negative regulator of leptin signaling, stabilization of oxPTP1B by co-expression of scFv45 also leads to potentiation of leptin signaling.

The striking phenotype of PTP1B-/- mice was characterized by resistance to diet-induced obesity due to increased leptin sensitivity and improved glucose homeostasis due to increased insulin sensitivity. The mice also exhibited sustained phosphorylation of IRβ in liver and increased phosphorylation of IRβ and IRS1 in muscle tissue compared to wild type mice. Mice with tissue specific knockouts of PTP1B in brain, liver, and skeletal muscle also had improved insulin sensitivity and glucose tolerance, suggesting these cells would be ideal tissue culture models in the further characterization of scFv45 and chemical inhibitors of oxPTP1B.

We have tested the effects of scFv45 on insulin signaling in a panel of cell lines. We initially focused on C2C12, mouse myoblasts. C2C12 cells are capable of differentiation to myotubes and a useful tool in the study of insulin signaling. We partially selected them in

anticipation of eventually studying the effect of scFv45 on insulin resistance, as one of the earliest tissues to experience insulin resistance is muscle. As described in the results section of this chapter we have encountered some technical difficulties, and have since proceeded to use human hepatic stellate cells. Human hepatic stellate cells are a resident mesenchymal cell type in the liver characterized in their quiescent state by retinoid (Vit A) storage, minimal proliferation and collagen synthesis. They become activated in both acute and chronic liver injury such as in response to viral infection, alcohol abuse, biliary cholestasis and notably, metabolic disease such as insulin resistance. Activation induces retinoid metabolism, synthesis of extracellular matrix components such as collagen, proteoglycans and more insoluble glycoproteins, such as dermatan sulfate and fibronectin.

Our lab has worked to develop a new approach to design PTP1B inhibitors that specifically target the reversibly oxidized form; they would mimic the insulin enhancing and potentiating effects of scFv45. We established a screen using DiFMUP, as a substrate for PTP1B phosphatase activity. We have shown as illustrated in Figure 3.3 that we can generate reversibly oxidized pools of PTP1B *in vitro* with reproducible reactivation by reducing agent, TCEP. The approach of the screening assay was to test the ability of small molecule inhibitors to bind to oxPTP1B and antagonize its reactivation by reducing agents. The assay was validated using the LOPAC library, which contains 1280 compounds (Sigma-Aldrich). The collection includes some of the latest, drug-like molecules shown to be effective in fields ranging from cell signaling to neuroscience. Examples of processes in which they have shown efficiency include apoptosis, gene regulation and expression, multi-drug resistance, neurotransmission, phosphorylation, lipid signaling, ion channels and G-proteins.

4.2 Methods

4.2.1 Expression of scFv45 in Mammalian Cells

We wanted to express scFv45 as an intrabody in mammalian cells to observe its interaction with oxPTP1B generated by exogenous treatment with H_2O_2 or insulin stimulation. We transiently expressed scFv45 from a pcDNA vector with a pCMV promoter (Thermo Fischer Scientific pcDNA3.2/V5-GW/D-TOPO). We used X-tremeGENE HP reagent for transfection because the cells we were using were more difficult to transfect than most cell lines (Sigma).

We stably expressed scFv45 from pBABE-puro retroviral constructs (Addgene). Retrovirus was produced in Phoenix cells co-transfected with viral DNA and packaging vectors VSVG and ampho in a 3:1:1 ratio with Lipofectamine (Thermo Fisher Scientific). The DNA was incubated with lipofectamine in Opti-MEM media for 30 min at RT and added dropwise to phoenix cells (70-80% confluent) in culture media. Cells were infected with virus containing media and Polybrene (8ug/mL final concentration) and selected with puromycin (1.5 ug/mL).

4.2.2 Potentiation of Insulin Signaling by scFv45 Expression

We tested both infected C2C12 and transiently transfected human hepatic stellate cells for potentiation effects on insulin signaling with expression of scFv45. We stimulated the cells with both a range of insulin concentrations (0-200nM) and for a series of time points in order to optimize conditions.

Transfected cells were serum starved 36 hours after transfection for ~16 hours and stimulated with a range of insulin prior to lysis. Cells were lysed in 50 mM Tris, pH 7.2, 150 mM NaCl, 10 mM $Na_2HPO_4/H_2PO_4^-$, 1mM EDTA, 1% NP-40 supplemented with Complete protease inhibitor cocktail (Roche). Soluble fractions from samples were processed with 6x SDS-loading dye + DTT and resolved on SDS-PAGE. These samples were blotted for phosphorylation of the IRβ and downstream effectors such as Akt, Erk and GSK3α/β.

In C2C12 cells we performed a co-immunoprecipitation for binding of scFv45 to PTP1B oxidized in response to insulin stimulation. The pull down was carried out with HA-agarose in IP buffer (50mM HEPES, pH 7.4, 150 mM NaCl, 0.1% Triton) at 4°C, overnight. The samples were washed times with IP buffer, and resolved on SDS-PAGE. We blotted with anti-PTP1B (clone FG6) in order to detect PTP1B oxidized in response insulin signaling. We tested for oxidation of PTP1B in C2C12 cells using an antibody raised against the oxidized signature motif of PTP1B oxidized to the sulfonic acid form ($VHC_{SO3H}SAG$) (Persson, Kappert et al. 2005). Cells were lysed under anaerobic conditions in degassed lysis buffer (50 mM Tris, pH 7.4 150 mM NaCl, 5 mM EDTA, 10% glycerol). PTP1B was immunoprecipitated from the lysate at 4°C, for 2 hours using anti-PTP1B antibody (clone FG6) coupled to protein A/G-agarose beads (25 µL slurry) (Santa Cruz). Reduced PTP1B was labeled with sulfhydryl reactive IAA probes (1-10µM final) while no change occurs to terminally oxidized PTP1B species (EZ-link iodoacetyl-PEO).

Addition of TCEP (5 mM final) reduces the reversibly oxidized PTP1B pool and subsequent addition of pervanadate converts reduced cysteine to sulfonic acid forms. The IP samples can then be resolved on SDS-PAGE and the oxPTP antibody detects the S-O_3H species that are located in the active site.

4.2.3 LOPAC Library screening

PTP1B was titrated with a range of H_2O_2 concentrations to identify a concentration at which the enzyme is stably reversibly oxidized for 30-60 minutes, a critical parameter as the completion of the assay could vary between 30-60 minutes. PTP1B was reversibly oxidized in large batches and subsequently incubated with each of the compounds (5 min) and subsequently reactivated with TCEP (Figure 4.6 a). Reversibly oxidized PTP1B was reactivated with TCEP (5mM) in the absence and presence of scFv45, which served as positive and negative controls, respectively. Conversion of the fluorogenic substrate DiFMUP to the fluorescent and stable product DiFMU was used to assay reactivation of oxPTP1B. The assay tested the ability of small molecule inhibitors to bind to the oxidized conformation of PTP1B and antagonize its reactivation by reducing agents. In the presence of small molecules that do not stabilize the oxidized form of PTP1B, we will observe restoration of PTP activity, and dephosphorylation of DiFMUP, to the level observed in controls treated with reducing agent alone. In contrast, with those small molecules that stabilize the oxidized conformation of PTP1B, the restoration of PTP activity will be impaired.

4.2.4 Chelerythrine Potentiates Insulin Signaling in Primary Hepatocytes and in Mice

Primary hepatocytes were used to test the insulin potentiation effects of LOPAC screen hits shown to binding and stabilize oxPTP1B, inhibiting its reactivation. We used primary murine hepatocytes, a gift from Dr. Geoffrey Girnun isolated in his lab (Bhalla 2014). Serum starved cells were incubated with the inhibitors, chelerythrine, palmitine and protopine, for 1 hour (2 μM final) and subsequently stimulated insulin (0-100 nM) for 10 min at 37°C. Cells were lysed in lysis buffer (50 mM Tris, pH 7.2, 150 mM NaCl, 10 mM $Na_2HPO_4/H_2PO_4^-$, 1 mM EDTA, 1% NP-40 supplemented with Complete protease inhibitor cocktail (Roche)) and lysates were prepared for SDS-PAGE analysis.

The in vivo efficacy of chelerythrine was tested in a diet-induced obesity (DIO) model. Specifically C57BL/6 mice were fed either regular diet or high-fat diet on which they gain weight

and develop metabolic deregulation similar to Type 2 diabetes in humans. Animals were maintained on either high fat (45 kcal) or normal diet from week 8 to 12 at which point saline, chelerythrine and protopine were used to treat daily at a dose of 3 mg/kg. The previously characterized PTP1B allosteric inhibitor MSI1436 was used as a positive control for PTP1B inhibition and administered on the same schedule as the other inhibitors, at 5mg/kg (Krishnan 2014).

4.3 Results and Discussion

4.3.1 Testing the Effects of scFv45 on Insulin Signaling in Muscle Cells

We tested the ability of scFv45 to potentiate insulin signaling in the mouse myotube cell C2C12. We were able to stably express scFv45 from a retroviral construct in C2C12 and test its effects on oxPTP1B stabilization and insulin signaling. We observed that insulin potentiation effects of scFv45 expression in C2C12 are not as pronounced compared what we observed in 293T and COS-1 in our lab (Haque 2011). In cells stably expressing scFv45 we were not able to detect an increase in phosphorylation of IRβ or of Akt as compared to parental myotubes (Figure 4.1 top 4 panels).

4.3.2 Murine PTP1B is Redox Regulated and Bound by scFv45 Similarly to Human PTP1B

We considered whether the reduced effect of scFv45 on insulin signaling in C2C12 cells was due to a difference in scFv45's ability to recognize murine PTP1B. As such, we first confirmed through *in vitro* assays that murine PTP1B is oxidized by H_2O_2 and reactivated by addition of reducing agent in a similar manner to human PTP1B (Figure 4.2). Activity for both enzymes is recovered after being oxidized within the same range of H_2O_2. Oxidation of both murine and human PTP1B with concentrations of H_2O_2 of 800 μM and higher caused a sharp decline in recovery of phosphatase activity up on addition of reducing agent. This means that they are reversibly oxidized and reactivated within the same range of peroxide and lack of the ability of murine PTP1B to be oxidized is not the underlying reason for lack of potentiation of insulin signaling with scFv45 expression in murine cells.

As we found the oxidation and reactivation profiles to be practically identical, we tested the ability of scFv45 to interact with human and murine oxPTP1B. Due to the high sequence

similarity between the catalytic domains of the two enzymes, 90% sequence identity, we expected that scFv45 would bind the enzymes with similar affinity. We observed that addition of scFv45 to oxPTP1B inhibited reactivation of both enzymes upon addition of reducing agent (Figure 4.3). We simultaneously confirmed the binding by *in vitro* co-immunoprecipitation with an affinity tag on scFv45. Immunoblotting for PTP1B we observed a direct correlation of the amount of phosphatase and scFv45 present in the binding assay. Both murine and human PTP1B are reversibly oxidized in a similar manner and both interact with scFv45 and are stabilized from reactivation following the same kinetics.

However in C2C12 cells we were not able to observe an interaction between oxPTP1B and stably expressed scFv45. Using an antibody that detects oxidized PTP active site peptides by western blot we were not able to detect oxidation of PTP1B in response to insulin stimulation (Figure 4.1). Phosphorylation of IRβ at pYpY1162/1163 occurred with stimulation with as much as 50-100 nM insulin, which is high by comparison to 293T's where 10 nM resulted in robust potentiation of signaling by scFv45. We speculated it could be a caveat of C2C12 cells that only low levels of PTP1B are oxidized and those levels could be at the limit of our ability to detect. Additionally, scFv45 expression in C2C12 was practically nonexistent by transient transfection and with retroviral infection it was as high as 50% of 293T expression, meaning that the levels of scFv45 expression we are able to achieve in C2C12 cells could be inadequate for the assay.

4.3.3 Expression of scFv45 Potentiates Insulin Signaling in Hepatic Stellate cells

We also tested a human hepatic cell line, stellate cells. High levels of insulin and leptin activated these cells; this is the case in obese patients in particular as they exhibit insulin and leptin resistance. Transient expression of scFv45 in hepatic stellate cells led to increased and sustained phosphorylation of IRβ at pYpY1162/1163 and pY1164. We also observed phosphorylation of effector proteins downstream of the insulin receptor such as phosphorylation of Thr308 and Ser473 of Akt as well as GSK-3α/β phosphorylation on Ser21 and Ser9. My results with stellate cells support the hypothesis that scFv45 stabilizes the reversibly oxidized conformational change of PTP1B induced by ROS produced in response to insulin stimulation. These data suggest a model in which scFv45 binds and stabilizes endogenous oxPTP1B, thereby attenuating PTP1B activity and leading to sustained insulin signaling, a desired signaling state in the insulin resistant context of diabetes. Our results with scFv45 expression in hepatic stellate cells were reassuring, however our investigation for a cell system relevant to

insulin signaling and diabetes continues. Identification of such a system is necessary for characterization of small molecule inhibitors, which mimic of the effects of scFv45 on potentiation of insulin signaling.

4.3.4 Screen of The LOPAC Library

The screen for small molecules that mimic scFv45 inhibitory effects identified two compounds in the LOPAC1280 library, sanguinarine and levamisole (Figure 4.6a). These two compounds were found to partially stabilize the oxidized conformation of PTP1B and addition of reducing agent, TCEP, was able to restore only up to 60% of the activity as illustrated in Figure 4.6b and 4.6c. Identification of such inhibitors provides proof-of-principle for a novel approach that circumvents the challenges associated with targeting the active site of PTP1B in the reduced form. As was reported for the scFv conformation-sensor antibodies, we anticipated that hits from the screen would attenuate the reduction and reactivation of oxidized PTP1B but not have a direct effect on the activity of the reduced form of PTP1B (Haque 2011). The two compounds identified as hits in the pilot screen of the LOPAC library stabilize the oxidized form of PTP1B, but they are unable to inhibit activity of the reduced form of PTP1B. Levamisole has previously been used in Europe to treat weight loss and as an appetite-suppressant. It is now withdrawn from the market due to adverse effects. It has recently been recently associated with agranulocytosis and vasculitis in cocaine users exposed to tainted cocaine as levamisole is still available as a veterinary drug for treatment of parasitic infections (Nolan 2015). Agranulocytosis is an acute blood condition in which patients neutrophil counts are so low they are unable to fight off infections. Studies have characterized levamisole as a potential adjuvant in the treatment of colorectal cancer along with 5-fluorouracyl (Rayter 1995). Sanguinarine is benzophenanthridine alkaloid isolated from the root of *Sanguinaria canadensis* and other poppy-fumaria species (Xu 2013). It has antibacterial, antifungal, antischistosomal, antiplatelet and anti-inflammatory properties (Lu 2012). It has been characterized to have anticancer potentials by sensitizing cancer cells to tumor necrosis factor and through cell cycle arrest or induction of apoptosis. Interestingly although it has been characterized as an anticancer drug due to its inhibition of mitogen-activated protein kinase phosphatase, MKP-1, a phosphatase that has also been validated as an important negative regulator of JNK and p38 and mkp1 -/- mice are resistant to diet induced obesity (Wu 2006). As sanguinarine exhibited better inhibition of oxPTP1B reactivation we investigated derivatives of this molecule and tested their inhibition efficiency.

4.3.5 Chelerythrine: a scFv45 Mimetic Small Molecule Inhibitor of oxPTP1B

One molecule in particular, chelerythrine, inhibited oxPTP1B reactivation with better efficiency (K_i~5) than sanguinarine (K_i~25) Figure 4.7a and 4.7b. Two other derivatives tested, palmatine and protopine, exhibited lower inhibition and no inhibition, respectively. Protopine would therefore be a useful control for off target or nonspecific effects in further experiments in vivo. Chelerythrine is an alkaloid isolated from *Toddalia asiatica* (Wu 2006*)*. It has been characterized as an inhibitor of protein kinase C (PKC) in cancer and PPARγ in T2DM (Chmura 2000, Zheng 2015).

Docking studies with oxPTP1B and sanguinarine indicated that lysine 36, 39 41, leucine 37 and asparagine 44 are important residues for stabilization and inhibition of reactivation in PTP1B. This was the same region that we identified to be important for interaction between scFv45 and oxPTP1B: PTP1B-mut2, which abrogated binding, contains mutations at leucine 37 and lysines 39 and 41. We hypothesized that chelerythrine stabilized oxPTP1B by a similar mechanism that scFv45 does, and tested its ability to potentiate insulin signaling in murine primary hepatocytes (Figure 4.8 B). Incubation with chelerythrine (2 μM) in primary murine hepatocytes followed by stimulation with insulin resulted in potentiation of intracellular insulin signaling as observed by increased phosphorylation of IRβ and Akt. By comparison in the control cells treated with protopine and palmitine the phosphorylation levels were low, indicating no potentiation of insulin signaling through stabilization of oxPTP1B. In diet-induced obese mice we observed that treatment with chelerythrine resulted in weight loss as early day 4 of treatment (Figure 4.8C). The mice exhibit significantly increased glucose tolerance and a mild increase in insulin sensitivity. The food intake for saline, protopine and chelerythrine treated mice was comparable. Mice on normal chow diet treated with chelerythrine did not exhibit weight loss, indicating the weight loss in the DIO mice is not due to drug induced nausea or lack of appetite.

4.4 Figures

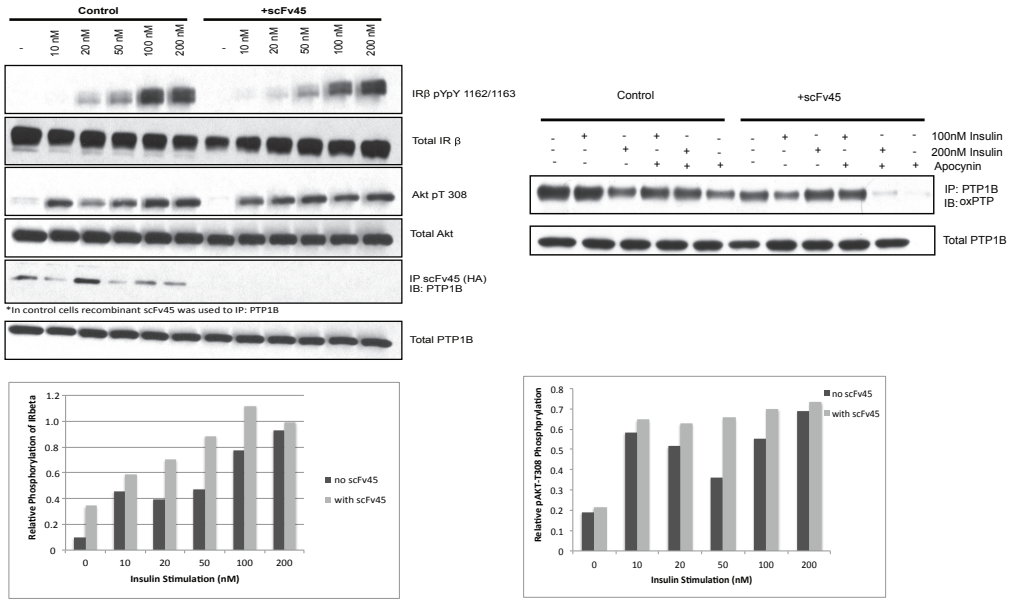

Figure 4.1 scFv45 Expression in Mouse Myoblasts (C2C12) Cells. Stable expression of scFv45 in C2C12 cells did not readily sensitize the cells to insulin signaling as illustrated by a lack of change in the phosphorylation profile of the IRβ and downstream effector Akt.

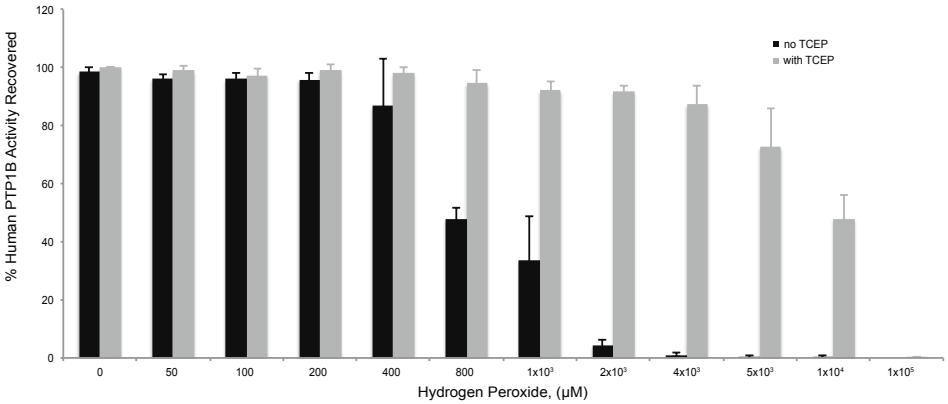

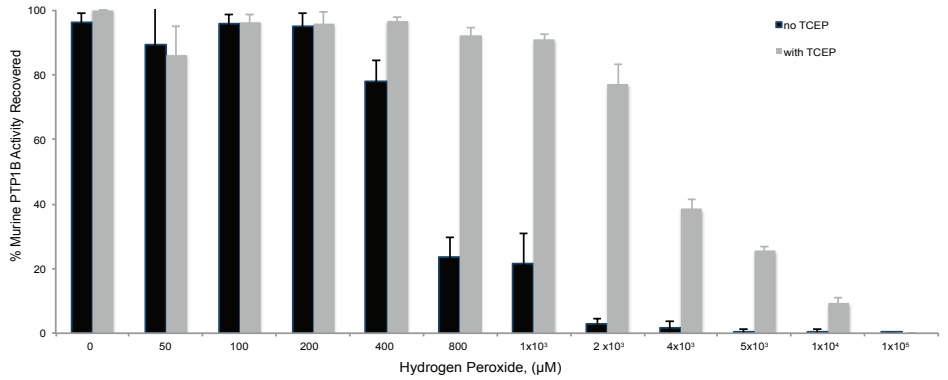

Figure 4.2 Oxidation and Reactivation of Human and Murine PTP1B. Up to 80% of activity of oxidized murine and human PTP1B can be recovered with addition of reducing agent in a after treatment with up to 400μM H_2O_2. At higher H_2O_2 concentrations the ability to reactive decreases sharply for both enzymes.

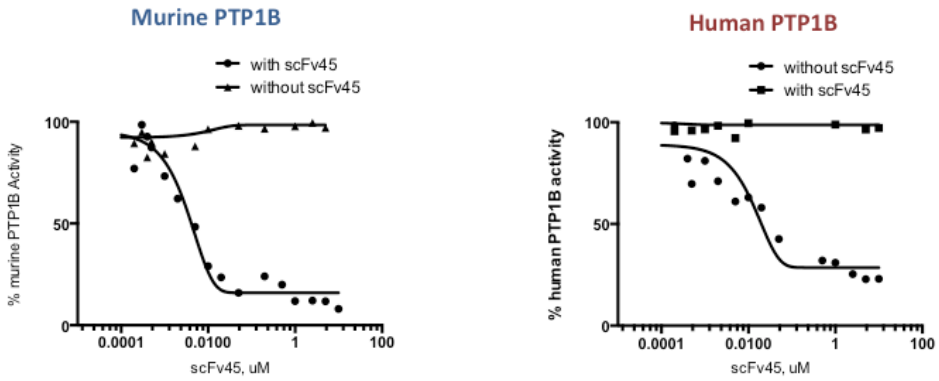

Figure 4.3 scFv45 inhibits reactivation of oxPTP1B. Incubation of oxPTP1B with scFv45 inhibited the ability of enzyme reactivation with the addition of reducing agent as indicated by lack enzyme activity.

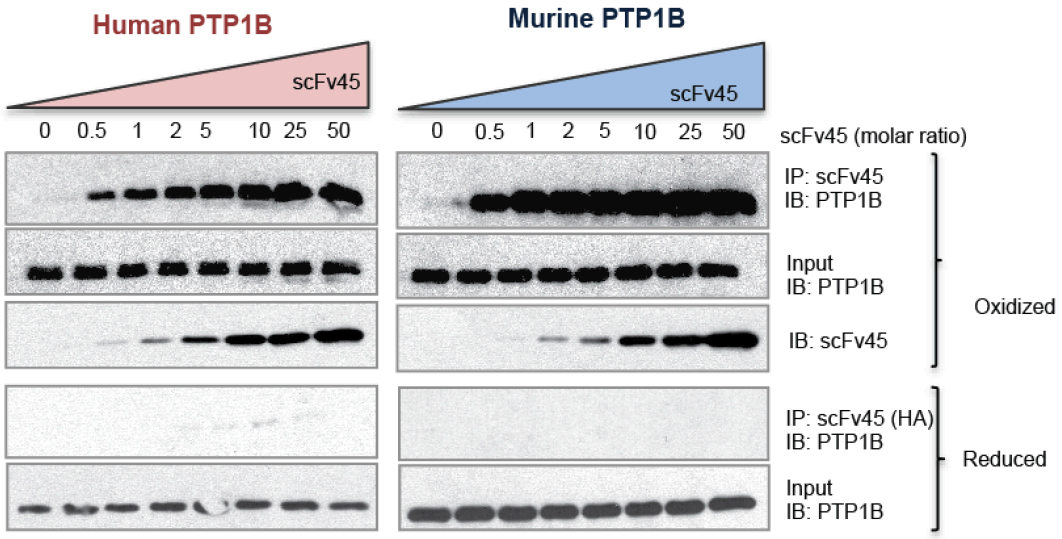

Figure 4.4 scFv45 Binds Murine oxPTP1B. Binding between oxidized murine PTP1B and scFv45 was confirmed by co-immunoprecipicating with a HA-tag on scFv45 for a range of concentrations of scFv45. By comparison, there was no binding observed between reduced murine or human PTP1B and scFv45.

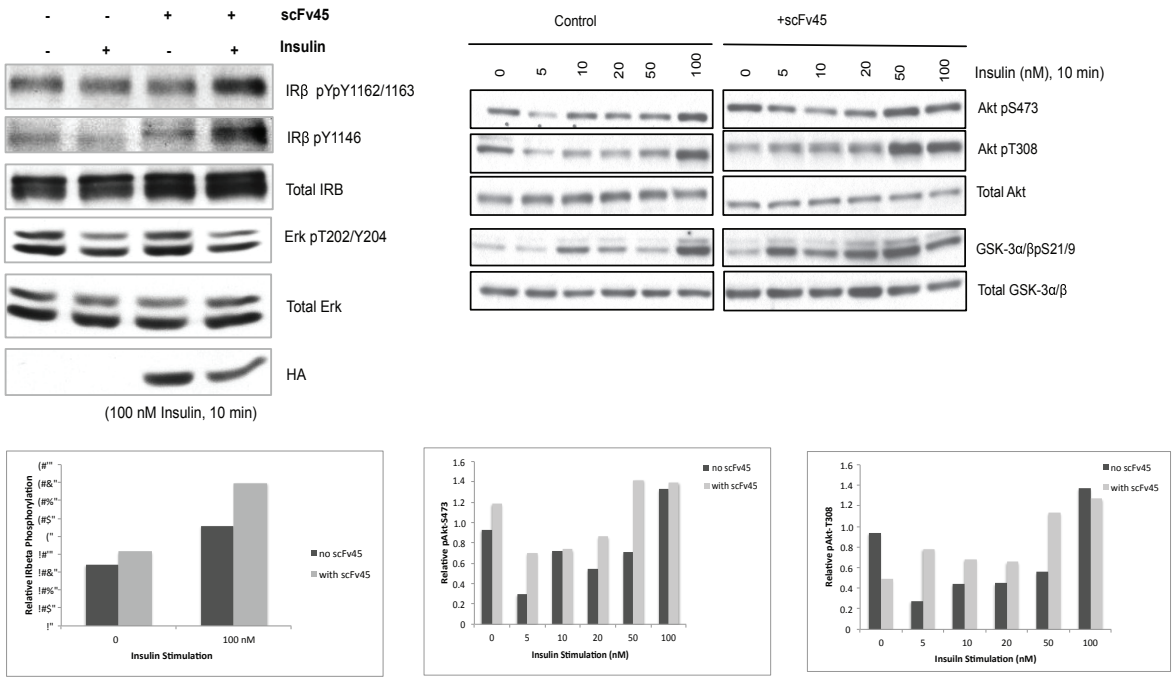

Figure 4.5 scFv45 Potentiates Insulin Signaling in Human Hepatic Stellate Cells. Transient expression of scFv45 in human hepatic stellate cells potentiated insulin signaling as observed by increased phosphorylation of IRβ, IRS1 and Akt at a lower concentration of insulin than in control cells.

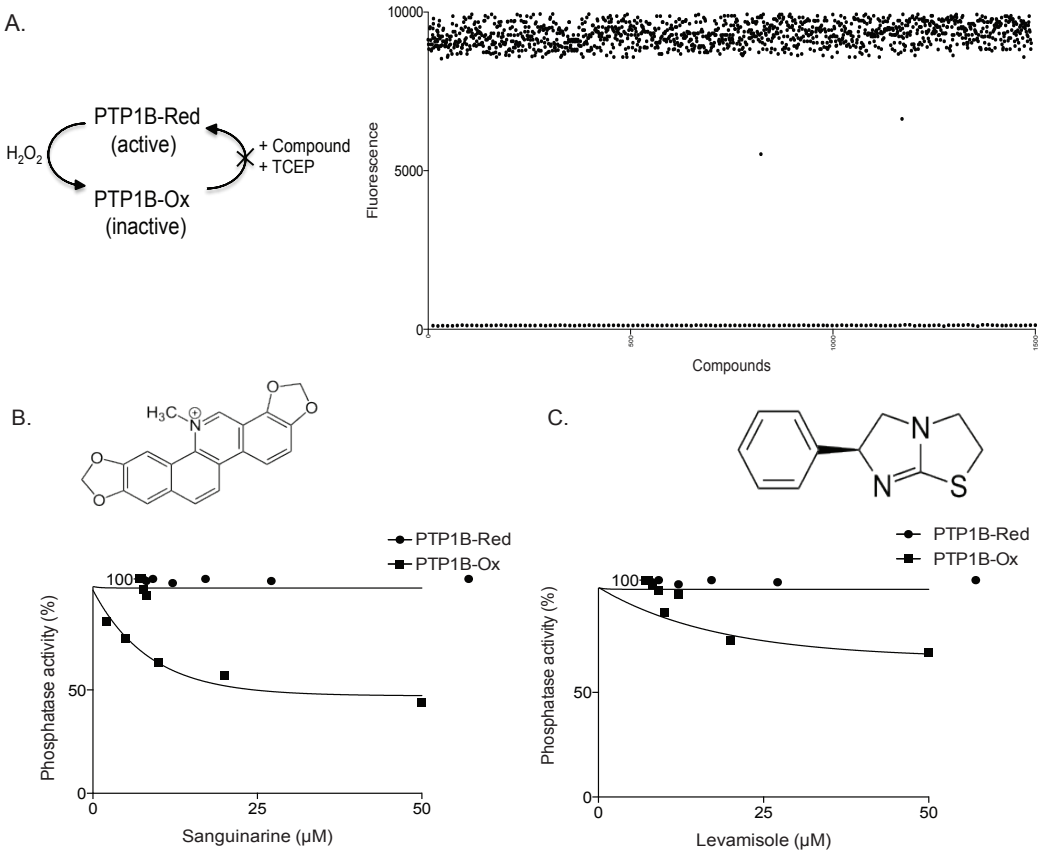

Figure 4.6 LOPAC Screen for Small Molecules Inhibitors of oxPTP1B Reactivation. (A) PTP1B-wt was reversibly oxidized with H_2O_2, incubated with each of the 1280 compounds in the LOPAC library and subsequently reactivated with TCEP. Ability of compounds to inhibit reactivation was quantified with the fluorogenic substrate DiFMUP. (B) Two compounds, sanguinarine and levamisole partially inhibited reactivation of oxPTP1B by 505 and 25%.

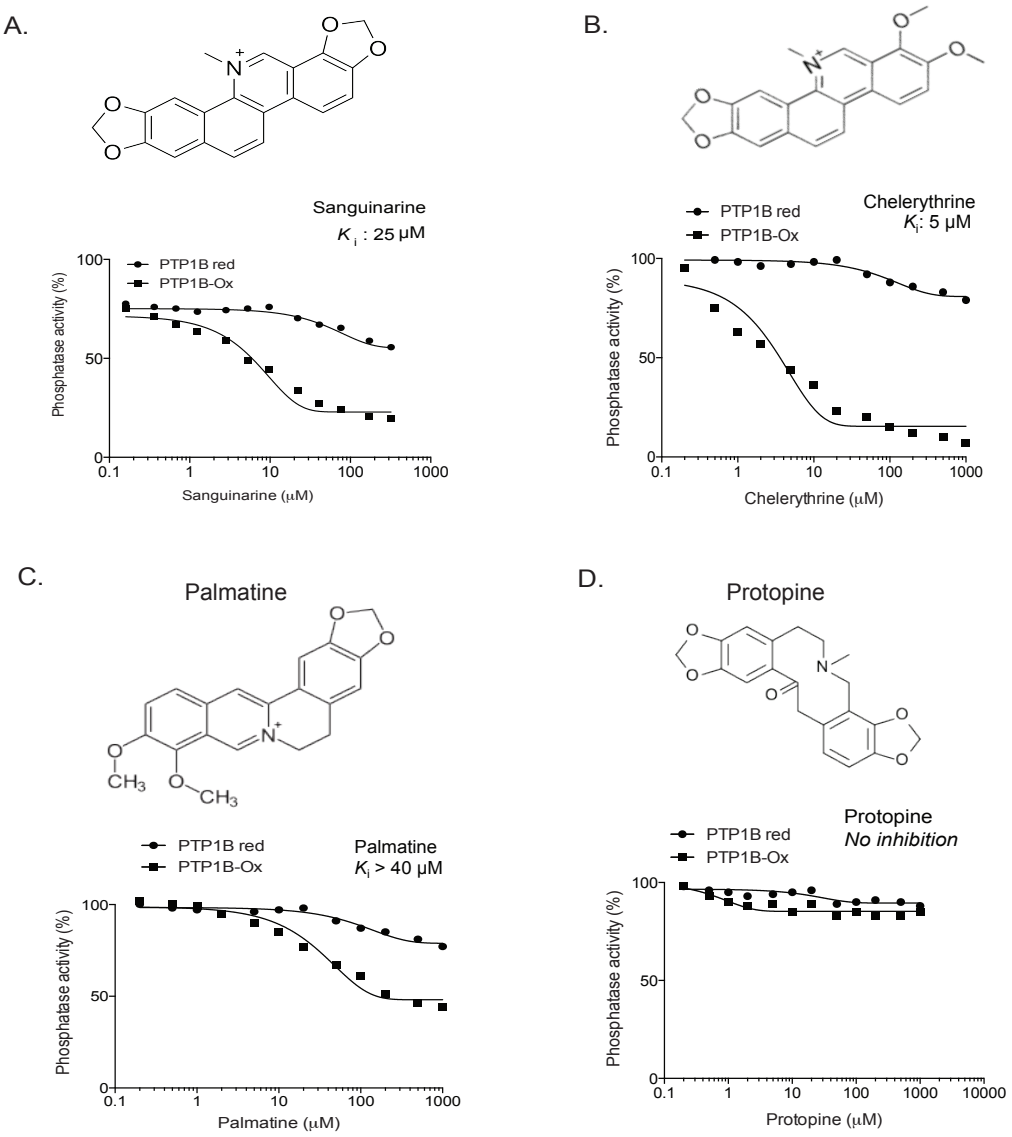

Figure 4.7 Derivatives of Sanguinarine Tested for Inhibition of oxPTP1B Reactivation. (A) Sanguinarine inhibited reversibly oxidized PTP1B with a K_i~25, and has no inhibitory effect on reduced PTP1B-wt. (B) Chelerythrine, a derivative of sanguinarine, exhibited more efficient inhibition of oxPTP1B and no inhibition of reduced PTP1B-wt. (C) Palmatine and (D) Protopine were two other derivatives of sanguinarine tested for inhibition of oxPTP1B reactivation and exhibited poor inhibitory ability

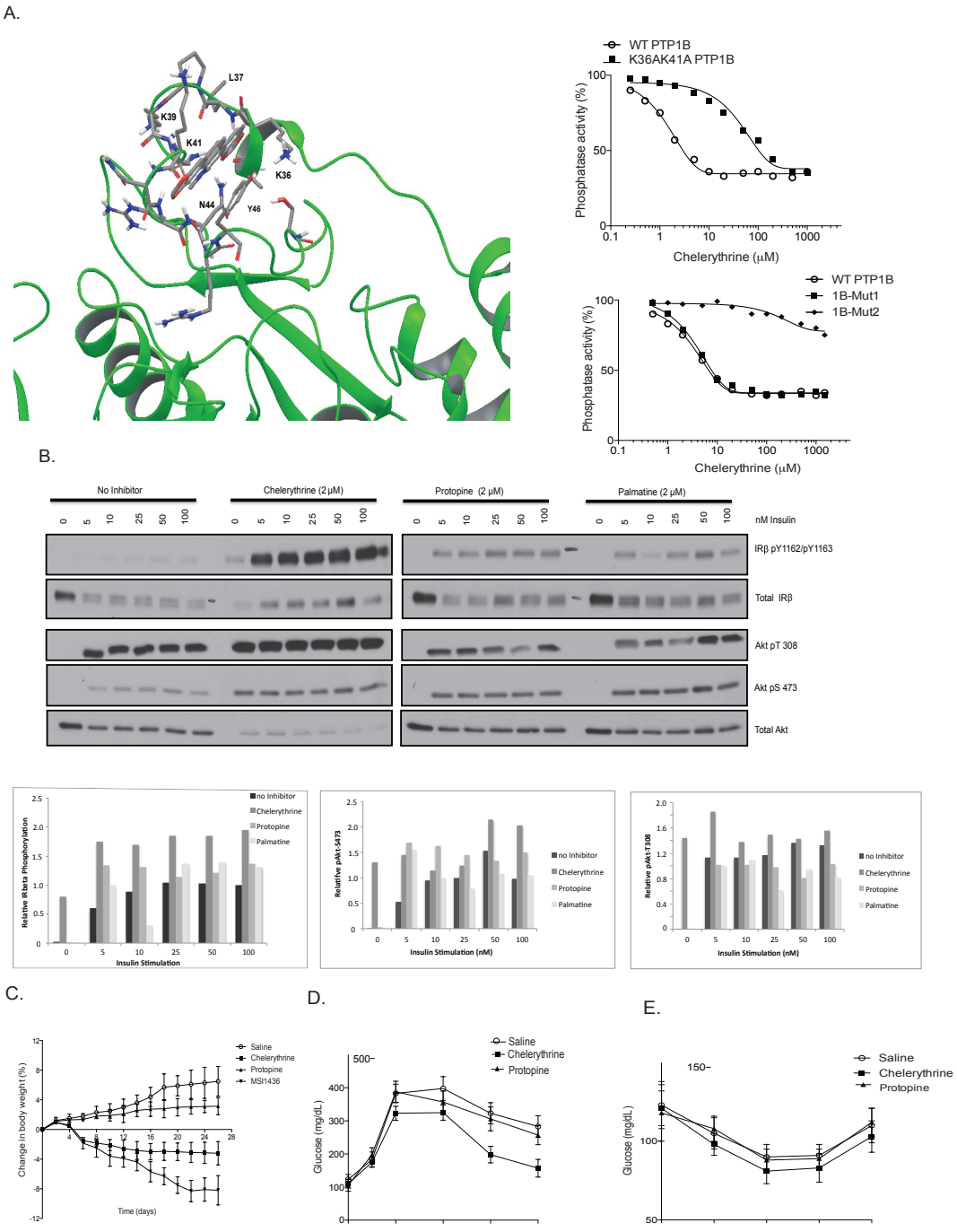

Figure 4.8 Chelerythrine potentiates insulin signaling by stabilizing oxPTP1B (A) Modeling of sanguinarine and oxPTP1B indicates lysine 36, 39 41, leucine 37 and asparagine 44 are important for stabilization. (B) Incubation with chelerythrine (2 μM) in primary murine hepatocytes followed by stimulation with insulin resulted in potentiation of intracellular insulin signaling as observed by increased phosphorylation of IRβ and Akt. By comparison in the control cells treated with protopine and palmitine the phosphorylation levels were low, indicating no potentiation of insulin signaling through stabilization of oxPTP1B. (C) Treatment with chelerythrine in mice with diet-induced obesity resulted in improved glucose tolerance, increased insulin sensitivity and weight loss.

Chapter 5

Summary and Perspectives

5.1 Crystallographic Screening of PTP1B-CASA in complex with scFv45

We were able to optimize the expression and purification of PTP1B-CASA and scFv45 in *E.coli* to obtain homogenous protein in sufficiently high amounts (~1-2mg/L of culture) that we could use for crystallographic trials. We reproduced crystals of PTP1B-CASA as well as found new conditions based on commercially available screens. We observe specific binding of scFv45 to PTP1B-CASA and we are able to isolate a stable complex that we have characterized with laser light dispersion and used for crystallographic screening. We analyzed a series of scFv45 constructs in which the peptide linkers between the V_L and V_H domains vary in length between 7 to 18 residues, and we observed a distinct difference in their stability and ability to maintain a homogeneous, monomeric protein population as discerned by their absorbance profile at 280nm during size exclusion chromatography. The construct with a linker of 7 residues was the least stable and aggregated at concentrations higher than 5mg/mL for the complex. However for the constructs with linkers of 12, 14, 15 and 16 residues protein homogeneity and stability did not improve with increase in linker length. In fact, the 14 residues linker construct was most stable of the four and it bound PTP1B-CASA better, forming a uniform peak by size exclusion chromatography, which indicated homogeneity of the complex. We analyzed constructs with a series of linker lengths because the scFv45 protein with an 18 residues peptide linker exhibited the high solubility. We hypothesized that an shorter linker length might slightly decrease solubility and thus help facilitate crystallization. Based on characterization of proteins generated from all of the constructs the homogeneity and stability exhibited by the protein with an 18 residues linker is preferred to any of the other constructs we tested and we can continue to use this scFv45 to form a complex and for subsequent crystal screening.

Our lab will continue to pursue crystallographic studies. As the purification of both proteins has been optimized, we will focus on screening as extensively as possible. A research technician, Om Shrestha, with several years of experience in structural work, crystallography as well as SAXS and NMR will continue this project in collaboration with the Joshua-Tor laboratory. We have thus far obtained crystals of scFv45 using the Hauptman-Woodward Institute screening facility. We will continue to conduct extensive crystallographic screening with PTP1B-CASA in complex with scFv4518 with the residue linker. We can continue to analyze more screening conditions, different types of experimental setup for the drop or chemical

modifications that might stabilize the complex such as methylation of the proteins after drops have been set up for crystallization. Off-campus screening facilities that offer fee-for-service screening offer the advantage of having many more conditions and might identify a crystallization condition faster. As scFv45 bound oxPTP1B-mut1 with higher affinity than oxPTP1B-CASA (Figure 3.6B) it is possible that a complex of PTP1B-CASA-mut1 : scFv45 could co-crystallize easier than PTP1B-CASA with scFv45. A complex of these 2 proteins could be a viable alternative to our current screening approach. The scFv45 protein itself is not susceptible to proteolytic cleavage, indicating that it has no disordered loops that might interfere with crystal formation. However analytic comparison with other scFv molecules already crystalized might indicate N- or C-terminal residues, which could be eliminated.

Obtaining coordinates important for the binding between scFv45 and oxPTP1B, would indicate residues in oxPTP1B that are important for its stabilization and prevention from reactivation. Mutagenesis and binding analysis could highlight residues that are most important to process of binding of the two proteins. The residues of oxPTP1B highlighted by crystallography and mutagenesis analysis could be informative in the process of designing or optimizing small molecule inhibitors that stabilize oxPTP1B and inhibit its reactivation.

5.2 Defining the Binding Specificity of scFv45 and oxPTP1B

There has been a concerted effort to characterize the function and regulation of PTP1B in the context of insulin signaling. The PTP1B-/- mice were resistant to development of diet-induced obesity due to increased leptin sensitivity. The mice also exhibited increased insulin sensitivity and decreased adipocyte size. The knock out mouse phenotype established PTP1B as a valid therapeutic target in the treatment of both obesity and type 2 diabetes. The charged nature of the catalytic site cleft of PTPs has caused difficulty in finding inhibitors that are orally bioavailable. The generation of the oxPTP1B conformation-sensing antibodies has shown that it is possible to target PTP1B through an alternative approach. By stabilizing the oxidized, inactive form of the enzyme and preventing its reduction and reactivation in cells, insulin signaling can be manipulated and cells sensitized to the insulin hormone.

Mutagenesis and binding analysis identified 3 residues of importance in the mechanism of binding between scFv45 and oxPTP1B: leucine 37, lysine 39 and lysine 41. Mutation of these 3 residues in PTP1B to phenylalanine, glutamic acid and arginine, which are the

equivalent residues in TCPTP generated PTP1B-mut2 and abrogated binding of scFv45. In TCPTP, by comparison, mutation of the phenylalanine 39 to leucine, and of aspartic acid 41 and arginine 43 to lysine residues introduced binding between scFv45 and oxTCPTP-mut2. As highlighted in Figure 5.1, one striking difference in oxidized PTP1B occurred in the positioning of lysine 39 with its side chain forming a hydrogen bond with the backbone of aspartic acid 63. In the reduced conformation, Lys39 points 180° away from Asp63. This is a model based on crystal structures of PTP1B, however it must be corroborated by mutagenesis to disrupt the H-bond between Asp63 and Lys39. Mutagenesis of Lys39 to hydrophobic residues such as Ala that does not form a H-bond might be optimal.

Reversibly oxidized TCPTP has not been crystallized yet, nor TCPTP-CASA and we are not able to model and estimate whether the lysine residues introduced in -mut2 could form a H-bonds as it does in oxPTP1B with Asp63. TCPTP does contain a glutamic acid at position 63 and an aspartic acid at position 65, which might be available for hydrogen bonding with the newly introduced Lys. In TCPTP-WT there is a glutamic acid at the position where Lys39 from PTP1B is substituted to generate -mut2 and it is unknown whether it undergoes a significant change in orientation in the oxidized state.

Obtaining a structure of oxTCPTP or TCPTP-CASA, a process that would not be trivial, would indicate the conformation of the residues altered in –mut2, however it is the structure of oxTCPTP-mut2 : scFv45 in complex that would indicate the mechanism of binding between these two proteins. A crystal structure of oxTCPTP alone could elucidate whether a cyclic sulphenamide is formed when the active site cysteine becomes reversibly oxidized. If a cyclic sulphenamide does not form in oxTCPTP-WT it would suggest that the presence of the conformational change occurring with formation of sulphenamide is important for the binding. We do not know whether a cyclic sulphenamide is formed in oxPTP1B-mut2, and whether the abrogation of binding with scFv45 is due to absence of cyclic sulphenamide. A structure that indicates whether oxTCPTP forms a cyclic sulphenamide would be an important addition to the phosphatase field

The lysine39 residue was highlighted along with leucine37 as important in the binding assays in Figure 2.5 wherein -mut2 residues were mutated back to parental residues. Reintroduction of Leu37 and Lys39 in PTP1B-mut2 reintroduced binding between oxPTP1B and scFv45. Mutation of Leu37 and Lys39 from TCPTP-mut2 to TCPTP-WT residues abrogated the

binding between scFv45 and TCPTP. Importantly, we only detected binding between scFv45 and oxTCPTP-mut2, and no binding with reduced TCPTP-mut2. Indicating that there is an important conformational change that occurs in TCPTP-mut2, particularly in the loop containing the 3 residues F39L/E41K/R43K. As a result we conclude that both the nature of the residues and the conformational change in response to oxidation confer specificity to the binding interaction between the two proteins.

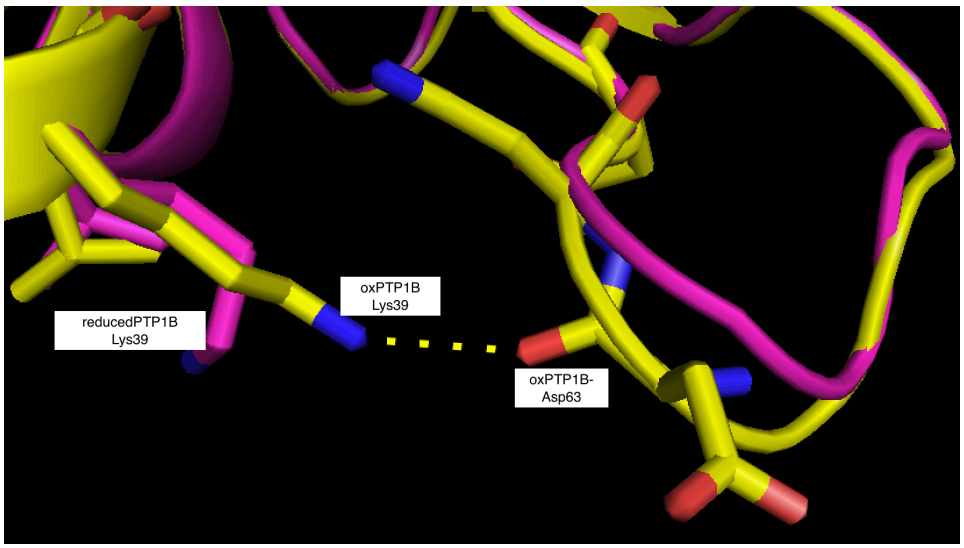

Figure 5.1 Differences in PTP1B-mut2 between the reduced and oxidized states. The major structural difference is the shift of the side chain of Lys39 and its formation of a H-bond with the backbone of Asp63. Reduced PTP1B is illustrated in magenta and oxPTP1b is illustrated in yellow.

Analysis of the binding interface from the perspective of the scFv45 molecule also illustrates residues of importance. There were several scFv residues other than scFv45 that bound to oxPTP1B and many that did not. Comparison of the residues in the complementarity determining region of both the binding and nonbinding scFvs indicates the presence and importance of Glu92, Asp93 and Asp114 is important for binding to oxPTP1B. There is a H-bond formed between Glu92 of scFv45 and Arg47 in PTP1B, and another H-bond formed between Asp110 in scFv45 and Lys41 in PTP1B. In the scFvs that do not bind oxPTP1B the Asp92 residue is conserved, however at position 91 there are Arg, Thr, Ala and Tyr residues, and at position 114 there are Val, Ala, and Thr residues. These interactions were determined based on computer modeling, which generated 10 models and one of which has been analyzed closely although in the absence of imposed restrictions as of this time. The observations from the model must and will be corroborated by mutagenesis of Glu91, Asp93 and Asp114 to residues such as Val, Ala and Thr and subsequent binding assays.

Figure 5.2 Differences in Complementarity Determining Region. The of scFv moecules highlighted in yellow are ones which bind oxPTP1B with a range of binding affinities and variation in their ability to stabilize it and prevent reactivation. Based on modeling we observe there are differences in residues in their CDR, shown here as an alignment. The scFvs that bind oxPTP1B contain Glu92, Asp93 and Asp114, whereas the scFvs that do not bind contain Val, Ala and Thr residues.

Proteolysis coupled with mass spectrometry indicated that a peptide containing residues 23-57, Figure 5.3 below, was protected from proteolytic cleavage through binding of scFv45. This peptide contains within it –mut2, which had been identified 3 residues highly important in mediating binding between scFv45 and oxPTP1B. Computer modeling has also illustrated that scFv45 binds and overlaps with –mut2 and this region protected from proteolysis.

Limited Proteolysis MS

Figure 5.3 Visual Summary of the Protection Proteolysis observations We conclude that binding of scFv45 protects PTP1B-CASA from proteolytic cleavage in its N-terminal cleavage within a peptide region including residues 23-57 highlighted in blue in the structure of PTP1B. The residues identified in PTP1B-CASA-mut2, which abrogated binding between oxPTP1B and scFv45 are indicated in yellow.

The ability to express scFv45 in cells also raises hopes that we could use it as an analytical tool for redox status and in particular redox regulation of PTP1B. This is particularly helpful as there is a need for better reagents to study redox regulation in cells. It would be worthwhile to co-express wild type and –mut2 forms of PTP1B and TCPTP in knock out or double knockout cells, such as mouse embryonic fibroblasts. PTP1B and TCPTP are similarly redox regulated by H_2O_2 and binding assays in cells in response to insulin, might reveal the extent to which the mutation introduced in –mut2 is relevant to their validated substrates, such as IRβ.

5.3 Understanding the Mechanism of PTP1B Redox Regulation in a Cell Model Relevant to Insulin Signaling

We have shown that scFv45 can stabilize oxPTP1B and inhibit its reactivation in mammalian cells. We have specifically searched for a suitable mouse cell line physiologically relevant to insulin signaling in diabetes considering that any future validation of small molecules that mimic scFv45 would likely be tested in mice. It will be interesting to investigate the effect of scFv45 overexpression in an animal model, particularly in one of diet-induced obesity as a proof of principle to which future inhibitors can be compared in the validation process. We expect to see similar effects to tissue specific PTP1B-/-, which exhibited increased insulin sensitivity and improved blood glucose homeostasis. It is likely that the phenotype with scFv45 will not be as striking as a full body or brain PTP1B-/- mouse. We have thus far not detected striking effects of scFv45 expression in murine myotube or adipocyte cell lines, although primary cells might be a better population. We did however encounter technical difficulties expressing comparative levels of scFv45 in these cells to other cell lines such as 293T and COS-1 in which we were able to detect potentiation of insulin signaling. As we have now identified a small molecule inhibitor, chelerythrine, as a mimic of scFv45 in potentiating insulin signaling and its effects could be tested in C2C12 cells.

We have confirmed that scFv45 expression does indeed potentiate insulin signaling in human hepatic stellate cells. These are an important hepatic cell population which become activated in response to hyperinsulinemia as would occur in insulin resistance that accompanies diabetes and type 2 diabetes. As such they are particularly relevant as a cell system for studying the effects of scFv45 in insulin resistance.

PTP1B has been considered a validated target for treating diabetes and obesity for its direct negative regulatory role in insulin and leptin signaling. Potent inhibitors targeting the active site have been identified but have not been developed for clinical use due to poor oral bioavailability. Our lab has shown as a proof of principle that scFv45 inhibition of PTP1B by targeting the reversibly oxidized enzyme is a means to manipulate insulin signaling. We have now also shown that we are able to identify compounds that inhibit oxPTP1B and potentiate insulin signaling through a screen of 1280 pharmacologically active compounds. Sanguinarine, one of the 2 lead compounds identified had a low affinity for oxPTP1B (K_i~25 μM). However one of its commercially available derivatives chelerythrine, has a K_i~ 5 μM. Stimulation with insulin after addition of Chelerythrine caused an increase in phosphorylation of IRβ at pYpY1162/1163 as well Akt pS473/pT308 and GSK-3α/β. This is an early observation of a compound readily available and without undergoing any chemical modification in order to optimize its binding to oxPTP1B. Importantly this data reveals a path to developing a small molecule inhibitor of oxPTP1B that sensitizes insulin signaling in T2DM and obesity just as scFv45 does, by selectively inhibiting that pool of PTP1B that regulates insulin and leptin signaling. The insulin potentiating effects of chelerythrine in primary mouse hepatocytes have formed the basis for further studies in mouse models of diet-induced obesity.

In summary, we have sought to characterize the source of selectivity of the conformation-sensing antibody, scFv45, for oxPTP1B. Through independent and complimentary methods we have identified several residues in oxPTP1B important in the molecular mechanism of recognition by scFv45. Screening assays for small molecule inhibitors of PTP1B have identified several compounds that bind to oxPTP1B and inhibit its reactivation. Both scFv45 and the small molecule inhibitors stabilize oxPTP1B by binding to the same region of the enzyme. Both scFv45 and the small molecule inhibitors are specific for oxPTP1B to the exclusion of reduced PTP1B and the closely related TCPTP. When expressed in cells both scFv45 and the inhibitor chelerythrine potentiate insulin. Overall our data reveal that conformation-sensing antibodies can serve on the path to development of small molecule inhibitors, particularly for protein targets that require alternative approaches, such as was the case with the oxidized, inactive form of PTP1B.

REFERENCES

Ahima, R., Osei, SY, (2004). "Leptin signaling." Physiol Behav **81**(2): 223-241.

Ahmad, F., Considine, R.V., Bauer, T.L., Channesian, J.P., Marco, C.C., Goldstein, B.J. (1997). "Improved Sensitivity to Insulin in Obese Subjects Following Weight Loss Is Accompanied by Reduced Protein-Tyrosine Phosphatases in Adipose Tissue." Metabolism **46**(10): 1140-1145.

Ahmad, F., Li, PM, Meyerovitch, J, Goldstein, BJ, (1995). "Osmotic loading of neutralizing antibodies demonstrates a role for protein-tyrosine phosphatase 1B in negative regulation of the insulin action pathway." J Biol Chem **270**: 20503-20508.

Alonso, A., Merlo, JJ, Na, S, Kholod, N, Jaroszewski, L, Kharitonenkov, A, Williams, S, Godzik, A, Posada, JD, Mustelin, T. (2002). "Inhibition of T cell antigen receptor signaling by VHR-related MKPX (VHX), a new dual specificity phosphatase related to VH1 related (VHR)." J Biol Chem **277**(7): 5524-5528.

Anderson, E., Lustig, ME, Boyle, KE, Woodlief, TL, Kane, DA, Lin, CT, Price, JW 3rd, Kang, L, Rabinovitch, PS, Szeto, HH, Houmard, JA, Cortright, RN, Wasserman, DH, Neufer, PD. (2009). "Mitochondrial H2O2 emission and cellular redox state link excess fat intake to insulin resistance in both rodents and humans." J Clin Invest **119**(3): 573-581.

Banno, R., Zimmer, D, De Jonghe, BC, Atienza, M, Rak, K, Yang, W, Bence, KK, (2010). "PTP1B and SHP2 in POMC neurons reciprocally regulate energy balance in mice." J Clin Invest **120**(3): 720-734.
Barford, D., Flint, AJ, Tonks, NK (1994a). "Crystal Structure of Human Protein Tyrosine Phosphatase 1B." Science **263**: 1398-1404.

Barford, D., Keller, JC, Flint ,AJ, Tonks, NK (1994b). "Purification and Crystallization of the Catalytic Domain of Human Tyrosine Phosphatase 1B Expressed in Escherichia coli."

Bence, K., Delibegovic, M, Xue, B, Gorgun, CZ, Hotamisligil, GS, Neel, BG, Kahn, BB (2006). "Neuronal PTP1B regulates body weight, adiposity and leptin action." Nat Med **12**(8): 917-924.

Bentires-Alj, M., Neel, BG (2007). "Protein-tyrosine phosphatase 1B is required for HER2/Neu-induced breast cancer." Cancer Res **67**(6): 2420-2424.

Bjorge, J., Pang, A, Fujita, DJ (2000). "Identification of protein-tyrosine phosphatase 1B as the major tyrosine phosphatase activity capable of dephosphorylating and activating c-Src in several human breast cancer cell lines." J Biol Chem **275**(52): 41439-41446.

Boivin, B., Zhang, S, Arbiser, JL, Zhang, ZY,Tonks, NK (2008). "A modified cysteinyl-labeling assay reveals reversible oxidation of protein tyrosine phosphatases in angiomyolipoma cells." Proc Natl Acad Sci U S A **105**(29): 9959-9964.

Brown-Shimer, S., Johnson, K.A., Hill, D.E., Bruskin, A. (1992). "Effect of Protein TYrosine Phosphatase 1B expression on Transformation by the Human new Oncogene." Cancer Research **52**: 478-482.

Brown-Shimer, S., Johnson, K.A., Lawrence, J.B., Johnson, C., Bruskin, A., Green, N.R., Hill, D.E. (1990). "Molecular cloning and chromosome mapping of the human gene encoding protein phosphotyrosyl phosphatase 1B." Proceedings of the National Academy of Sciences of the United States of America **87**: 5148-5152.

Bryant, N., Govers, R, James, DE (2002). "Regulated transport of the glucose transporter GLUT4." Nat Rev Mol Cell Biol **3**(4): 267-277.

Buckley, D., Cheng, A, Kiely, PA, Tremblay, ML, O'Connor, R (2002). "Regulation of Insulin-Like Growth Factor Type I (IGF-I) Receptor Kinase Activity by Protein Tyrosine Phosphatase 1B (PTP-1B) and Enhanced IGF-I-Mediated Suppression of Apoptosis and Motility in PTP-1B-Deficient Fibroblasts." Molecular and Cellular Biology **22**(7): 1998-2010.

Cervantes, F., Vannucchi, AM, Kiladjian, JJ, AL-Ali, HK, Sirulnik A, Stalbovskaya, V, McQuitty, M, Hunter, DS, Levy, RS, Passamonti, F, Barbui, T, Barosi, G, Harrison, CN, Knoops, L, Gisslinger, H, (2013). "Three-year efficacy, safety, and survival findings from COMFORT-II, a phase 3 study comparing ruxolitinib with best available therapy for myelofibrosis." Blood **122**(25): 4047-4053.

Charbonneau, H., Tonks, N.K., Kumar, S., Diltz, C.D., Harrylock, M., Cool, D.E., Krebs, E.G., Fischer, E.H., Walsh, K.A. (1989). "Human placenta protein-tyrosine-phosphatase: Amino acid sequence and relationship to a family of receptor-like proteins." Proc.Natl.Acad.Sci. USA **86**: 5252-5256.

Chen, X., Zaro, JL, Shen, WC, (2013). "Fusion protein linkers: property, design and functionality." Adv Drug Deliv Rev **65**(10): 1357-1369.

Cheng, A., Uetani, N, Simoncic, PD, Chaubey, VP,Lee-Loy, A, McGlade, CJ, Kennedy, BP,Tremblay, ML, (2002). "Attenuation of leptin action and regulation of obesity by protein tyrosine phosphatase 1B." Dev Cell **2**(497-503).

Chernoff, J., Schievella, A.R., Jost, C.A., Erikson, R.L., Neel, B.G., (1990). "Cloning of a cDNA for a major human protein-tyrosine-phosphatase." Proceedings of the National Academy of Sciences of the United States of America **87**: 2735-2739.

Cheung, A., Kusari, J., Jansen, D., Bandyopadhyay, D., Kusari, A., Bryer-Ash, M. (1998). "Marked impairment of protein tyrosine phosphatase 1B activity in adipose tissue of obese subjects with and without type 2 diabetes mellitus." J Lab Clin Med **134**(2): 115-123.

Chmura, S., Dolan ME, Cha, A, Mauceri, HJ, Kufe, DW, Weichselbaum, RR (2000). "In Vitro and in Vivo Activity of Protein Kinase C Inhibitor Chelerythrine Chloride Induces Tumor Cell Toxicity and Growth Delay in Vivo." Clin Cancer Res **6**: 737-742.

Cicirelli, M., Tonks, NK, Diltz, CD, Weiel, JE, Fischer, EH, Krebs, EG (1990). "Microinjection of a protein-tyrosine-phosphatse inhibits insulin action in Xenopus oocytes." Proc Natl Acad Sci U S A **87**: 5514-5518.

Cohen, P. (2002). The origins of protein phosphorylation. Nat. Cell Biol. **4:** E127-130.

Combs, A. P. (2010). "Recent advances in the discovery of competitive protein tyrosine phosphatase 1B inhibitors for the treatment of diabetes, obesity, and cancer." J Med Chem **53**(6): 2333-2344.

Cool, D., Tonks, NK, Charbonneau, H., Walsh, KA, Fischer, EH, Krebs, EG (1989). "cDNA isolated from a human T-cell library encodes a member of the protein-tyrosine-phosphatase family." Proc Natl Acad Sci U S A **86**: 5257-5261.

Cromlish, W., Tang, M, Kyskan, R, Tran, L, Kennedy, BP, (2006). "PTP1B-dependent insulin receptor phosphorylation/residency in the endocytic recycling compartment of CHO-IR cells." Biochem Pharmacol **72**(10): 1279-1292.

Delibegovic, M., Bence, KK, Mody, N, Hong, EG, Ko, HJ, Kim, JK, Kahn, BB, Neel, BG (2007). "Improved glucose homeostasis in mice with muscle-specific deletion of protein-tyrosine phosphatase 1B." Mol Cell Biol **27**(21): 7727-7734.

Delibegovic, M., Zimmer, D, Kauffman, C, Rak, K, Hong, EG, Cho, YR, Kim, JK, Kahn, BB, Neel, BG, Bence, KK (2009). "Liver-specific deletion of protein-tyrosine phosphatase 1B (PTP1B) improves metabolic syndrome and attenuates diet-induced endoplasmic reticulum stress." Diabetes **58**(3): 590-599.

Denu, J. M., Tanner, K.G. (1998). "Specific and Reversible Inactivation of Protein Tyrosine Phosphatases by Hydrogen Peroxide: Evidence for a Sulfenic Acid Intermediate and Implications for Redox Regulation." BIochemistry **37**: 5633-5642.

Echwald, S., Bach, H, Vestergaard, H, Richelsen, B, Kristensen, K, Drivsholm, T, Borch-Johnsen, K, Hanse, T, Pedersen, O (2002). "A P387L Variant in Protein Tyrosine Phosphatase-1B Is Associated with Type 2 Diabetes and Impaired Serine Phosphorylation of PTP-1B In Vitro." Diabetes **51**: 1-6.

Elchebly, M., Payette, P, Michaliszy, E, Cromlish, W, Collins, S, Loy, AL, Normandin, D, Cheng, A, Himms-Hagen, J, Chan, CC, Ramachandran, C, Gresser, MJ, Tremblay, ML, Kennedy, BP (1999). "Increased Insulin Sensitivity and Obesity Resistance in Mice Lacking the Protein Tyrosine Phosphatase-1B Gene." Science **283**(5407): 1544-1548.

Fischer, E. H. and E. G. Krebs (1955). "Conversion of Phosphorylase b to Phosphorylase a in muscle extracts." J. Biol. Chem **216**(1): 121-132.

Flint, A., Tiganis, T, Barford, D, Tonks NK (1997). "Development of "substrate-trapping" mutants to identify physiological substrates of protein tyrosine phosphatases." Proc Natl Acad Sci U S A **94**: 1680-1685.

Frangioni, J., Oda, A, Smith, M, Selzman EW, Neel, BG, (1993). "Calpain-catalyzed cleavage and subcellular relocation of protein phosphotyrosine phosphatase 1B (PTP-1B) in huma platelets." EMBO J **12**(12): 4843-4856.

Frangioni, J. V., Beahm, P.H., Shifrin, V., Jost, C.A., Neel, B.G., (1992). "The Nontransmembrane Tyrosine PHosphatase PTP-1B Localizes to the Endoplasmic-Reticulum Via Its 35 Amino-Acid C-Terminal Sequence." Cell **68**: 545-560.

Galic, S., Hauser, C, Kahn, BB, Haj, FG, Neel, BG, Tonks, NK, Tiganis, T (2005). "Coordinated regulation of insulin signaling by the protein tyrosine phosphatases PTP1B and TCPTP." Mol Cell Biol **25**(2): 819-829.

Galic, S., Klingler-Hoffmann, M, Fodero-Tavoletti, MT, Puryer, MA, Meng, TC, Tonks, NK,Tiganis, T (2003). "Regulation of Insulin Receptor Signaling by the Protein Tyrosine Phosphatase TCPTP." Molecular and Cellular Biology **23**(6): 2096-2108.

Gu, F., Dube, N, Kim, JW, Cheng, A, Ibarra-Sanchez, MdJ, Tremblay, ML, Boisclair, YR (2003). "Protein Tyrosine Phosphatase 1B Attenuates Growth Hormone-Mediated JAK2-STAT Signaling." Molecular and Cellular Biology **23**(11): 3753-3762.

Guan, K. L., Haun, R.S., Watson, S.J., Geahlen, R.L. Dixon, J.E. (1990). "Cloning and Expression of a protein-tyrosine-phosphatase." Proceedings of the National Academy of Sciences of the United States of America **87**: 1501-1515-1505.

Haj, F., Verveer, PJ, Squire, A, Neel, BG, Bastiaens PI (2002). "Imaging sites of receptor dephosphorylation by PTP1B ont he surface of the endoplasmic reticulum." Science **295**: 1708-1711.

Haque, A., Andersen, JN, Salmeen, A, Barford, D, Tonks, NK (2011). "Conformation-sensing antibodies stabilize the oxidized form of PTP1B and inhibit its phosphatase activity." Cell **147**(1): 185-198.

Heinonen, K. M., Nestel, F.P., Newell, E.W., Charette, G., Seemayer, T.A., Tremblay, M.L., Lapp, W.S. (2004). "T-cell protein tyrosine phosphatase deletion results in progressive systemic inflammatory disease." Blood **103**(9): 3457-3464.

Iversen, L., Moller, KB, Pedersen, AK, Peters, GH, Petersen, AS, Andersen, HS, Branner, S, Mortensen, SB, Moller, NP, (2002). "Structure determination of T cell protein-tyrosine phosphatase." J Biol Chem **277**(22): 19982-19990.

Jia, Z., Barford, D., Flint, A.J., Tonks, N.K. (1995). "Structural Basis for Phosphotyrosine Peptide Recognition by Protein Tyrosine PHosphatase 1B." Science **268**: 1754-1758.

Julien, S., Dube, N, Read, M, Penney, J, Paquet, M, Han, Y, Kennedy, BP, Muller, WJ, Tremblay, ML (2007). "Protein tyrosine phosphatase 1B deficiency or inhibition delays ErbB2-induced mammary tumorigenesis and protects from lung metastasis." Nat Genet **39**(3): 338-346.

Karaman, M., Herrgard, S, Treiber, DK, Gallant, P, Atteridge C E, Campbell BT, Chan KW, Ciceri P, Davis MI, Edeen PT, Faraoni R, Floyd M, Hunt JP, Lockhart DJ, Milanov ZV, Morrison MJ, Pallares G, Patel HK, Pritchard S, Wodicka LM, Zarrinkar PP (2008). "A quantitative analysis of kinase inhibitor selectivity." Nat Biotechnol **26**(1): 127-132.

Kenner, K., Anyanwu E, Olefsky JM, Kusari J (1996). "Protein-tyrosine phosphatse 1B is a negative regulator of insulin- and insulin-like growth factor-I-stimulated signaling." J Biol Chem **271**: 19810-19816.

Klaman, L., Boss, O, Peroni, OD, Kim, JK, Martino, JL, Zabolotny, JM, Moghal, N, Lubkin, M, Kim, YB, Sharpe, AH, Krongrad, AS, Shulman, GI, Neel, BG, Kahn, BB (2000). "Increased Energy Expenditure, Decreased Adiposity, and Tissue-Specific Insulin Sensitivity in Protein-Tyrosine Phosphatase 1B-Deficient Mice." Molecular and Cellular Biology **20**(15): 5479-5489.

Krebs, E., Fischer, EH, (1955). "Phosphorylase activity of skeletal muscle extracts." Biochim Biophys Acta **20**(1): 113-120.

Krishnan, N., Koveal, D, Miller, DH, Xue, B, Akshinthala, SD, Kragelj, J, Jensen, MR, Gauss, CM, Page, R, Blackledge, M, Muthuswamy, SK, Peti, W, Tonks, NK (2014). "Targeting the disordered C terminus of PTP1B with an allosteric inhibitor." Nat Chem Biol **10**(7): 558-566.

Krishnan, N., Krishnan, K, Connors, CR, Choy, MS, Page, R, Peti, W, Van Aelst, L, Shea, SD, Tonks, NK (2015). "PTP1B inhibition suggests a therapeutic strategy for Rett syndrome." J Clin Invest **125**(8): 3163-3177.

Lam, M. H. C., Michell, B.J., Fodero-Tavoletti, M.T., Kemp, B.E., Tonks, N.K., Tiganis, T. (2001). "Cellular Stress Regulates the Nucleocytoplasmic Distribution fo the Protein-Tyrosine Phosphatase TCPTP." J Biol Chem **276**(40): 37700-37377-37707.

Lammers, B., Bossenmaier, B., Cool, D.E., Tonks, N.K., Schelessinger, J., Fischer, E.H., Ullrich, A (1993). "Differential Activities of Protein Tyrosine Phosphatases in Intact Cells." J Biol Chem **268**: 22456-22462.

LaMontagne, K. J., Flint, AJ, Franza, BR Jr, Pandergast, AM, Tonks, NK (1998). "Protein tyrosine phosphatase 1B antagonizes signalling by oncoprotein tyrosine kinase p210 bcr-abl in vio." Mol Cell **18**: 2965-2975.

Lee, S., Yang, KS, Kwon, J, Lee, C, Jeong, W,Rhee, S. G. (2002). "Reversible inactivation of the tumor suppressor PTEN by H2O2." J Biol Chem **277**(23): 20336-20342.

Lohse, D. L., Denu J.M., Santoro, N,, Dixon J.E. (1997). "Roles of Aspartic Acid-181 and Serine-222 in Intermediate Formation and Hydrolysis of the Mammalian Protein-Tyrosine-Phosphatase PTP1." Biochemistry **36**: 4568-4575.

Lu, J., Bao, JL, Chen, XP, Huang, M, Wang, YT (2012). "Alkaloids isolated from natural herbs as the anticancer agents." Evid Based Complement Alternat Med **2012**: 485042.

Mahadev, K., Motoshima, H, Wu, X, Ruddy, JM, Arnold, RS, Cheng, G, Lambeth, JD, Goldstein, BJ (2004). "The NAD(P)H Oxidase Homolog Nox4 Modulates Insulin-Stimulated Generation of H2O2 and Plays an Integral Role in Insulin Signal Transduction." Molecular and Cellular Biology **24**(5): 1844-1854.

Mahadev, K., Zilbering, A, Zhu, L, Goldstein, BJ (2001). "Insulin-stimulated hydrogen peroxide reversibly inhibits protein-tyrosine phosphatase 1b in vivo and enhances the early insulin action cascade." J Biol Chem **276**(24): 21938-21942.

Meng, T., Buckley, DA, Galic, S, Tiganis, T, Tonks, N K (2004). "Regulation of insulin signaling through reversible oxidation of the protein-tyrosine phosphatases TC45 and PTP1B." J Biol Chem **279**(36): 37716-37725.

Meng, T., Fukada, T, Tonks, NK (2002). "Reversible Oxidation and Inactivation of Protein Tyrosine Phosphatases In Vivo." Molecular Cell **9**: 387-399.

Mohi, M., Neel, BG, (2007). "The role of Shp2 (PTPN11) in cancer." Curr Opin Genet Dev **17**(1): 23-30.

Myers, M., Andersen, JN, Cheng, A, Tremblay, ML, Horvath, CM, Parisien, JP, Salmeen, A, Barford, D, Tonks NK (2001). "TYK2 and JAK2 are substrates of protein-tyrosine phosphatase 1B." J Biol Chem **276**: 47771-47774.

Myers, M., Leibel, RL, Seeley, RJ, Schwartz, MW (2010). "Obesity and leptin resistance: distinguishing cause from effect." Trends Endocrinol Metab **21**(11): 643-651.

Newsholme, P., Haber, EP, Hirabara, SM, Rebelato, EL, Procopio, J, Morgan, D, Oliveira-Emilio, HC, Carpinelli, AR,Curi, R (2007). "Diabetes associated cell stress and dysfunction: role of mitochondrial and non-mitochondrial ROS production and activity." J Physiol **583**(Pt 1): 9-24.

Nolan, A., Jen, KY (2015). "Pathologic manifestations of levamisole-adulterated cocaine exposure." Diagn Pathol **10**: 48.

Palmer, C., Bento, JL, Mychaleckyj, JC, Langefeld, CD, Campbell, JK, Norris, JM, Haffner, SM, Bergman, RN, Bowden, DW, (2004). "Association of Protein Tyrosine Phosphatase 1B Gene Polymorphisms With Measures of Glucose Homeostasis in Hispanic Americans " Diabetes **53**: 3013-3019.

Pannifer, A. D. B., Flint, A.J., Tonks, N.K., Barford, D., (1998). "Visualization of the Cysteinyl-phosphate Intermediate of a Protein-tyrosine Phosphatase by X-ray Crystallography." J Biol Chem **273**(17): 10454-10462.

Patti, M., Kahn, CR, (1998). "The Insulin Receptor - A Critical Link in Glucose Homeostasis and Insulin Action." Journal of Basic and Clinical Physiology and Pharmacology **9**(2-4).

Persson, C., K. Kappert, U. Engstrom, A. Ostman and T. Sjoblom (2005). "An antibody-based method for monitoring in vivo oxidation of protein tyrosine phosphatases." Methods **35**(1): 37-43.

Persson, C., Savenhed, C, Bourdeau, A, Tremblay, ML, Markova, B, Bohmer, FD, Haj, FG, Verveer, PJ, Squire, A, Neel, BG, Bastiaens PI, Neel, BG, Elson, A, Heldin, CH, Ronnstrand, L, Ostman, A, Hellberg, C (2004). "Site-Selective Regulation of Platelet-Derived Growth Factor Receptor Tyrosine Phosphorylation by T-Cell Protein Tyrosine Phosphatase." Molecular and Cellular Biology **24**(5): 2190-2201.

Pocal, A., Lam, TKT, Gutierres-Juares, R, Obici, S, Schwarts, GJ, Bryan, J, Aguillar-Bryan, L, Rossetti, L (2005). "Hypothalamic K-ATP channels control hepatic glucose production." Nature **434**: 1026-1031.

Rayter, Z., Leicester, RJ, Mansi, JL (1995). "Adjuvant chemotherapy for colorectal cancer." Ann R Coll Surg Engl **77**: 81-84.

Reaven, G. M. (2011). "The metabolic syndrome: time to get off the merry-go-round?" J Intern Med **269**(2): 127-136.

Reynaud, C., Anques, V, Grimal, H, Weill, JC (1987). "A Hyperconversion Mechanism Generates the Chicken Light Chain Preimmune Repertoire." Cell **48**: 379-388.

Reynaud, C., Dahan, A, Anques, V, Weill, JC (1989). "Somatic Hyperconversion Diversified the Single VH Gene of the Chicken with a High Incidence in the D Region." Cell **59**: 171-183.

Romsicki, Y., Reece, M, Gauthier, JY, Asante-Appiah, E, Kennedy, BP, (2004). "Protein tyrosine phosphatase-1B dephosphorylation of the insulin receptor occurs in a perinuclear endosome compartment in human embryonic kidney 293 cells." J Biol Chem **279**(13): 12868-12875.

Salmeen A, A. J., Myers MP, Meng TC, Hinks JA, Tonks NK, Barford D (2003). "Redox regulation of protein tyrosine phosphatase 1B involves a sulphenyl-amide intermediate." Nature **423**: 769-773.

Salmeen, A., Andersen, JN, Myers, MP, Tonks, NK, David, B (2000). "Molecular Basis for the Dephosphorylationof the Activation Segment of the Insulin Receptor by Protein Tyrosine Phosphatase 1B." Molecular Cell **6**: 1401-1413.

Salmeen, A., Barford, D, (2005). "Functions and Mechanisms of Redox Regulation of Cysteine-Based Phosphatases." Antioxidants & Redox Signaling **7**: 560-577.

Saltiel, A., Pessin JE (2002). "Insulin signaling pathways in time and space." Trends in Cell Biology **12**(2): 65-71.

Saltier, A., Kahn, CR, (2001). "Insulin signaling and the regulation of glucose and lipid metabolism." Nature **414**: 799-806.

Savitsky, P., Finkel, T (2002). "Redox regulation of Cdc25C." J Biol Chem **277**(23): 20535-20540.

Scherer, T., O'Hare, J, Diggs-Andrews, K, Schweiger, M, Cheng, B, Lindtner, C, Zielinski, E, Vempati, P, Su, K, Dighe, S, Milsom, T, Puchowicz, M, Scheja, L, Zechner, R, Fisher, SJ, Previs, SF, Buettner, C (2011). "Brain insulin controls adipose tissue lipolysis and lipogenesis." Cell Metab **13**(2): 183-194.

Shields, B., Hauser, C, Bukczynska, PE, Court, NW,Tiganis, T (2008). "DNA replication stalling attenuates tyrosine kinase signaling to suppress S phase progression." Cancer Cell **14**(2): 166-179.

Simoncic, P., Lee-Loy, A, Barber, DL, Tremblay, ML, McGlade, CJ (2002). "The T Cell Protein Tyrosine Phosphatase Is a Negative Regulator of Janus Family Kinases 1 and 3." Current Biology **12**: 446-453.

Sundaresan, M., Yu, Z.X., Ferrans, V.J., Irani, K., Finkel, T., (1995). "Requirement for Generation of H2O2 for Platelet-Derived Growth Factor Signal Transduction." Science **270**: 296-299.

Taghibiglou, C., Rashid-Kolvear, F, Van Iderstine, SC, Le-Tien, H, Fantus, IG, Lewis, GF, Adeli, K (2002). "Hepatic very low density lipoprotein-ApoB overproduction is associated with attenuated hepatic insulin signaling and overexpression of protein-tyrosine phosphatase 1B in a fructose-fed hamster model of insulin resistance." J Biol Chem **277**(1): 793-803.

Thie, H., Schirrmann, T, Paschke, M, Dubel, S, Hust, M, (2008). "SRP and Sec pathway leader peptides for antibody phage display and antibody fragment production in E. coli." N Biotechnol **25**(1): 49-54.

Tiganis, T., Bennett, AM, Ravichandran, KS, Tonks, NK (1998). "Epidermal Growth Factor Receptor and the Adaptor Protein p52Shc Are Specific Substrates of T-Cell Protein Tyrosine Phosphatase." Molecular and Cellular Biology **18**(3): 1622-1634.

Tonks, N., Diltz, CD, Fischer EH (1988a). "Purification of the Major Protein-tyrosine-phosphatase of Human Placenta." The Journal of Biological Chemistry **263**(14): 6722-6730.

Tonks, N., Diltz, CD, Fischer, EH, (1988b). "Characterization of the Major Protein-tyrosine phosphatases of Human Placental." The Journal of Biological Chemistry **263**(14): 6731-6737.

Tonks, N. K. (2003). "PTP1B: From the sidelines to the front lines!" FEBS Letters **546**(1): 140-148.

Tonks, N. K. (2003). PTP1B: from the sidelines to the front lines! FEBS Lett. **546:** 140-148.

Tonks, N. K. (2006). "Protein tyrosine phosphatases: from genes, to function, to disease." Nat Rev Mol Cell Biol **7**(11): 833-846.

Van Montfort, R., Congreve, M, Tisi, D, Carr, R, Jhoti, H (2003). "Oxidation state of the active-site cysteine in protein tyrosine phosphatase 1B." Nature **423**(6941): 773-777.

van Vliet, C., Bukczynska, PE, Puryer, MA, Sadek, CM, Shields, BJ, Tremblay, ML, Tiganis, T (2005). "Selective regulation of tumor necrosis factor-induced Erk signaling by Src family kinases and the T cell protein tyrosine phosphatase." Nat Immunol **6**(3): 253-260.

Wiede, F., Shields, BJ, Chew, SH, Kyparissoudis, K, van Vliet, C, Galic, S, Tremblay, ML, Russell, SM, Godfrey, DI, Tiganis, T (2011). "T cell protein tyrosine phosphatase attenuates T cell signaling to maintain tolerance in mice." J Clin Invest **121**(12): 4758-4774.

Woodford-Thomas, T. A., Rhodes, J.D., Dixon, J.E. (1992). "Expression of a Protein Tyrosine Phosphatase in Normal and v-src-Transformed Mouse 3T3 Fibroblasts." J Cell Biol **117**(2): 401-414.

Wu, J., Roth, RJ, Anderson, EJ, Hong, EG, Lee, MK, Choi, CS, Neufer, PD, Shulman, GI, Kim, JK, Bennett, AM (2006). "Mice lacking MAP kinase phosphatase-1 have enhanced MAP kinase activity and resistance to diet-induced obesity." Cell Metab **4**(1): 61-73.

Xu, J., Meng, QH, Chong, Y, Jiao, Y, Zhao, L, Rosen, EM, Fan, S (2013). "Sanguinarine is a novel VEGF inhibitor involved in the suppression of angiogenesis and cell migration." Mol Clin Oncol **1**(2): 331-336.

Yamamoto, T., Sekine, Y, Kashima, K, Kubota, A, Sato, N, Aoki, N, Matsuda, T, (2002). "The nuclear isoform of protein-tyrosine phosphatase TC-PTP regulates interleukin-6-mediated signaling pathway through STAT3 dephosphorylation." Biochemical and Biophysical Research Communications **297**: 811-817.

You-Ten, K. E., Muise, E.S., Itie, A., Michaliszyn, E., Wagner, J., Jothy, S., Lapp, W.S., Tremblay, M. (1997). "Impaired Bone Marrow Microenvironment and Immune Function in T Cell Protein Tyrosine Phosphatase-deficient Mice." J Exp Med **186**(5): 683-693.

Zabolotny, J., Bence-Hanulec, KK, Stricker-Krongrad, A, Haj, F, Wang, Y, Minokoshi, Y, Kim, YB, Elmquist, JK, Tartaglia, LA, Kahn, BB, Neel, BG (2002). "PTP1B Regulates Leptin Signal Transduction in Vivo." Dev Cell **2**: 489-495.

Zhang, K., Geddie, ML, Kohli, N, Kornaga, T, Kirpotin, DB, Jiao, Y, Rennard, R, Drummond, DC, and U. Nielsen, Xu, L, Lugovskoy, AA. (2015). "Comprehensive optimization of a single-chain variable domain antibody fragment as a targeting ligand for a cytotoxic nanoparticle." MAbs **7**(1): 42-52.

Zheng, W., Qiu, L, Wang, R, Feng, X, Han, Y, Zhu, Y, Chen, D, Liu, Y, Jin, L, Li, Y. (2015). "Selective targeting of PPARgamma by the natural product chelerythrine with a unique binding mode and improved antidiabetic potency." Sci Rep **5**: 12222.

Zinker, B., Rondinone, CM, Trevillyan, JM, Gum, RJ, Clampit, JE, Waring, JF, Xie, N, Wilcox, D, Jacobson, P, Frost, L, Kroeger, PE, Reilly, RM, Koterski, S, Opgenorth, TJ, Ulrich, RG, Crosby, S, Butler, M, Murray, SF, McKay, RA, Bhanot, S, Monia, BP, Jirousek, MR (2002). "PTP1B antisense oligonucleotide lowers PTP1B protein, normalizes blood glucose, and improves insulin sensitivity in diabetic mice." Proc Natl Acad Sci U S A **99**(17): 11357-11362.